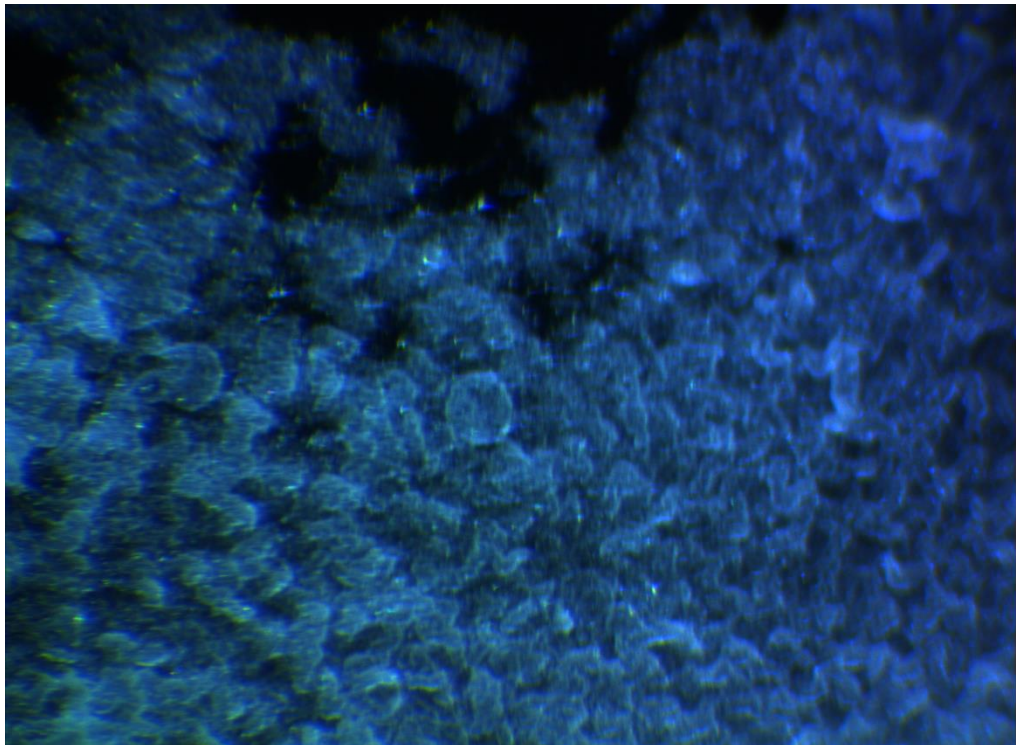


Master of Science by Research
The University of Kent
The School of Physical Sciences

Gold Nanoparticles as Adjuncts in Electrophoretic Analysis of Biopolymers.

By Emerald. R. Taylor



Submitted in fulfilment of the degree of Master of Science by Research
September 2017

Abstract:

This thesis discusses two projects which investigate the analysis and application of biomolecules. Chapter 1 provides the background and context of this work. Chapter 2 discusses the synthesis and characterisation of three types of gold nanoparticles, sodium citrate, cetyltrimethyl ammonium bromide (CTAB) and 4-dimethylamino pyridine (DMAP) protected gold nanoparticles, as well as two types of polyacrylamide gel, TBE and tris-HCl. Successful characterisation of these gold nanoparticles was carried out by dynamic light scattering, ultra-violet visible spectroscopy and transmission emission microscopy. The characterisation of polyacrylamide gels was achieved by investigation by rheology, optical coherence tomography and scanning electron microscopy. Rheological analysis demonstrated that the addition of gold nanoparticles to polyacrylamide reduces the elasticity of the gel but stabilises the linear viscoelastic range, while not changing the core properties of the material. These materials were then used to separate sulfur containing biomolecules by polyacrylamide gel electrophoresis.

Chapter 3 discusses the efficacy of the three types of gold nanoparticles to separate sulfur containing biomolecules when added to polyacrylamide gel electrophoresis. Citrate and CTAB gold nanoparticles were unsuccessful when used to analyse phosphorothioated DNA, however, DMAP gold nanoparticles showed promising results. DMAP gold nanoparticles were further tested with the proteins lysozyme, bovine serum albumin (BSA), glutathione-S-transferase (GST) and RNase A (RNase). The retention of BSA and GST was successful however there was continued problems with visualising lysozyme and RNase. This led to the development of ATP polyacrylamide gel electrophoresis.

Chapter 4 discusses the theoretical application of the development of catalytic DNA aptamers using in vitro selection. We synthesised a DNA aptamer library, two primers and two biotinylated strands of DNA, to be used in the selection process. However due to poor purity and yields, the

Master of Science by Research

project remains in its infancy. We discuss the methods by which we would conduct this research and our justifications for these processes.

Contents

List of Abbreviations	6
<i>Acknowledgements:</i>	8
Chapter 1.0 Introduction:	9
1.1 Gold Nanoparticles as Adjuncts in Electrophoretic Analysis of Biomolecules:.....	10
1.2 Design and Synthesis of Catalytic DNA Aptamers:.....	16
Chapter 2: Synthesis, Concentration and Characterisation of Gold Nanoparticles and Polyacrylamide Gels.....	20
2.1 Introduction:.....	20
2.2 Experimental:	21
2.2.1 Materials:	21
2.3 Methods:	21
2.3.1 Gold Nanoparticle Synthesis:	21
2.3.1.1 Dimethylamino Pyridine Protected Gold Nanoparticle (DMAP AuNPs) Synthesis: .	21
2.3.1.2 Sodium Citrate Protected Gold Nanoparticle (Citrate AuNPs) Synthesis:	22
2.3.1.3 Cetyltrimethyl-ammonium Bromide Protected Gold Nanoparticle (CTAB AuNPs) Synthesis:	22
2.3.2 Gold Nanoparticle Concentration:	23
2.3.2.1 DMAP AuNPs Concentration:.....	23
2.3.2.2 Citrate AuNPs Concentration:.....	23
2.3.2.3 CTAB AuNPs Concentration:.....	23
2.3.3 Characterisation of Gold Nanoparticles:.....	24
2.3.3.1 Dynamic Light Scattering (DLS):.....	24
2.3.3.2 Ultra-violet Visible (UV-Vis) Spectroscopy:	24
2.3.3.3 Transmission Electron Microscopy (TEM):	24
2.4 Characterisation of Polyacrylamide Gels:	25
2.4.1 Rheology:	25
2.4.3 Scanning Electron Microscopy (SEM):.....	27
2.5 Results and Discussion:	27
2.5.1 AuNPs Characterisation:	27
2.5.1.1 DLS and UV-Vis:.....	27
2.5.1.2 Transmission Electron Microscopy:.....	29
2.6 Characterisation of Polyacrylamide Gels:	30
2.6.1 Rheology:	30
2.6.2 Optical Coherence Tomography:.....	38
2.6.3 Scanning Electron Microscopy:	42

2.7 Conclusions:	44
Chapter 3: Analysis of Biomolecules using Gold Nanoparticles as Adjuncts in Polyacrylamide Gel Electrophoresis.	46
3.1 Introduction:	46
3.2 Experimental:	47
3.2.1 Materials:	47
3.3 Methods:	47
3.3.1 DNA Samples:	47
3.3.2 DNA Sample Preparation:	48
3.3.3 Tris Borate EDTA (TBE) Native Denaturing PA Gel:	49
3.3.4 Tris Magnesium Acetate (TAMg) Native PA Gel:	49
3.3.4 Protein Reduction:	49
3.3.5 Tris-HCl Native PA Gel:	50
3.3.6 SDS Gradient Polyacrylamide Gel (4-15 %):	50
3.3.7 Tris-HCl Native Gradient Gels:	51
3.3.8 ATP Tris-HCl Native PA Gel Buffers:	51
3.3.9 ATP Tris-HCl Native PA Gel:	52
3.4 Results and Discussion:	52
3.4.1 AuNPs Gel Electrophoresis:	52
3.4.2 Citrate-AuNPs Polyacrylamide Gel Electrophoresis:	52
3.4.3 CTAB-AuNPs Polyacrylamide Gel Electrophoresis:	55
3.4.4 DMAP-AuNPs Polyacrylamide Gel Electrophoresis:	56
3.4.5 SDS Polyacrylamide Gel Electrophoresis:	57
3.4.6 Tris-HCl Polyacrylamide Gel Electrophoresis:	59
3.5 Conclusion:	63
Chapter 4: Catalytic DNA Aptamers.	65
4.1 Introduction:	65
4.2 Materials:	65
4.3 Methods:	66
4.3.2 Cleavage, De-protection and Purification of Synthesised DNA Components:	67
4.3.3 Quantification:	68
4.3.4 Selection Buffers:	68
4.4 Results and Discussion:	69
4.5 Conclusions:	73
Chapter 5: Conclusions, Further Work and References.	74
5.1 Conclusions and Further Work:	74
5.2 References:	76

List of Abbreviations:

%, Percentage
≈, Approximately
°C, Degrees celsius
μL, Microlitre
μM, Micromolar
2-ME, β-mercaptoethanol
3', Three prime
3D, 3-dimensional
5', Five prime
A, Adenosine
Abs, Absorption
AFM, Atomic force microscopy
ATP, Adenosine triphosphate
AuNPs, Gold nanoparticles
BSA, Bovine serume albumin
C, Cytosine
CD, Circular dichroism
cm, Centimetre
CTAB, Cetyltrimethyl ammonium bromide
Cys, Cysteine
DG, Diffraction grating
DLS, Dynamic light scattering
DMAP, 4-dimethylamino pyridine
DNA, Deoxyribose nucleic acid
DNA ref, DNA reference
EtOH, Ethanol
g, Gravity
G, Guanine
G'', Loss modulus
G', Storage modulus
GST, Glutathione-S-transferase
Hg-PAGE, Mercury polyacrylamide gel electrophoresis
HSAB, Hard soft acid base
Hys-tag, Histadine tag
Hz, Hertz
ICP-MS, Inductively coupled plasma-mass spectrometry
intS, Internal sulfur
extS, External sulfur
kba, kilobase
keV, Kilo electron voltage
LC-MS, Liquid chromatography mass spectrometry
LVER, Linear viscoelastic range
LxWxB, Length by width by breadth
M, Molarity

mg mL⁻¹, milligram per millilitre
mins, Minutes
mM, millimolar
mRNA, messenger ribo nucleic acid
MS, Mass spectrometry
n, Number
NEM, N-ethyl maleimide
nm, Nanometre
nmol, Nanomoles
OCT, Optical coherence tomography
Pa, Pascals
PA, Polyacrylamide
PAGE, Polyacrylamide gel electrophoresis
PCR, Polymerase chain reaction
PDB, Protein data bank
R, Reduced
rads⁻¹, Radians per second
RNA, Ribo nucleic acid
RNAi, Ribo nucleic acid interference
RNase, RNase A
SB-OCT, Spectrometre based optical coherence tomography
SDS, Sodium dodecyl sulfate
SEM, Scanning electron microscopy
SLD, Super-luminscent diode
Sp-OCT, Spectral domaine optical coherence tomography
SPR, Surface plasmon resonance
ss-DNA, Single stranded DNA
T, Thymine
TBE, Tris borate EDTA
TD-OCT, Time domanie optical coherence tomography
TEM, Transmission electron microscopy
TLC, Thin layer chromatography
Tris-HCl, Tris hydrochloric acid
tRNA, Transfer ribo nucleic acid
TS, Transition state
UV, Ultraviolet
UV-Vis, Ultraviolet visible spectroscopy
V, Voltage
vp, Variable pressure
XPS, X-ray photoelectron spectroscopy

Acknowledgements:

I would like to thank my supervisor Dr Christopher Serpell for giving me the opportunity to complete this work.

I would also like to thank the Kent Faculty of Sciences Research Fund for funding.

I would like to thank, Dr Dave Beal for teaching me how to work in a biosciences laboratory and aiding in the protein based research. Dr Jennifer Hiscock for teaching me how to use the rheometer. Ian Brown for running TEM analysis, Luke Alsebrook for running SEM analysis and Sophie Caujolle for imaging my gels using OCT.

Finally I would like to thank; my friends in the Serpell and Hiscock groups, and loved ones for always having faith in me.

Chapter 1.0 Introduction:

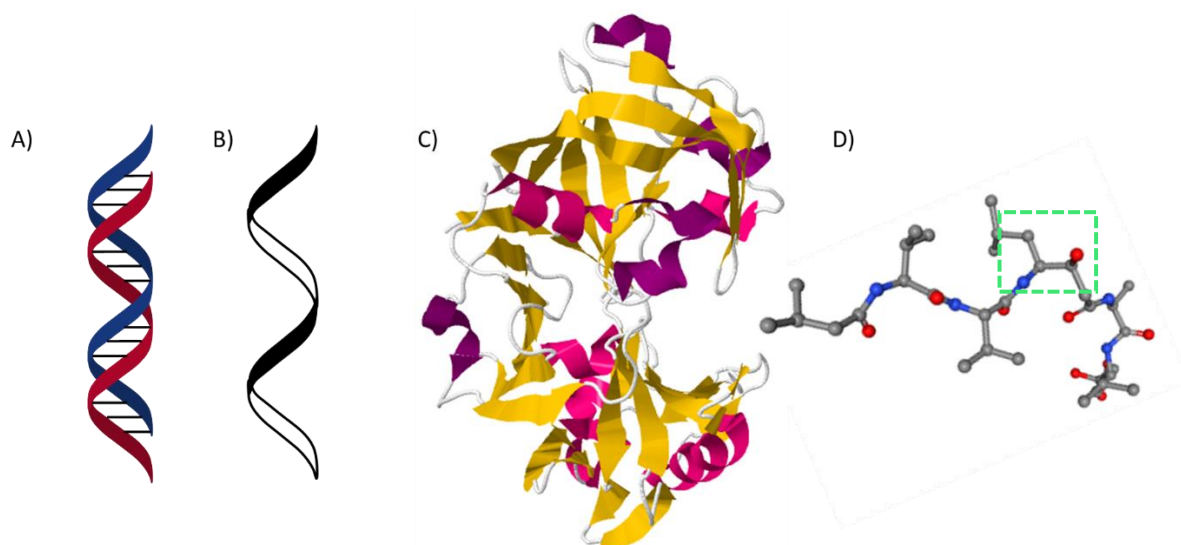


Figure 1.1: A, representation of DNA. B, representation of RNA. C, biological assembly of human pepsin 3b (3UTL) taken from PDB¹. D, ball and stick structure of pepstatin, an inhibitor of pepsin. Tetrahedral structure imperative in pepsin-pepstatin bonding, highlighted by dashed box. Taken from PDB (PRD_000557)².

This thesis discusses two projects related to the analysis and application of biomolecules. Biomolecules fall into four main categories: carbohydrates, lipids, proteins / peptides and nucleic acids. These relatively simple structures ultimately act as the building blocks of life itself. Lipids are small molecules with structural properties primarily related to their amphiphilic nature, meaning that they have hydrophilic heads and hydrophobic chains or 'tail's.³ This property allows lipids to form structures such as liposomes and micelles, as well as cell membranes.³ Carbohydrates in their simplest form take the form of mono- and disaccharides such as glucose and sucrose respectively.⁴ Glucose especially is considered one of the main energy sources in cell function.⁴ However polysaccharides also form complex multi-layered folded structures such as cellulose which is the key component of cell walls.⁵ Polysaccharides can also be found on the cell membrane of animal cells; these conjugated carbohydrates act as signalling beacons.⁵ Nucleic acids fall into two categories, according to whether they have a ribose or deoxyribose sugar. Both of these forms are linked by phosphates to form the backbone associated with DNA and RNA. Each sugar phosphate unit is then connected to a base; A, C, G and T for DNA or A, C, G, U for RNA. RNA is mainly responsible for transport and transfer of

information from the nucleus to organelles.⁶ DNA is basis upon which all genetic information is stored and passed onto future generations it holds the genetic code upon which daily biological processes are carried out in all life.⁶ Amino acids are the monomer components from which proteins are formed. Proteins are responsible for carrying out the biological processes living creatures rely on the most, including but not limited to photosynthesis, the breakdown of food and nutrients, mediation of messenger RNA and gene expression.⁷ Proteins will be discussed in further detail through this chapter.

1.1 Gold Nanoparticles as Adjuncts in Electrophoretic Analysis of Biomolecules:

The biological importance of sulfur can be easily overlooked. Historically considered toxic⁸ in its form as hydrogen sulfide, it has been discovered that sulfur is key to many biological pathways.⁹ Sulfur can be found in each of the four key categories of biomolecules; it is due to sulfur having a number of mechanisms for making and breaking bonds, as well as redox diversity, meaning that sulfur can be extremely versatile.^{8,9} Sulfur has a similar reactivity to that of oxygen however its position lower on the periodic table allows it to be both a nucleophile and electrophile dependent on its environment.¹⁰ Disulfide bonds are also more stable than peroxide bonds, for this reason they are key in protein structure.^{9,11} Cysteine, a sulfur containing amino acid is the building block of many key metabolites such as: coenzyme A, glutathione and mycothiol because of the presence of sulfur in its structure.¹⁰ Metal sulfates such as iron sulfate, can have useful redox properties such as the interconversion of α -hydroxy acids and α -keto acids, such as lactate and pyruvate as well as acting as ligands in biological pathways.¹²

Proteins are complex 3D structures formed by folding long polypeptide chains with a high level of structural definition. Many proteins work through binding small molecules (ligands).⁴ Cysteine is the only known amino acid which contains the uniquely reactive thiol (SH) group, which when deprotonated exceeds the nucleophilic capacity of any other protein side chain.¹³ This is why residue modification is the most common method of protein tagging.^{14,15}

Thiolated biomolecules, natural and synthetically modified, can be used to 'tag' biological processes; the use of biotin, free cysteines and antibodies conjugated with sulfur are all popular methods.^{16,17} Biotin is common due to its affinity for streptavidin and the separation which can be achieved between complexes which have formed disulfide bonds.¹⁶ Thiol containing biomolecules can be labelled with thiol active species such as triphenylphosphonium, which is utilised in the detection of thiols produced in mitochondrion phosphorylation.¹⁸ These tagged products are then separated by gel electrophoresis and detected by the interaction with an antibody which has been activated for triphenylphosphonium.¹⁸ Tagging of phosphorylation sites found in proteins are of use when trying to understand specific protein function and structure, this can be done using a modified poly histidine-tag, which has a thiol containing cysteine residue (Hys-tag).¹⁹ Protein tagging is useful in the observation and understanding of protein interactions and the understanding of drug delivery.^{14,20-22} Tagging is also beneficial in that it does not generally modify the chemical structure or reactivity of the target molecule.²² Classical modification reagents such as 4-vinylpyridine and N-substituted maleimides were thought to be the pinnacle of cysteine related tagging however recent studies have shown that these methods can lead to structure instability and undesirable side reactions.^{13,20} The instability of the adduct in biological media has become particularly difficult with the rise of antibody-drug conjugates,²¹ the development of alternative chemical markers has led to the use of molecules such as vinyl sulfones.^{13,23,24} These complications make the analysis of sulfur all the more important.

Nucleic acids can be labelled by a number of methods; sulfur's reactivity makes it a prime element to act as the intermediate binding point between the molecules. Labelling can aid in a number of processes such as, separation, purification and identification. Some types of tagging are fluorescent labelling with fluorophores, tagging with biotin and phosphorothiolation of nucleic acids.²⁵⁻²⁷ Phosphorothioates are resistant to enzymatic degradation and because of this are useful in the development of nucleic therapeutics design.²⁸ Thiophosphates do occur

naturally via the phosphorylation of RNA but they are also synthetically generated, through phosphoramidite and solid phase chemistry.^{28,29} Natural thiophosphates produced from RNA have a wide application which I will be discussed in further detail.

The post transcriptional modification of ribonucleic acid (RNA) is a characteristic property of the molecule, with many modifications occurring naturally.³⁰ Transfer (tRNA) RNA has many thiol containing derivatives, these are important biomolecules in gene expression, codon recognition and structural stability.³⁰ Post translational modifications of tRNA follow the ubiquitin-like pathway for modifying eukaryotic proteins.^{30,31} Sulfur-modified RNA is not only important in terms of biological function but also therapeutics.³² An example of this is in the testing RNA oligomers which work by RNA interference (RNAi), these short double stranded lengths of RNA work by manipulating cellular machinery to degrade specific strands of messenger RNA (mRNA) before they are translated in to proteins.³³⁻³⁵ Antisense oligomers are perhaps the most direct way of targeting RNA; once bound to the target RNA antisense oligomers edit the RNAs function through post binding events.^{33,35} Very recently an RNAi therapeutic has succeeded in phase 3 clinical trials for a previously untreatable illness. This important breakthrough highlights the importance of this technology. Sulfur containing RNAs have led to the development of a number of interesting research avenues, thus highlighting the need to separate sulfur containing biomolecules from non-thiolated biomolecules.

Observing sulfur and sulfur containing biomolecules can be completed by a number of methods, some of these are: mass spectrometry (MS), X-ray photoelectron spectroscopy (XPS) and inductively coupled plasma-mass spectrometry (ICP-MS)³⁶⁻³⁹. MS can be used in the analysis of sulfur containing compounds however the different charge states and a mixture of these states can cause varied splitting of the molecules making it difficult to interpret the spectra⁴⁰. Sulfur has four stable isotopes at; 32,33,34 and 36, this can cause uncertainty in the assigned masses but is useful in MS analysis³⁶. The most common MS analysis techniques of sulfur biomolecules involve prior separation steps.^{41,42} Coupled techniques include liquid chromatography MS (LC-

MS) and gas chromatography MS (GC-MS). These techniques are preferable over sulfur derivatisation methods which often only work for free thiols, unlike the coupled techniques which can analyse sulfur in all of its forms.³⁹

ICP-MS was at its inception considered to be only a “metal detector” but has seen a recent rebirth in its ability to analyse the majority of elements present in the periodic table.^{36,43} The ability of ICP-MS to analyse sulfur biomolecules has been greatly improved by the coupling of separation techniques as with traditional MS coupled techniques.^{19,36,39,40} XPS is a method which interrogates surface based interactions. This is especially key when analysing sulfur containing molecules. Sulfur and its surface molecules have different binding energies depending on their state and environment XPS is a useful tool in the interrogation of this property as well as distinguishing the oxidation states of sulfur.^{44,45} Sulfur identifications achieved by analysis of S2p information is important in identifying the reactions and pathways in which different types of sulfur contribute.^{44,45}

A common method of Identifying the presence of reduced thiols in proteins is the use of a colour changing assay which uses 5, 5'-dithiobis (2-nitrobenzoic acid) or Ellman's reagent as the indicator.^{46,47} Ellman's reagent contains a weak disulfide bond. When in the presence of oxidised sulfur, the assay remains colourless, however in the presence of free thiols from reduced proteins the disulfide bond within the Ellman's reagent is reduced. The free thiols from the protein and separated Ellman's reagent form new disulfide bonds causing the solution to change from colourless to yellow,^{22,46-49} Figure 1.2 shows a representation of this process.

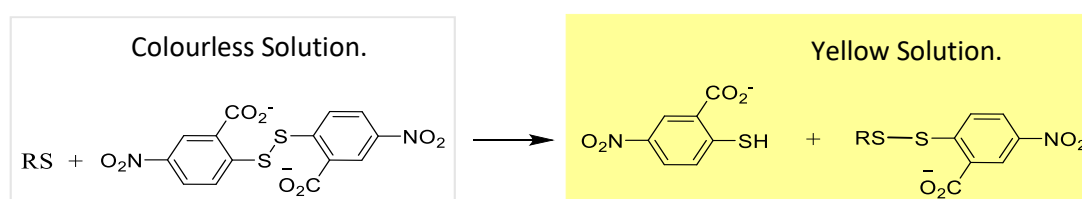


Figure 1.2: The reaction which occurs when Ellman's reagent reacts with free thiol to generate a colour change.

Sulfur is key in the formation of the secondary structures of proteins due to cysteine – cysteine (Cys-Cys) disulfide bonds. This complex structure of proteins can be investigated by a method called circular dichroism (CD). CD investigates the structural conformation of proteins by resolving the absorbance of left and right hand polarised light.^{50,51} CD effects are focused around the peptide bond, aromatic amino acid side groups and the disulfide bond, with the disulfide bond showing absorption centred around 260 nm.⁵⁰ A wealth of data can be collected from CD analysis of proteins, such as: secondary structure composition, tertiary structure fingerprint, conformational changes and the integrity of cofactor binding sites, the secondary structure composition is especially useful in identifying the overall formation of disulfide bonds.^{50,51}

A method which has been used is the use of mercury modified mediums such as: mercurial columns⁵² and modified polyacrylamide gel electrophoresis (Hg-PAGE)⁵³. PAGE is a suitable medium to modify with mercury because of its well-developed use in the separation and analysis of RNA as well as its simplicity to use and interpret when compared to other methods such as chromatography⁵². The separation of sulfur biomolecules by mercury is based upon the chemistry of these two elements. They are both 'soft' elements, meaning that they form strong covalent-like interactions when they interact⁵³. These interactions are strong enough to hinder the migration of sulfur containing biomolecules in Hg-PAGE⁵³. tRNA which has been complexed with mercury during PAGE can also show reduced migration; with tRNA strands with differing numbers of sulfur showing different migrations⁵². Biondi and Burke⁵³ discovered that the charge state of sulfur determined the degree of separation as well as the number of sulfurs found on the analysed molecules.⁵³



Figure 1.3: Image of tRNA retention by organomercury polyacrylamide gel electrophoresis, asterisk (*) bound sequences, spot (●) unbound sequences. Dashed line represents the organomercury layer. Adapted from reference 53.⁵³

The success of the method is reflective of the chemistry but there are drawbacks associated with this method, such as the health and safety implications associated with the use of mercury and the cost of mercury disposal.⁵⁴ As stated before, mercury is toxic to the human body and fatal with prolonged exposure, mercury toxicity can cause serious neurological and physical problems through inhalation, contact and ingestion.⁵⁵ Mercury is very good at separating sulfur containing molecules because of the soft-soft interactions. However other 'soft' acids also exist which present fewer problems; such as gold nanoparticles (AuNPs).⁵⁶ Gold nanoparticles are considerably safer than the use of mercury and can be just as easily incorporated into polyacrylamide gel.⁵⁷

Our method utilise gold nanoparticles as adjuncts in PAGE to examine sulfur containing biomolecules, building on the work of Biondi and Burke⁵³ but in place of a mercury containing modified gel layer we inserted a layer containing gold nanoparticles. The replacement of weakly bound ligands by sulfur is common practice with gold nanoparticles,⁵⁸ and therefore it is reasonable to expect that AuNPs will retain sulfur containing biomolecules. AuNPs have garnered a great deal of investigation, especially in biological applications such as therapeutics and drug delivery, due to the ease and range of surface modifications possible⁵⁹⁻⁶¹ They have not yet been discovered to cause undesirable health or environmental issues but work into the long term effects of AuNPs use in chemistry and medicine are being investigated.⁶¹⁻⁶³ In this work we discuss the process in which we developed our method as well as the successes and

failures we encountered. Chapters 2 and 3 discuss the creation, characterisation and use of the materials.

1.2 Design and Synthesis of Catalytic DNA Aptamers:

A catalyst is a substance which when added to a reaction will aid in the progression of the reaction but will not be used up in, or effect the equilibrium of, the reaction.⁶⁴ Catalysis is key in industrial chemistry and also plays very important roles in biology and medicine.^{64–66} There are two main types of catalyst in chemistry, homogeneous and heterogeneous. Homogeneous catalysts are in the same state as the reaction they are influencing, heterogeneous catalysts catalyse reactions in different phases to their own.^{67,68} Figure 1.3 shows the development of catalysis through history. There are positives and negatives with both type of catalyst, a few of these are detailed below. Heterogeneous catalysts can endure high temperatures but they have poorly defined active sites.^{69,70} Heterogeneous catalysts also have low selectivity but are cheaper and easier to recycle than homogeneous catalysts.^{64,69} Homogeneous catalysts in contrast: operate at low temperatures, have well defined active sites, well established reaction mechanisms, high selectivity and are easily modified.^{64,68,70}

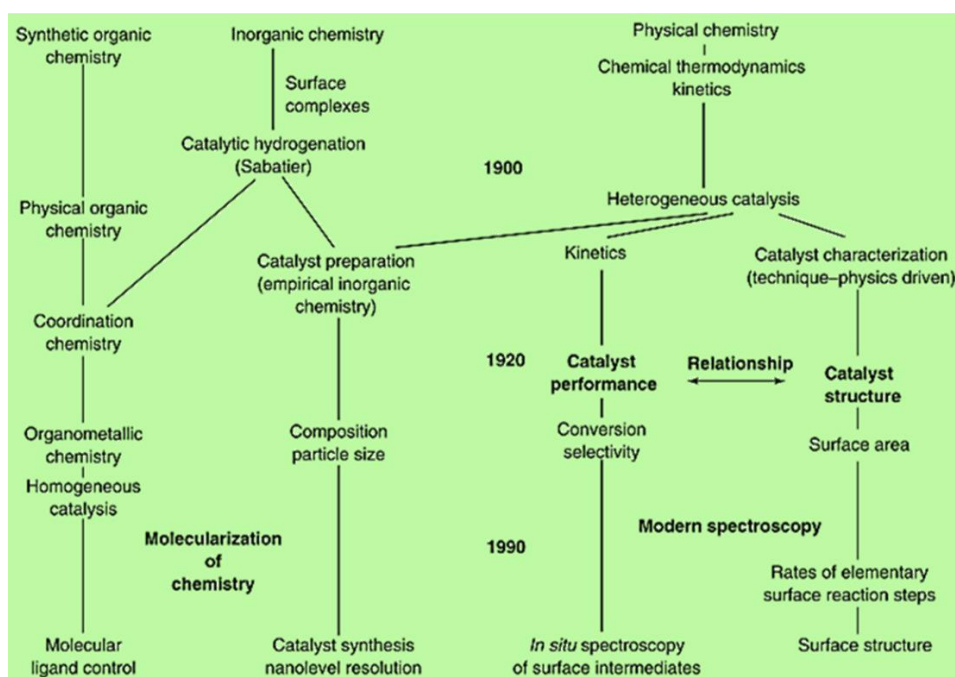


Figure 1.3: Catalyst development through history, adapted from reference 64 .⁶⁴

Biological reactions without the aid of catalysts would take years; protein enzymes, for the most part are responsible for catalysing almost all biological processes, with a few being catalysed by ribozymes.^{71,72} Proteins form complex folded structures which allows peptide side chains to form enzymatic active sites.⁷² Intermolecular forces within an enzyme active site facilitate ligand binding and catalysis by stabilising the transition state.^{6,73–75} These microenvironments are highly selective and they modulate the catalytic cycle of an enzyme by ensuring only compatible ligands and enzymes bind.⁷³ If RNA can be used naturally to catalyses biological reactions such as, RNA cleavage and ligation. Would artificial single stranded DNA, which has similar properties to RNA, be able to perform catalytic activities?^{72,76}

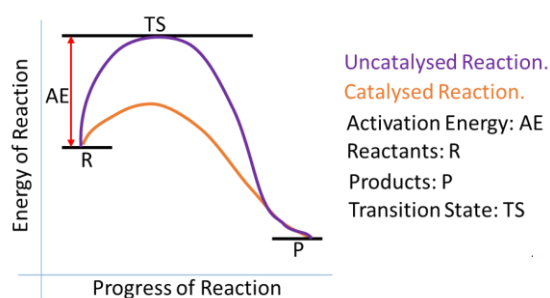


Figure 1.5: Representation of how catalysts lower the activation energy of a reaction, adapted from reference 71.⁷¹

A class of biological entity which relies on recognition are antibodies; antibodies raised to bind TS-mimics have been shown to catalyse reactions.⁷⁷ Catalytic antibodies can be spliced and manipulated to generate a wide range of site specific generalisation but they are expensive and inefficient.^{78,79}

DNA based catalysts open up a large area of application in both biology and chemistry, given that enzymes catalyse reactions by binding strongly to their transition states it would then follow that an enzyme would bind a molecule which closely represents this transition state. This in fact is often the basis of competitive inhibition.^{6,72,80} It would follow that if you could design and synthesise a DNA strand which mimics the binding site of a protein it would show similar catalytic activity to the protein.^{72,76,81} An advantage of DNA aptamers over enzymes is the design and selection process, the number of different sequences produced is directly related to the length

of variable regions of the aptamer (4ⁿ). Some specific examples of aptamer catalysis are: cancer therapeutics, synthetic photosynthesis for energy production and tagging of biological processes,⁸²⁻⁸⁵ these were not avenues available to chemists before their discovery.

The Hammond postulate states that transition states (TS) and temporary intermediates in a chemical reaction have structures which only require minimal rearrangement.⁸⁶⁻⁸⁸ The Hammond postulate theorises that the type of reaction dictates TS structure; endothermic reactions will have a TS which closely resemble the structure of the products, an exothermic reaction will have a TS which resemble the reactants.^{86,88} The Hammond postulate is not recommended for thermoneutral reactions (Fig 1.6).⁸⁶

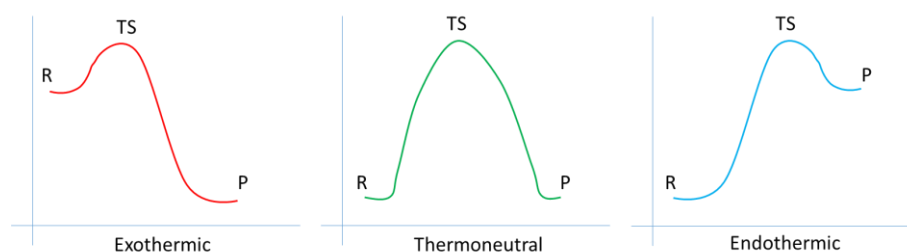


Figure 1.6: Representation of the Hammond postulate, adapted from reference 86.⁸⁶

The use of nucleic aptamers or nucleic antibodies are a more cost-effective method of producing highly selective catalytic materials.⁸⁹ The benefits of DNA aptamers over antibodies is not only limited to the ethical and monetary considerations; they are smaller and more flexible allowing them to bind small molecules and form a wider range of secondary structures.⁸⁹ Aptamers are not limited to only targeting immunological targets like antibodies but can also target: toxins, organs and ions to name a few. The time taken to produce antibodies is from six months whereas aptamers can be selected in hours (automated) or weeks (unautomated), they also are unlikely to experience contamination or batch variation unlike antibodies the structural basis for binding is more easily analysed.^{34,89}

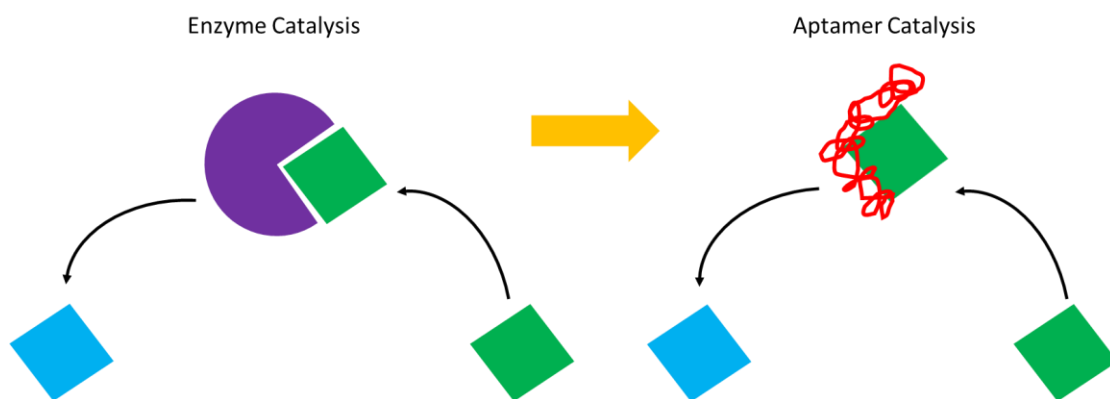


Figure 1.7: Representation of the breakdown of a target analyte by enzyme and aptamer catalysis.

We aim in this work to replicate a well-established biological mechanism, the catalytic breakdown of haemoglobin by pepsin, using aptamers.^{90,91} Pepsin is an acid protease which is inhibited by pepstatin a TS-mimic, our research aims at synthesising a DNA aptamer with selectivity for pepstatin. It follows given what we have discussed previously that this aptamer would then show similar catalytic activity to pepsin, for example in the breakdown of haemoglobin.⁹⁰ We developed an in vitro selection protocol based on literature from Li and Nutiu;⁹² due to time constraints we were unable to fully complete the work, chapter 4 discusses our method development and justification.

Chapter 2: Synthesis, Concentration and Characterisation of Gold Nanoparticles and Polyacrylamide Gels.

2.1 Introduction:

Nanoparticles are fine dispersions of materials often metallic but not always, generally with a size in the nanometre range.^{93,94} My research focuses on gold nanoparticles (AuNPs), these nanoparticles do not exist as small spheres of metal but require stabilising agents to prevent agglomeration.^{95,96} There are three methods for stabilising AuNPs; co-ordination with ligands, and coating by polymers and surfactants. Ligands and polymeric conjugation both aid in avoiding agglomeration by acting a physical barrier between the gold cores; surfactants act by creating an electrical double layer like effect causing repulsion by charge.^{59,63,94}

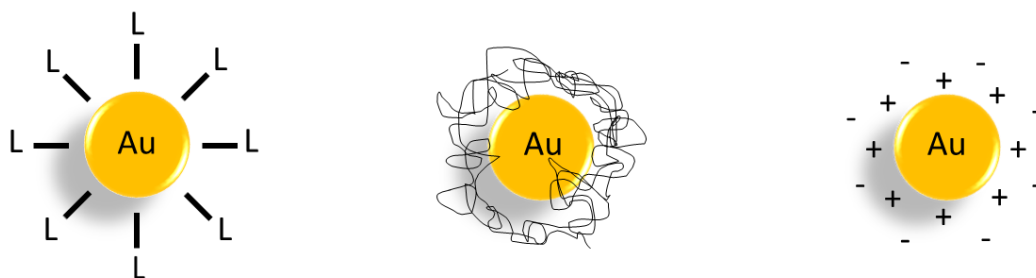


Figure 2.1: Gold nanoparticle stabilisation techniques; from left to right: ligand, polymeric, surfactant.

Some current uses of gold nanoparticles are in catalysis, therapeutics and nanomaterials.^{62,97} Although these areas are of interest to many, my research focuses on the interactions of gold with sulfur for application in biotechnology. According to hard soft acid base (HSAB) theory, nucleophiles and electrophiles are classified by their polarizability; 'soft' are relatively polarisable and hard are relatively unpolarisable.⁵⁶ HSAB theory also states that compounds with similar chemistry i.e. 'soft' and 'soft' or 'hard' and 'hard' compounds will preferentially interact with each other.⁵⁶ Gold and sulfur are both 'soft' according to HSAB theory meaning that they will form strong covalent like interactions.⁵⁶ This property of both gold and sulfur has been

utilised in AuNPs research, often related to the conjugation of thiolated ligands to the AuNPs surface.⁹⁶

2.2 Experimental:

2.2.1 Materials:

Hydrogen tetrachloroaurate, Aliquat[®] 336 and sodium borohydride, urea and EDTA were purchased from Acros. 4-Dimethylamino pyridine was purchased from Fluorochem. Toluene, boric acid and acrylamide / bisacrylamide 37.5:1 solution was purchased from Fisher Scientific. Ammonium persulfate, N, N, N', N'-tetramethylethylenediamine (TEMED) and cetyltrimethylammonium bromide were purchased from Sigma Aldrich. Sodium citrate was purchased from Fisons. Chemicals were used without further purification and to produce stock solutions.

2.3 Methods:

2.3.1 Gold Nanoparticle Synthesis:

2.3.1.1 Dimethylamino Pyridine Protected Gold Nanoparticle (DMAP AuNPs) Synthesis:

DMAP-protected AuNPs were synthesised from precursor AuNPs, which were prepared by the Brust two phase method⁹⁸ Aliquat 336 in Toluene (612 mg / 20 mL). An aqueous solution of hydrogen tetrachloroaurate (HAuCl_4) was prepared in deionised water (100 mg in 8 mL). The two solutions were transferred to a round bottom flask and stirred for one hour. Transferring the biphasic mixture to a separating funnel allowed a distinct separation between the clear yellow organic phase and the creamy inorganic phase. The organic phase was transferred to a clean round bottom flask and a magnetic stir bar added. A fresh solution of sodium borohydride was prepared (109 mg in 6 mL) in deionised water the sodium borohydride was added drop-wise to the stirring gold solution. A colour change was observed as the borohydride was added, yellow, to orange and to red. This was due to the reduction of Au^{III} to Au^0 . After two hours of stirring the solution was transferred to a separating funnel and the phases left to separate. The inorganic layer was removed and the organic layer was washed three times with 25 mL deionised water. A solution of 4-dimethylamino pyridine (DMAP) was prepared in deionised water (610

mg in 50 mL), the solution was then added to the separating funnel. The DMAP solution causes the nanoparticles to move into aqueous phase by ligand substitution.

The DMAP-protected nanoparticles (DMAP AuNPs) were stored in 50 mL falcon tubes at 4 °C. The DMAP AuNPs were at an approximate concentration of 2 mg Au / mL. The nanoparticles were stable for a minimum of two months. Characterisation of the nanoparticles was carried out by UV-Vis, DLS and TEM. The diluted samples for DLS and UV-Vis were prepared by diluting 40 µL of DMAP AuNPs in 2 mL deionised water.

2.3.1.2 Sodium Citrate Protected Gold Nanoparticle (Citrate AuNPs) Synthesis:

Citrate-protected nanoparticles were synthesised by the Frens-Turkevich method.² A solution of HAuCl₄ was prepared in deionised water (25 mg in 50 mL). The solution was heated, while stirring and brought to a vigorous boil. A solution of sodium citrate was prepared in deionised water (25 mg in 2 mL). Once boiling the citrate solution was added and an immediate colour change from yellow to dark purple occurred.

The citrate-protected nanoparticles were stored at 4 °C for up to two months. The approximate concentration of citrate AuNPs was 0.5 mg Au / mL. The nanoparticles were characterised by DLS and UV-Vis. The solutions for DLS and UV-Vis were prepared by diluting 160 µL citrate AuNPs in 2 mL deionised water.

2.3.1.3 Cetyltrimethyl-ammonium Bromide Protected Gold Nanoparticle (CTAB AuNPs) Synthesis:

CTAB AuNPs were synthesised by using an adapted version of the Brust method. A solution of HAuCl₄ was prepared in deionised water (200 mg in 16 mL). This solution was placed into a round bottom flask containing a magnetic stir bar. To this a solution of CTAB in deionised water (1.224 g in 40 mL) was added and the solution left to stir for one hour, a solution of sodium borohydride in deionised water (210 mg in 12 mL) was added drop-wise to the stirring solution. A colour change from orange, to brown, to dark red occurred and the solution left to stir for a minimum of twenty hours. The resulting solution was dark purple.

The CTAB-protected nanoparticles were collected into 50 mL falcon tubes, labelled and stored at 4 °C for at least six weeks. The approximate concentration of CTAB AuNPs was 3.33 mg Au / mL. The CTAB AuNPs were then characterised by DLS and UV-Vis. The solutions used for DLS and UV-Vis were made by diluting 40 µL of CTAB AuNPs in 20 mL deionised water.

2.3.2 Gold Nanoparticle Concentration:

2.3.2.1 DMAP AuNPs Concentration:

DMAP AuNPs (≈ 2 mg Au / mL) were concentrated by precipitation using ethanol (EtOH). 30 mL of DMAP AuNPs volume was reduced by two thirds by rotary evaporation at 70 °C. The solution was split into 500 µL aliquots in 1.5 mL centrifuge tubes; to each 1 mL of 100 % EtOH was added. The tubes were inverted and centrifuged at 21100 x g for 40 minutes. A clear ruby coloured supernatant and a dark red pellet were formed. The supernatant was removed and the pellets collected and re-suspended in 1 ml deionised water (≈ 60 mg Au / mL).

2.3.2.2 Citrate AuNPs Concentration:

Citrate AuNPs (≈ 0.5 mg Au / mL) were concentrated by centrifugation. 120 mL of citrate AuNPs were split into 1.5 mL aliquots. The aliquots were centrifuged at 9.8 ms^{-2} (gravity) for 10 minutes. A clear colourless supernatant and purple pellet was produced, the supernatant was discarded and the pellets collected and re-suspended in 1 mL deionised water (≈ 60 mg Au / mL).

2.3.2.3 CTAB AuNPs Concentration:

CTAB AuNPs (≈ 3.33 mg Au / mL) were concentrated by a similar method to the DMAP AuNPs. The solvent volume was reduced by one quarter, the nanoparticles were split into 500 µL aliquots and 750 µL of 100 % EtOH was added. The centrifuge tubes were inverted and centrifuged at 9.8 ms^{-2} for 3 minutes. The resultant supernatant was colourless and the pellet black in colour, the supernatant was discarded and the pellets collected and re-suspended in 1 mL deionised water (≈ 50 mg Au / mL).

2.3.3 Characterisation of Gold Nanoparticles:

2.3.3.1 Dynamic Light Scattering (DLS):

Dilute solutions of the AuNPs were analysed by DLS, the operating procedure was developed from pre-determined parameters as defined by the manufacture. DLS analysis was carried out on a Malvern Zetasizer Nano ZS. The sample was equilibrated to 25 °C before 14 consecutive scans of the sample were taken.

2.3.3.2 Ultra-violet Visible (UV-Vis) Spectroscopy:

UV-Vis Spectroscopy was used as an additional method for characterising the size of AuNPs. The parameters of the scan were set to scan between 400-600 nm. 2 mL of the diluted AuNPs sample was deposited into a clean cuvette and placed into the spectrometer. The sample was scanned and a graph with a single peak was produced. The data values were collected and used to calculate the AuNPs diameter using literature.⁹⁹ A ratio between the peak value and the value at 450 nm was used to give the diameter of the AuNPs.⁹⁹ UV-Vis data was collected on a Shimadzu UV-1800 spectrometer and reported in nM. This method was used analyse all samples.

2.3.3.3 Transmission Electron Microscopy (TEM):

3 µL of DMAP AuNPs was deposited onto the surface of a carbon copper grid. The grid was left to dry under the direct heat of a lamp. Images of the nanoparticles were taken by Ian Brown (Biosciences) on a Jeol 1230, operating at an accelerating voltage of 80 kV and the images were recorded with a Gatan Multiscan 790 digital camera. Seventeen images were obtained of DMAP AuNPs. These images were analysed using Fiji Image J software¹⁰⁰. The analysis parameters were: size nm² (5-100), circularity (0.50-1.00), show outlines, display results and exclude edges. The data collected was used to back calculate, the diameter of each particle from its area.

2.4 Characterisation of Polyacrylamide Gels:

2.4.1 Rheology:

Five concentrations of polyacrylamide gel were investigated; 5, 10, 12, 15, and 20 %, without and without DMAP AuNPs. 10 mL solutions of each concentration were prepared from a 20 % polyacrylamide stock solution and diluted to the required concentration with TBE buffer. The gels were polymerised in between glass plates with 1.5 mm spacers to ensure even thickness of the polyacrylamide samples. The samples were wrapped in cling film and stored in the fridge to prevent drying.

Experimental parameters:

Two tests were carried out: an amplitude sweep to establish the linear viscoelastic range (LVER) and a frequency sweep within the established LVER to investigate the gel properties of each sample.

Table 2.1: Table listing rheological experiment data for amplitude and frequency sweeps.

-	Amplitude Sweep	Frequency Sweep
Rheometer Set Strain. (Pa)	3	5
Frequency Range. (Hz)	0.01-100	0.1 - 15
Plate Temperature. (°C)	25	25
Wait Time. (mins)	5	5
Experiment Time. (mins)	5	5
Relaxation Time. (mins)	5	5
Number of Repeats.	3	3

2.4.2 Optical Coherence Tomography (OCT):

OCT was used to visualise gold nanoparticles in two types of polyacrylamide gel (TBE / tris-HCl), in order to investigate the dispersion of gold within the gel matrix. Figure 2.2 shows a representation of the OCT set-up.

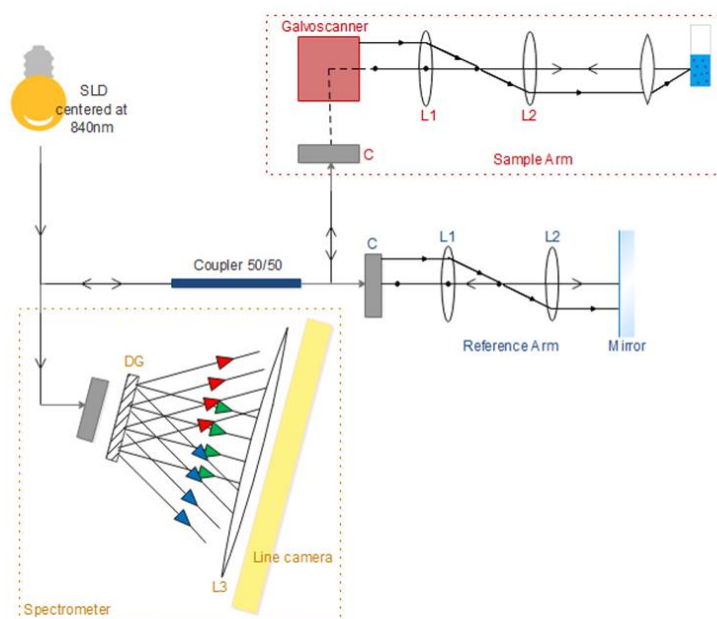


Figure 2.2: SB-OCT set-up. L, lens, DG, diffraction grating.

The samples were interrogated in a 10 x 10 x 30 mm quartz cuvette at a penetration depth of 2 mm and with a resolution of 14 μm in the axial and 12 μm in the lateral directions. Images were obtained of: dilute and concentrated DMAP protected gold nanoparticles; and a 12 % polyacrylamide gel, made with TBE buffer, with and without DMAP AuNPs, as well as the interface between the two. These images were also obtained for a 10-15 % gradient polyacrylamide gel made with tris-HCl buffer, as used in the protein testing portion of this research. The gels were prepared as follows:

TBE polyacrylamide gels were prepared from a 20 % denaturing polyacrylamide stock solution which was diluted with TBE buffer to the required concentrations (12 %). Tris-HCl gels were prepared from a 30 % polyacrylamide stock solution and diluted with 1.5 M tris buffer (10 – 15 %) for the resolving gels and 0.375 M tris buffer (10 % + AuNPs) for the gold gel.

1.5 mL of the non-AuNPs containing gel was deposited into a clean polished cuvette, after being activated by the TEMED and APS. The gel was left to polymerise before 1.5 mL of the AuNPs containing gel was deposited onto the surface and left to polymerise. Once the gels had fully polymerised the cuvette was attached to a stand and placed in front of the sample beam. The top and bottom layers were imaged separately before the interface was also visualised. A 3D

image or volume was then obtained of the interface. This method was repeated for both gel types and a volume was also taken of the TBE AuNPs gel. Images were obtained by the same method for the as synthesised DMAP AuNPs and the concentrated DMAP AuNPs. A clean cuvette was filled (3 mL) with un-concentrated DMAP AuNPs, and the sample was scanned and an image obtained. This was repeated for the concentrated DMAP AuNPs sample.

2.4.3 Scanning Electron Microscopy (SEM):

1 cm by 1.5 mm by 1 cm (L x W x B), polyacrylamide gel samples were deposited onto carbon sticky tabs and analysed by SEM. SEM images were obtained on a Hitachi 54000 in backscatter mode (BSE). With a variable pressure of 50 vp and with an electron beam energy of 20 keV. The images were taken and analysed using Aztec software provided by Oxford instruments. 12 % polyacrylamide gel was prepared from a 20 % polyacrylamide gel stock solution by dilution with TBE buffer. Another 12 % polyacrylamide gel was prepared with the addition of 500 μ L of concentrated DMAP AuNPs. 10 % 8 mM ATP polyacrylamide was prepared from a 30 % polyacrylamide stock solution with 8 mM tris-HCl buffer and 500 μ L of DMAP AuNPs. A 10 % polyacrylamide tris-HCl gel was also prepared from a 30 % acrylamide stock solution and diluted with tris-HCl buffer and 500 μ L DMAP AuNPs.

2.5 Results and Discussion:

Three types of gold nanoparticles were synthesised, which when added to polyacrylamide gel as adjuncts, underwent electrophoresis with phosphorothioated DNA. This was to investigate the ability of the gold nanoparticles to interact with the modified DNA due to 'soft' gold-sulfur interactions, it was predicted that strong interactions would hinder or halt the migration of the DNA through the polyacrylamide gel. This will be discussed in detail in chapter 3.

2.5.1 AuNPs Characterisation:

2.5.1.1 DLS and UV-Vis:

DLS and UV-Vis were used to evaluate the diameters of the synthesised gold nanoparticles. DLS is a characterisation method, used to analyse the size distribution of particles such as proteins, nanoparticles and small polymers. UV-Vis gives data about the absorbance of energy at different

wavelengths of light. Using a method developed by Haiss,¹⁰¹ we can calculate the diameter of gold nanoparticles in solution based on the surface plasmon resonance peak (SPR) and absorption at 450 nm. All of the nanoparticles investigated gave absorption graphs of the following shape (Figure 2.3).

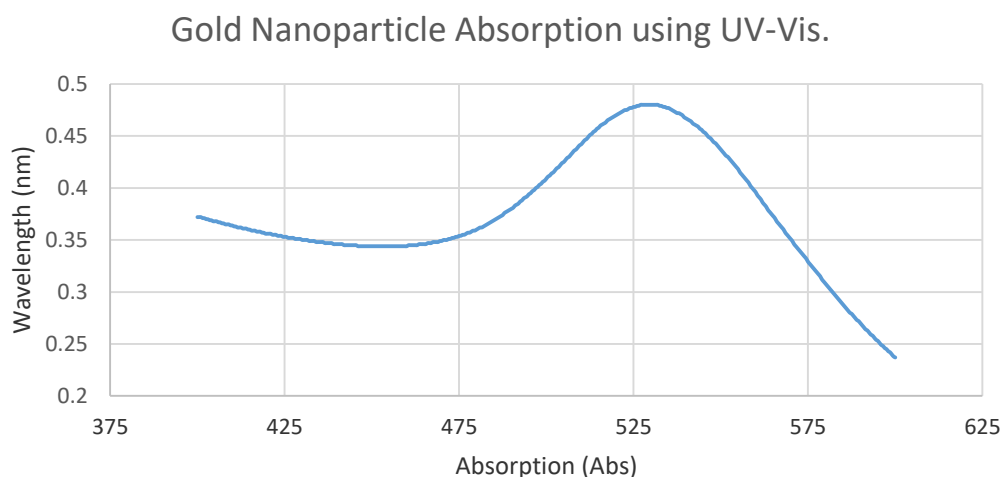


Figure 2.3: Graph showing absorption of light against wavelength for UV Visible Spectroscopy for gold nanoparticles in deionised water with a calculated diameter of 8 nm.¹⁰²

The peak absorption is representative of the surface plasmon resonance (SPR) band emitted by the AuNPs, this changes between nanoparticles depending on their size.

Table 2.2: Table showing dynamic light scattering and UV-Visible results for, 4-dimethylamino pyridine, citrate and cetyltrimethylammonium bromide protected gold nanoparticles in deionised water.

<i>Batch</i>	<i>DMAP AuNPs Diameter DLS (nm)</i>	<i>DMAP AuNPs Diameter UV-Vis (nm)</i>	<i>Citrate AuNPs Diameter DLS (nm)</i>	<i>Citrate AuNPs Diameter UV-Vis (nm)</i>	<i>CTAB AuNPs Diameter DLS (nm)</i>	<i>CTAB AuNPs Diameter UV-Vis (nm)</i>
<i>A</i>	15.62	8	50.75	10	2.33	20
<i>B</i>	24.36	8.5	4.19	10	2.32	25
<i>C</i>	68.06	8.5	4.18	10	-	-
<i>D</i>	37.84	7	4.19	25	-	-
<i>E</i>	615.1	10	-	-	-	-
<i>F</i>	8.72	25	-	-	-	-
<i>G</i>	4.19	25	-	-	-	-
<i>H</i>	4.18	25	-	-	-	-
<i>I</i>	28.21	25	-	-	-	-

The expected diameters from literature for DMAP, citrate and CTAB are expected to be: 8 nm, 10 nm and 8 nm respectively.^{98,103} As seen in table 2.2, there is little correlation between the results obtained for the diameters of the AuNPs between DLS and UV-Vis. The DLS results for

CTAB and citrate protected nanoparticles show relatively similar results. The result for citrate A DLS is due to an error during synthesis resulting in larger nanoparticles. The inconsistency in the DLS results for the DMAP AuNPs may be attributed to the fact that DLS measures the hydrodynamic radius of particles in solution;¹⁰⁴ also given that DMAP AuNPs prefer to form clusters,¹⁰⁵ it is possible that the DLS is measuring the hydrodynamic radius of these clusters resulting in larger diameters than expected from literature.¹⁰⁵⁻¹⁰⁷ The DLS results for the CTAB AuNPs are much smaller than expected, this may be because CTAB AuNPs tend to form rod-like nanoparticles not spheres, due to the long carbon chain tail on the CTAB ligand. DLS only works for spherical analytes or analytes which form spherical hydration spheres, which a rod-like structure would not.^{104,108} The UV-Vis method gave results which were consistent between small volume synthesis and large volume synthesis but not between the two, this may be due to residues being present in the solution left over from synthesis. However this may be attributed that the method we used to calculate the diameter of the nanoparticles was developed from citrate AuNPs, it is possible that this method is not compatible with other types of nanoparticle. The difference between nanoparticle types is to be expected, this is because the ligands are different as well as the concentration of gold used to synthesise the AuNPs, larger ligand to gold ratio will result in smaller nanoparticles and vice versa. TEM was used as an orthogonal method to validate the findings either by DLS or UV-Vis.

2.5.1.2 Transmission Electron Microscopy:

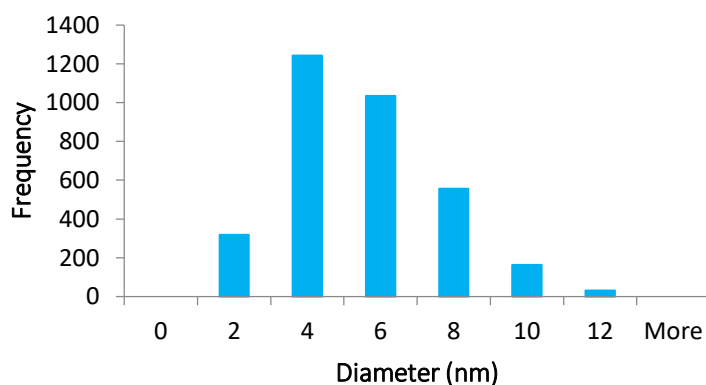


Figure 2.4: Histogram showing the distribution of DMAP capped AuNPs (n = 3347).

The majority of particles fall in the 4 – 8 nm range with a standard deviation of 2.099 nm and a mean of 4.445 nm (Figure 2.4), this is within keeping with the literature and UV-Vis but contrary to DLS. The majority of particles examined exhibit spherical morphology. The DMAP-protected AuNPs appear to form closely packed clusters, with larger particles at the centre of groupings and smaller particles surrounding these (Figure 2.5).

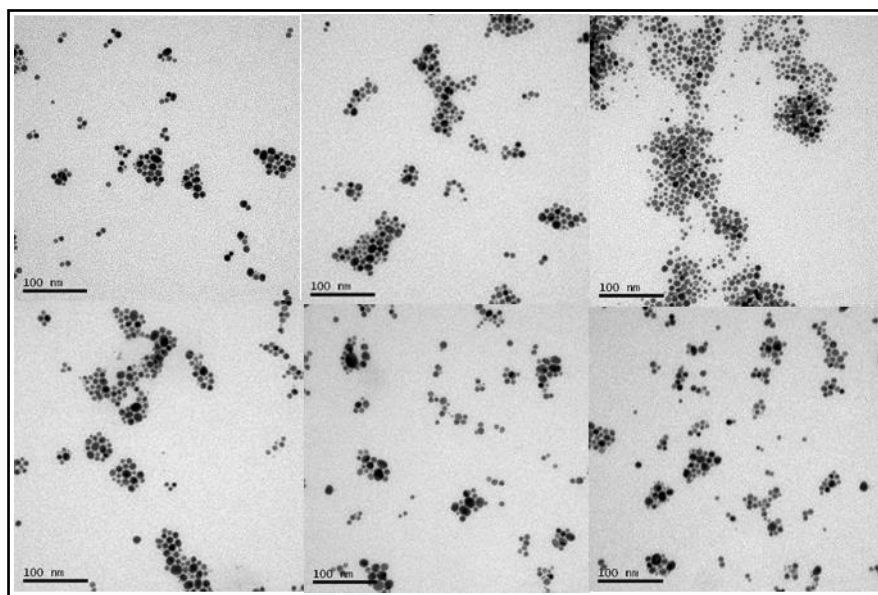


Figure 2.5: Transmission Electron Microscopy images showing 4-dimethylamino pyridine capped gold nanoparticles. The scale bar represents 100 nm.

2.6 Characterisation of Polyacrylamide Gels:

The motivation for investigating DMAP AuNPs in PA gel was so that we could evaluate the way in which AuNPs position themselves during gelation. This is because there is a noticeable difference in setting time between AuNP and non-AuNP containing gels of the same concentration. We wanted to investigate whether the nanoparticles appear homogenous throughout the PA gel or whether they are interacting with the matrix, instead of being independent adjuncts within the matrix as first theorised. This would be represented by regions of high a low intensity suggesting clustered nanoparticles.

2.6.1 Rheology:

The first investigation of the samples was an amplitude sweep, which was used to establish the linear viscoelastic range (LVER) for each sample; this allows us to set the parameters for the frequency experiment, as these can only be carried out in the LVER. The amplitude sweep is an

investigation of sheer strain as a function of the storage modulus (G') and its exponential function the loss modulus (G'')¹⁰⁹. G' denotes how viscous a gel is and G'' denotes the elasticity of the gel.

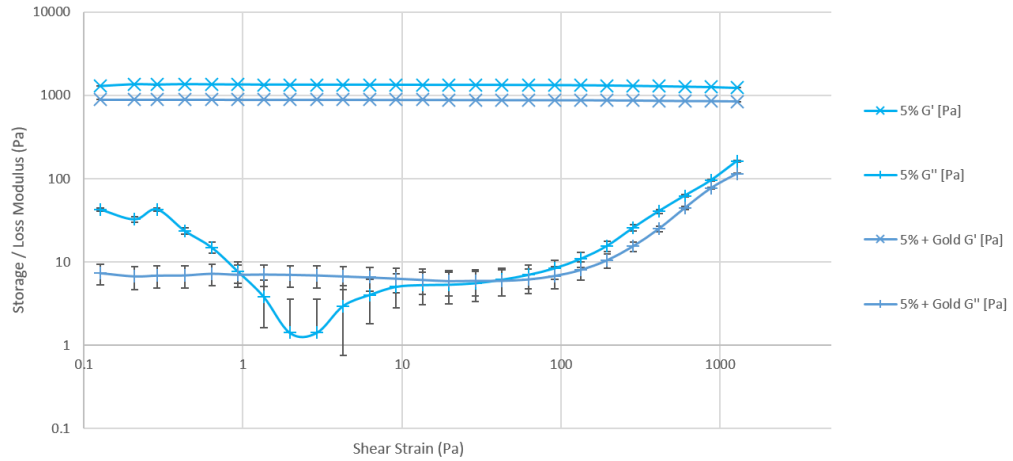


Figure 2.6: Comparison of average amplitude sweep data for 5% polyacrylamide with and without gold. Error bars represent the Log spread of data.

As can be seen from Figure 2.6 there appears to be a small amount of difference between the storage moduli for the gel with and without gold. Adding gold to the 5% polyacrylamide gel does stabilise the LVER.

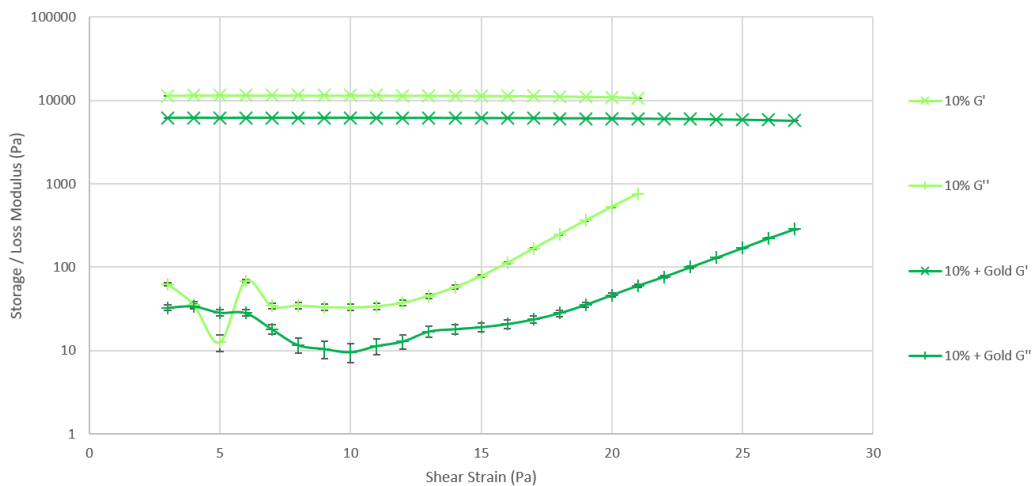


Figure 2.7: Comparison of average amplitude sweep data for 10% polyacrylamide with and without gold. Error bars represent the Log spread of data.

The 10% polyacrylamide with gold has a lower loss modulus than the 10% gel without gold at shear strains above 5 Pa as can be seen in Figure 2.7. The storage modulus for the 10% polyacrylamide gel with gold is also lower than that of the without gold gel. This would suggest

that the DMAP AuNPs are reducing the elasticity and viscosity of the 10 % polyacrylamide gel.

See Figure 2.7.

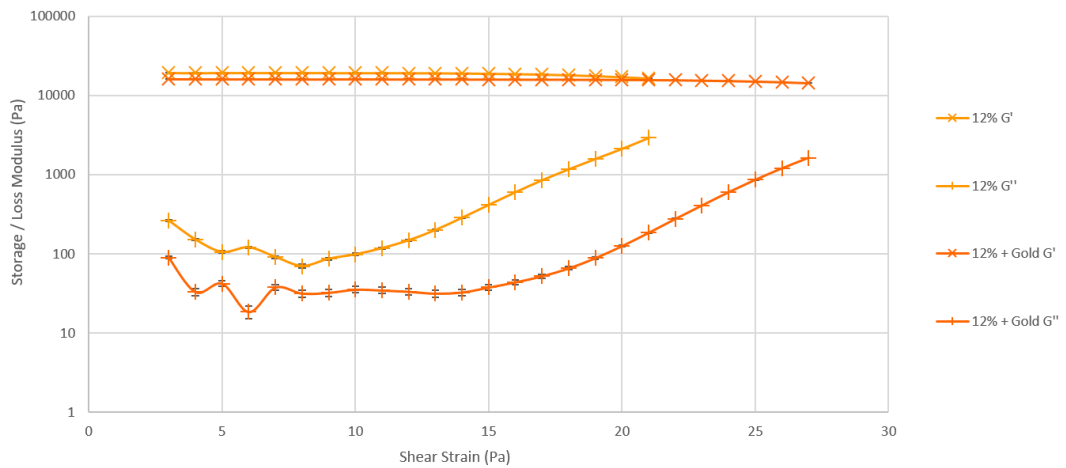


Figure 2.8: Comparison of average amplitude sweep data for 12 % polyacrylamide with and without gold. Error bars represent the Log spread of data.

The storage moduli for the 12 % with and without gold show less differentiation than that of the 10 % polyacrylamide gels. The loss moduli however, do show a significant difference between the two gels as can be seen from Figure 2.8. 12 % polyacrylamide gel with gold has a stabilised LVER when compared with the without gold gel.

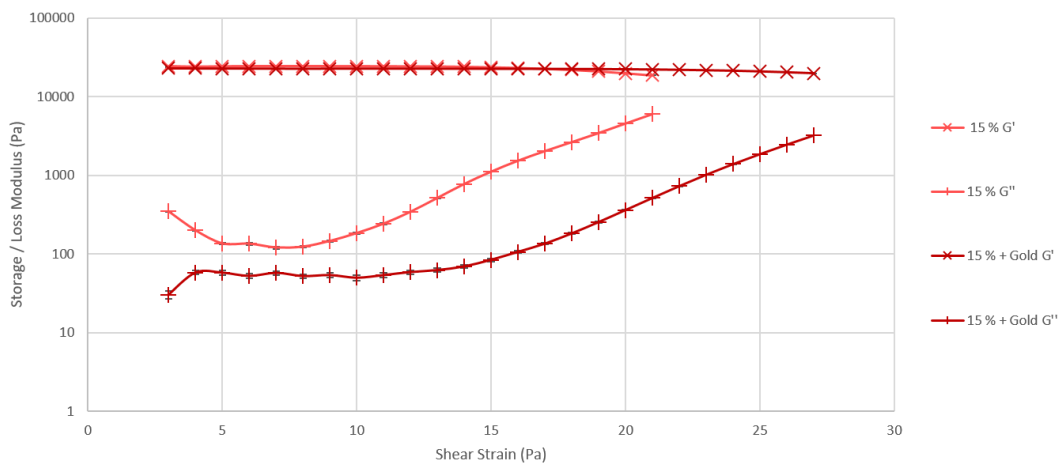


Figure 2.9: Comparison of average amplitude sweep data for 15 % polyacrylamide with and without gold. Error bars represent the Log spread of data.

From Figure 2.9 we can see there is no statistical difference in the storage moduli between 15 % polyacrylamide gel with and without gold, however there is a noticeable lowering of the loss modulus for 15 % polyacrylamide with gold as well as an extension of the LVER.

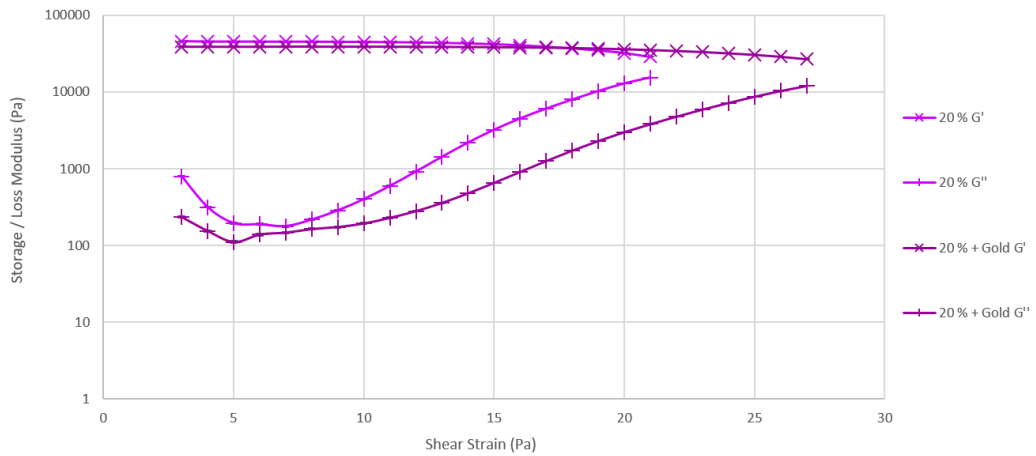


Figure 2.10: Comparison of average amplitude sweep data for 20 % polyacrylamide with and without gold. Error bars represent the Log spread of data.

As can be seen from Figure 2.10 there is only a very small difference between the storage moduli for 20 % polyacrylamide gel with and without gold. The loss moduli however do differ between the two after a shear strain of approximately 7.5 Pa, suggesting that the gold is effecting the elasticity of the gel especially at higher strains. Although the amplitude sweep data, does show some initial differences between polyacrylamide gels which contain gold nanoparticles and those that do not, these experiments were only conducted to obtain the LVER values to set the parameters for the frequency sweep.

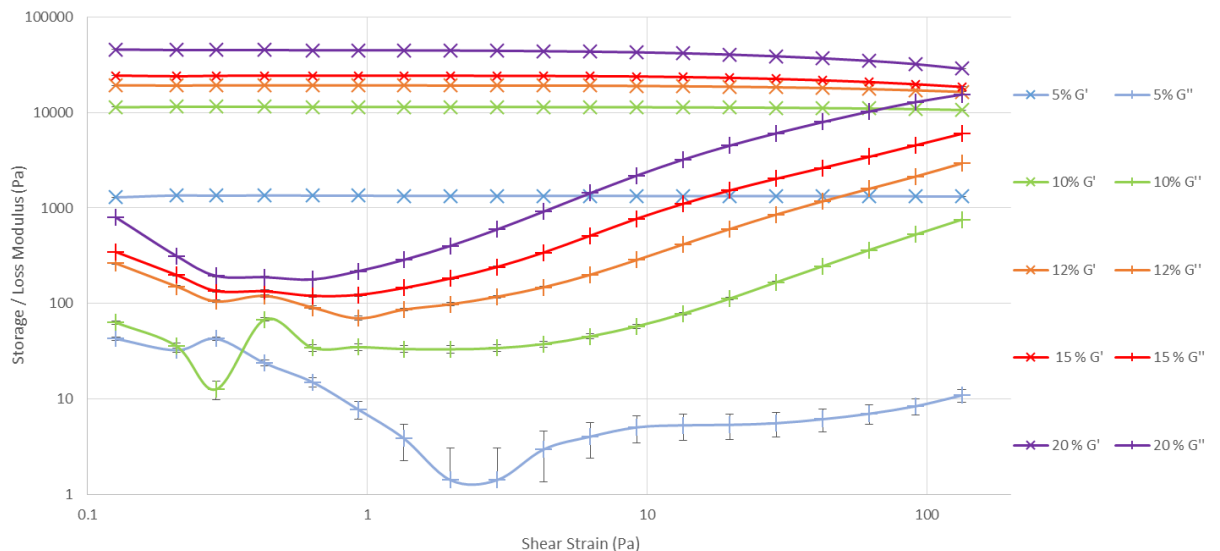


Figure 2.11: Averaged amplitude sweep rheology data for polyacrylamide gel without gold, for percentages; 5, 10, 12, 15 and 20%. Error bars depict the Log spread of data.

Figure 2.11 depicts the averaged amplitude sweep data for the polyacrylamide gels without gold, the LVERs were chosen by picking a point in the centre of the most linear range of the data. The

LVERs were; 5 % - 3 Pa, 10 % - 0.2 Pa, 12 % - 0.1 Pa, 15 % - 0.1 Pa and 20 % - 0.04 Pa. These strain values were used to set the parameters for the frequency sweep experiments. From Figure 2.11 it can be interpreted that lower percentage polyacrylamide gels have a smaller LVER compared to higher percentage gels. As well as being more stable at high strains than higher percentage gels.

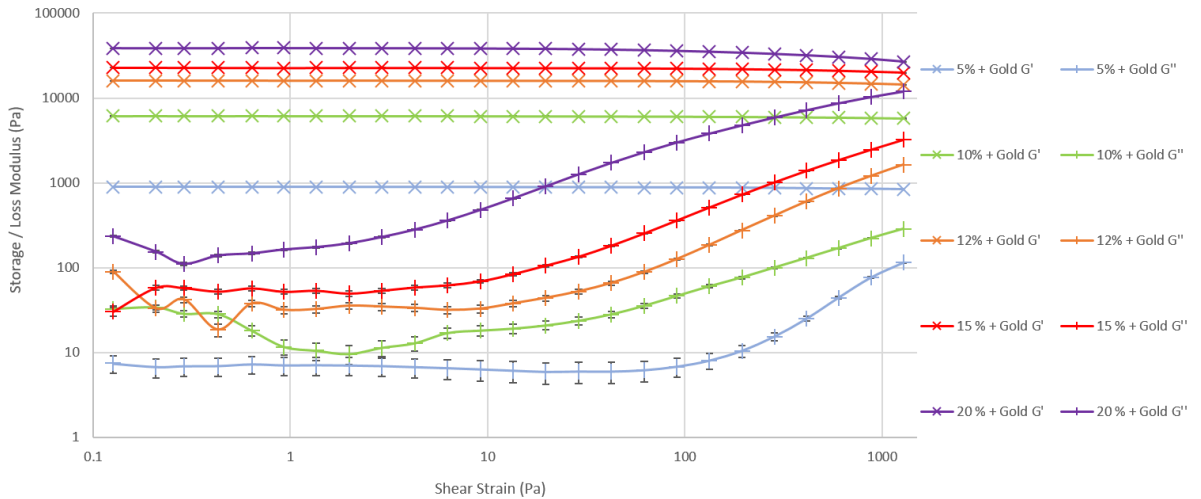


Figure 2.12: Average amplitude sweep rheology data for polyacrylamide gel with gold, for percentages; 5, 10, 12, 15 and 20 %. Error bars depict the Log spread of data.

Figure 2.12 depicts the averaged amplitude sweep for polyacrylamide gels with gold. The LVERs for the gold gels were: 5 % - 3 Pa, 10 % - 0.2 Pa, 12 % - 0.06 Pa, 15 % - 0.03 Pa and 20 % - 0.03 Pa. These strain values were used to set the parameters for the gold gels frequency sweep experiments. As can be seen from Figure 2.12 adding gold to the polyacrylamide gel extends the range of the LVER. Adding gold to the gel also lowers the loss modulus of the gels, suggesting there is a loss in elasticity when compared to the gels without gold (see Figure 2.11). There is a slight drop in the storage modulus, suggesting that gold also reduces the viscosity of the material.

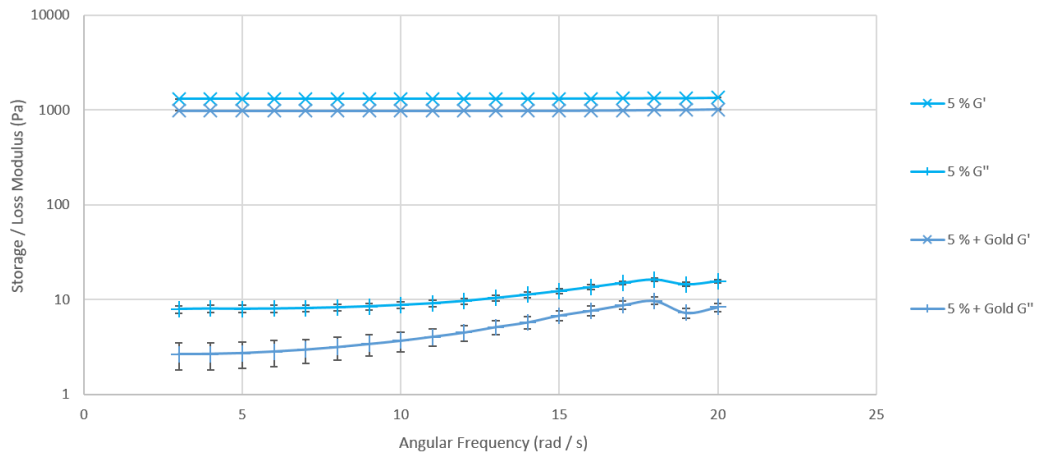


Figure 2.12: Comparison of average frequency sweep data for 5 % polyacrylamide with and without gold. Error bars represent the Log spread of data.

5 % polyacrylamide gel with gold has a lower elasticity than the 5 % polyacrylamide gel without gold and this is reflected in Figure 2.12. There is also less consistency in the data for the gold gel as can be seen from the error bars on Figure 2.12. This suggests that the gel is not fully relaxing between repeats of the experiment, this may be related to the reduced elasticity of the gel caused by the AuNPs. There is a noticeable reduction in the viscosity of the 5 % polyacrylamide gel due to the addition of gold.

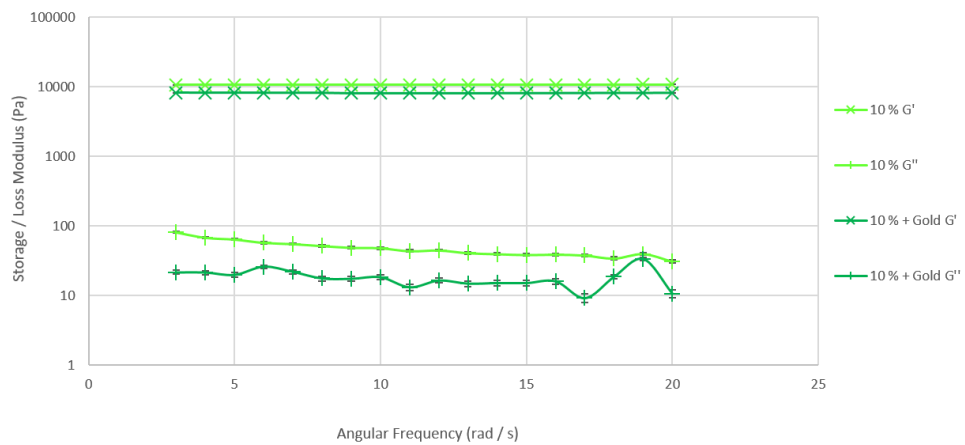


Figure 2.13: Comparison of average frequency sweep data for 10 % polyacrylamide with and without gold. Error bars represent the Log spread of data.

The addition of gold has destabilised the frequency sweep data for 10 % polyacrylamide gel, which can be seen from the less linear appearance of the data in Figure 2.13. This is in contrast to the stabilisation of the LVER by gold as seen in Figure 2.7. However in contrast the 5 %

polyacrylamide gold gel the error bars are much smaller suggesting that the 10 % polyacrylamide gel recovers between experiments more readily.

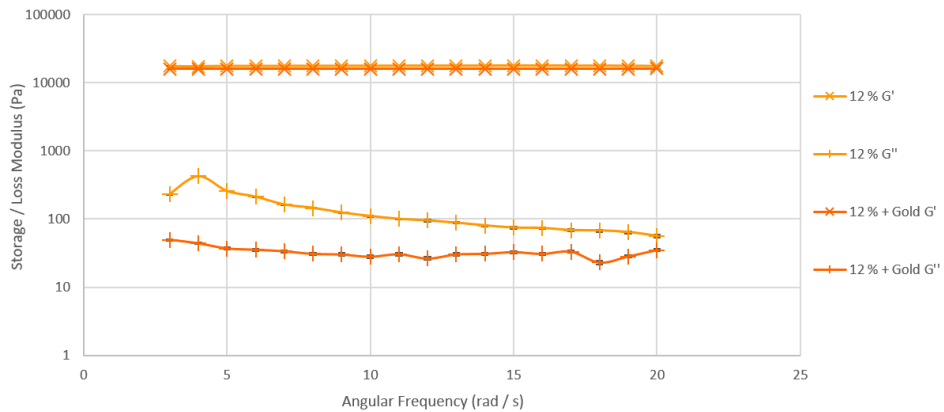


Figure 2.14: Comparison of average frequency sweep data for 12 % polyacrylamide with and without gold. Error bars represent the Log spread of data.

For 12 % polyacrylamide with gold the frequency sweep data is more linear than that of the non-gold gel, however there is still a reduction in the elasticity of the gold. This does not appear to effect the ability of the gel to recover between experiments. There is also little change between the storage moduli for the 12 % gels. See Figure 2.14.

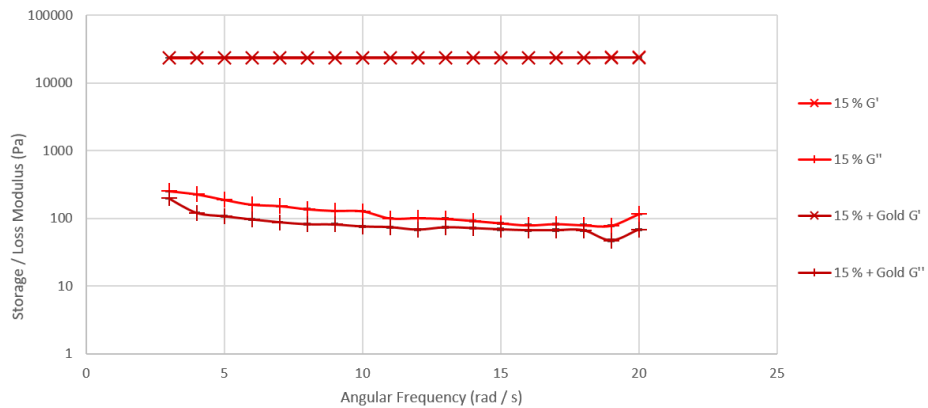


Figure 2.15: Comparison of average frequency sweep data for 15 % polyacrylamide with and without gold. Error bars represent the Log spread of data.

The 15 % polyacrylamide gels show similar frequency data trends. There is less change in the loss moduli for the 15 % polyacrylamide gels in comparison to lower percentage gels. The storage moduli for the 15 % polyacrylamide gels show no differentiation between gold and non-gold gels (Figure 2.15). This may be attributed to the increase in the crosslinking of the polymer associated with higher percentage polyacrylamide gels.

Master of Science by Research

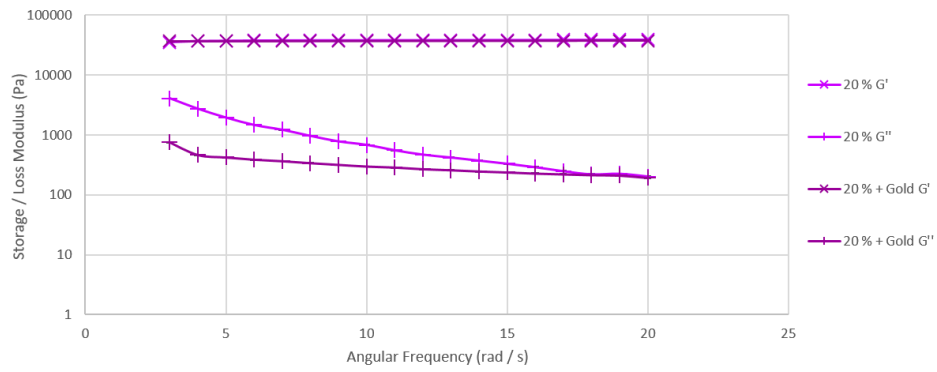


Figure 2.16: Comparison of average frequency sweep data for 20 % polyacrylamide with and without gold. Error bars represent the Log spread of data.

There is a visible difference between the loss moduli for the 20 % polyacrylamide gels up until an angular frequency of 15 rads^{-1} , at which the gold and non-gold gels begin to show similar elastic properties (Figure 2.16). Again likely due to the higher percentage of the polyacrylamide gels there is no distinguishable difference between the storage moduli of the two gels.

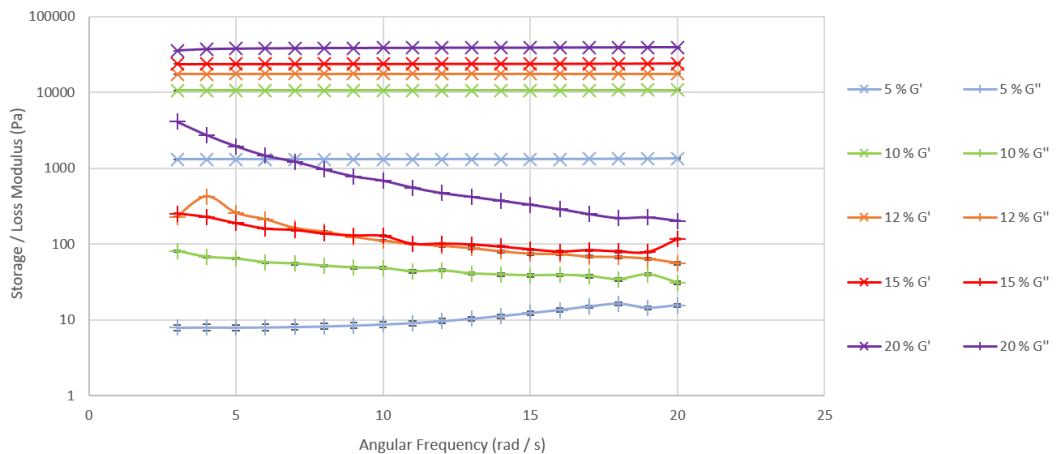


Figure 2.17: Averaged frequency sweep rheology data for polyacrylamide gel without gold, for percentages; 5, 10, 12, 15 and 20%. Error bars depict the Log spread of data.

From Figure 2.17 we can see that there is a discernible difference between the different concentrations of polyacrylamide in both the storage and loss moduli, accepting the 12 % and 15 % gels. This is related to crosslinking of the polyacrylamide matrix, as polyacrylamide concentration increase so does crosslinking. The 12 % and 15 % shows very little difference in frequency results suggesting while undergoing these experiments they have very similar properties (Figure 2.17).

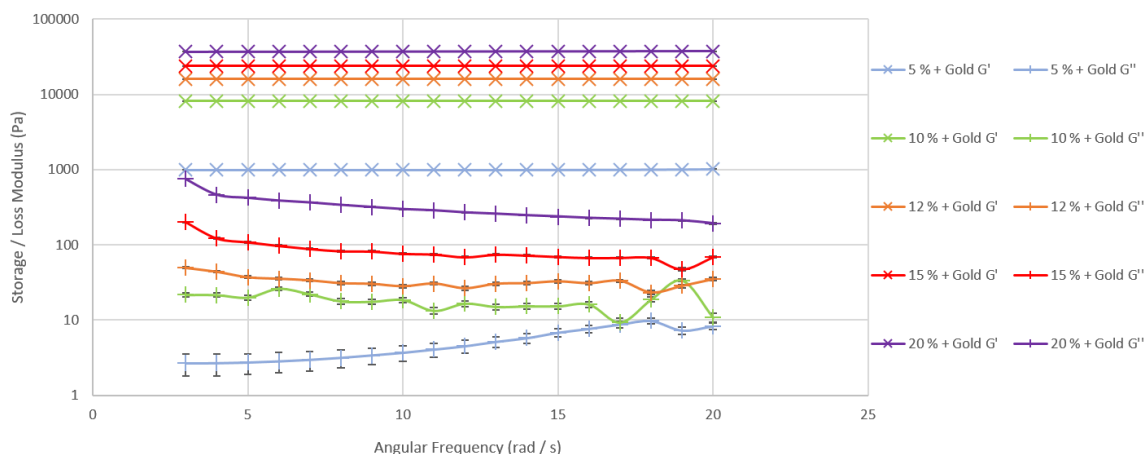


Figure 2.18: Averaged frequency sweep rheology data for polyacrylamide gel with gold, for percentages; 5, 10, 12, 15 and 20 %. Error bars depict the Log spread of data.

The frequency sweep data for the gold containing gels, shows little change in the storage moduli when compared to the non-gold containing gels (see Figures 2.17 and 2.18), this would suggest that the gold is not effecting the viscosity of the gels during frequency studies. On the other hand the loss moduli for the gold containing gels exhibit lower elasticities than the non-gold containing gels. See Figures 2.17 and 2.18. The most noticeable change between the gold and non-gold gels are between the polyacrylamide concentrations 12 % and 15 %. Having shown near identical data in Figure 2.17 the addition of gold has dramatically changed the properties of the 12 % polyacrylamide gel as can be seen in Figure 2.18 there is now a statistical difference between the two. The error bars on lower concentrations of polyacrylamide with gold seem to show a lesser ability to recover between experimental repeats however this is not the case for these percentages without gold, suggesting that the AuNPs are interfering with the properties of the gel on a molecular scale. Importantly this is not to say that these slight differences in the elasticity and viscosity prevent the gels from fulfilling their purpose; in fact it would appear they aid in stabilising the gel properties, resulting in a more linear trend in the data.

2.6.2 Optical Coherence Tomography:

Optical coherence tomography (OCT) is a non-invasive imaging technique typically used in the analysis and investigation of biological surfaces such as embryos and retinas. Traditionally the resolution of OCT is in the micrometre range, however due to the high scattering of colloidal gold, gold nanoparticles can be viewed by many methods. An image is typically generated by

analysing interference in a reflected sample beam, when compared to a reference beam. There are two types of OCT which form the basis of other methods; time-domain (TD-OCT) and spectral-domain (SD-OCT). Both have differing strengths and weaknesses; however for resolution purposes we have used a sub-type of spectral-domain OCT to visualise gold nanoparticles within polyacrylamide gel matrices. The spectrometer based (SB) OCT method relies on a low coherence light source. Our method utilised a super-luminescent diode (SLD) centred around 840 nm.

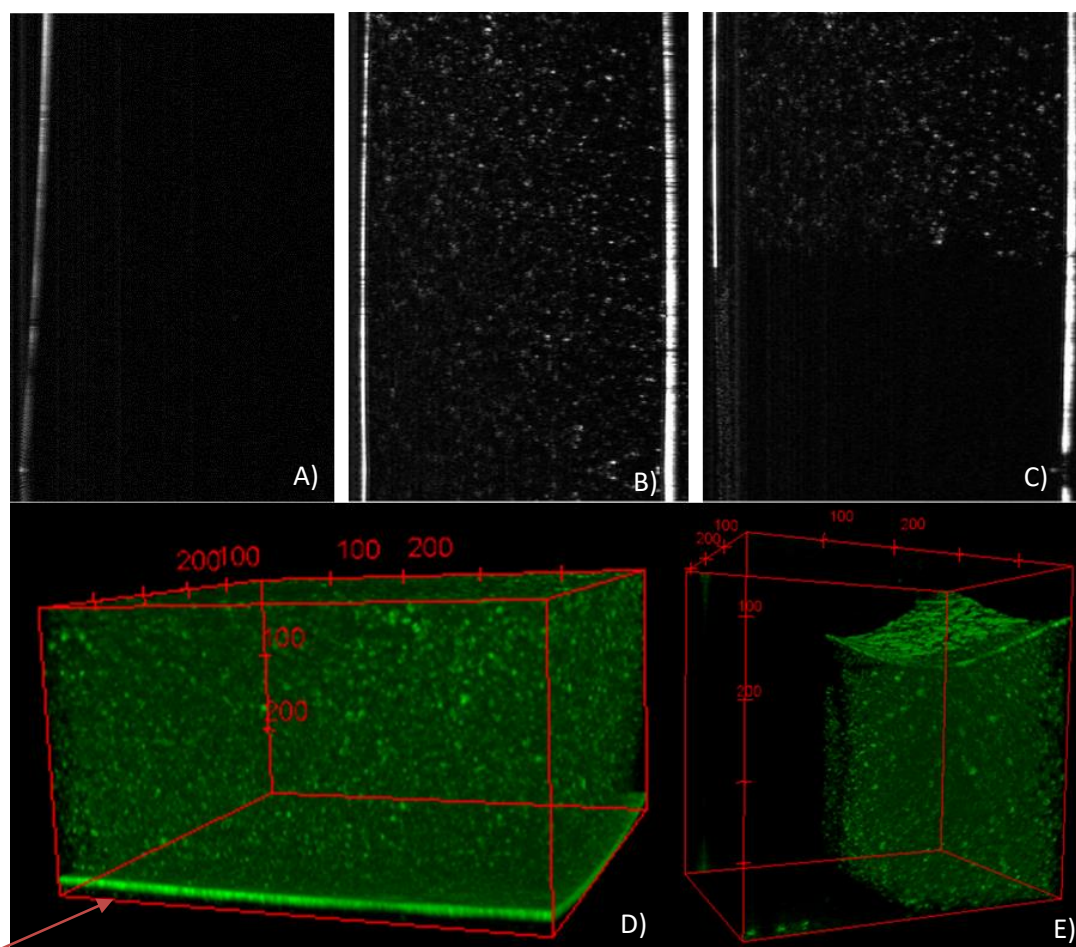


Figure 2.19: A, Non-AuNP containing 1 x TBE native PA gel. B, AuNP containing 1 x TBE native PA gel. C, Non-AuNP containing / AuNP containing 1 x TBE PA gel interface. D, Volume image showing AuNP containing 1 x TBE gel. E, Volume image showing the AuNP / non-AuNP 1 x TBE containing PA gel interface.

Figure 2.19 A, shows an image obtained of the non-AuNP containing TBE PA gel. The surface of the quartz cuvette has a different reflective index to that of the PA gel. This image shows the cuvette face followed by a black space, this is because the refractive index of the PA gel does not change throughout the cuvette, and therefore there is no reflectance of the beam. However

if we look at Figure 2.19 B, we can see that there is now the appearance of white spots. These white spots are the light reflected from gold nanoparticles due to the difference of their refractive index. We see that there are AuNPs spread throughout the gel however we also see that there are brighter spots. These regions would be suggestive of clustered nanoparticles or aggregation. Figure 2.19 D, is a 3D volume image generated from the AuNP containing TBE gel, this image allows us to show that these regions of higher intensity are spread throughout the gel but there is an even dispersion of much smaller nanoparticles.

Images showing the stark difference between the AuNP containing and non-AuNP containing TBE gels is highlighted by the interface images obtained (Figure 2.19 C, E). Figure 2.19 E, is a volume obtained of the TBE gel interface, the green region shows the AuNP containing gel and the blank space within the rest of the box parameters is the non-AuNP containing gel. This is because there is no reflectance generated from this gel, however the green region shows the contrast between reflected AuNPs and the gel matrix. This image along with Figure 2.19 C, shows there is a clear boundary between the two gels and that there is no migration of nanoparticles suggesting they are fixed within the gel matrix.

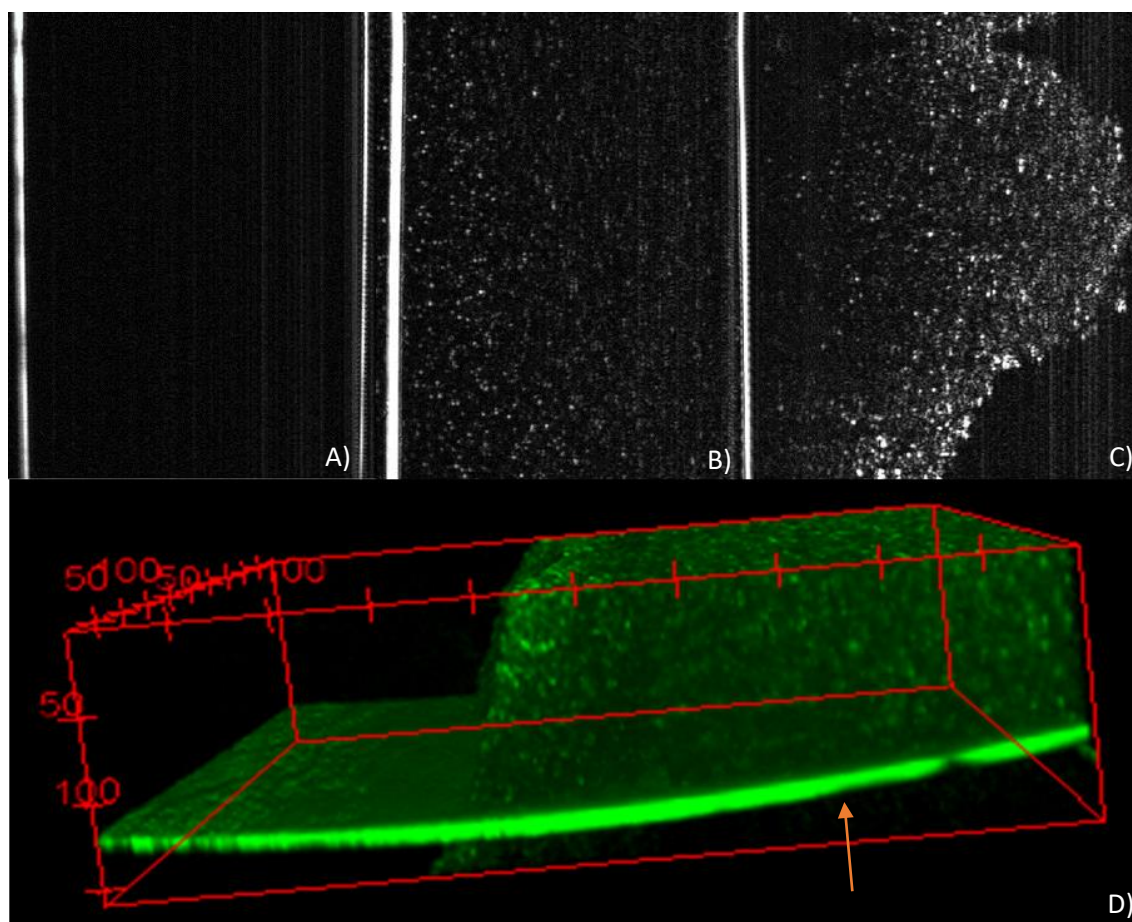


Figure 2.20: OCT images showing, A, Non-AuNP containing Tris-HCl native PA gel. B, AuNP containing Tris-HCl native PA gel. C, AuNP / non-AuNP containing Tris-HCl PA gel interface. D, Volume image showing the AuNP / non-AuNP containing Tris-HCl PA gel interface. Arrows highlight Cuvette face.

Similarly to Figure 2.19, Figure 2.20 A and B, show us the tris-HCl gels, with and without DMAP AuNPs respectively. As can be seen from Figure 2.20 B and D, there are larger clusters of nanoparticles which are brighter than smaller clusters or individual particles. We would expect to see consistently bright spots if all of the DMAP AuNPs were forming large clusters, however we see a more even spreading of duller particles suggesting that the DMAP AuNPs are relatively well dispersed throughout the gel matrix. Figure 2.20 C, images the interface between the AuNPs containing and non-AuNPs containing gels, as can be seen from this image larger clusters appear to congregate at the bottom of the AuNPs gel, most likely due to their size and gravitational effects during polymerisation. Given that we do not see very bright spots throughout the gel images it would suggest that the majority of DMAP AuNPs are monodisperse throughout both polyacrylamide gel matrices.

2.6.3 Scanning Electron Microscopy:

SEM was employed to visualise DMAP gold nanoparticles in different polyacrylamide gel matrices; TBE without gold, TBE with gold, tris-HCl with gold and tris-HCl ATP with gold.

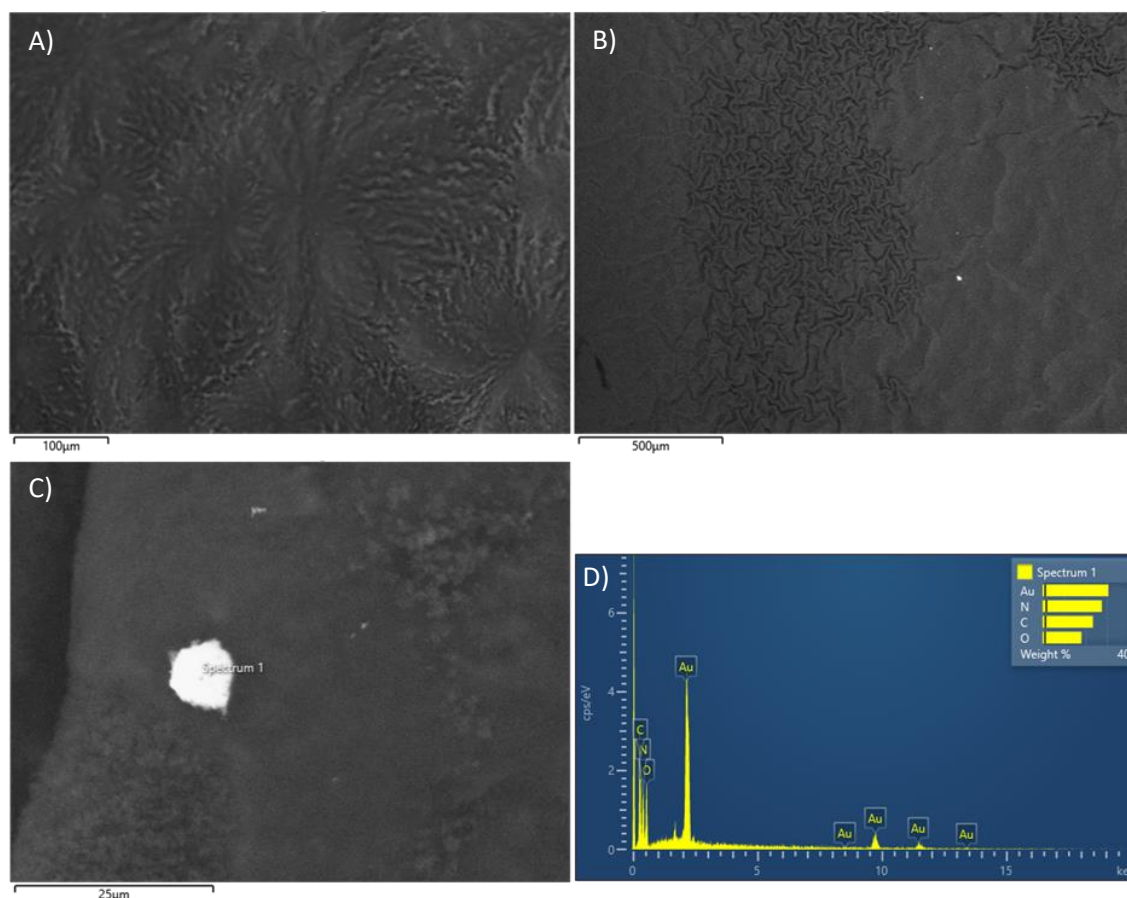


Figure 2.21: A, 12 % TBE polyacrylamide gel without gold. B, 12 % TBE polyacrylamide gel with DMAP AuNPs. C, DMAP gold nanoparticle cluster in 12 % TBE polyacrylamide gel. D, elemental spectrum of DMAP AuNPs cluster from C.

Figure 2.21 shows a selection of SEM images of TBE polyacrylamide gels. Image A (Figure 2.21) allows us to visualise the surface of a TBE polyacrylamide gel, the swirl like pattern may be an artefact of the glass surface the gel was cast in or represent nucleation points at which the polymerisation of the gel occurred or even drying effects. Figure 2.21 B, shows troughs in the surface of the polyacrylamide with gold gel, the gel has begun to desiccate. We believe this pattern is indicative of pores within the matrix losing moisture faster because they are near the surface. The size of the synthesised DMAP AuNPs are between 6 – 8 nm, therefore the nanoparticle visualised in Figure 2.21 C, must be a cluster due to its size, Figure 2.21 D is the elemental spectrum on the DMAP AuNPs cluster.

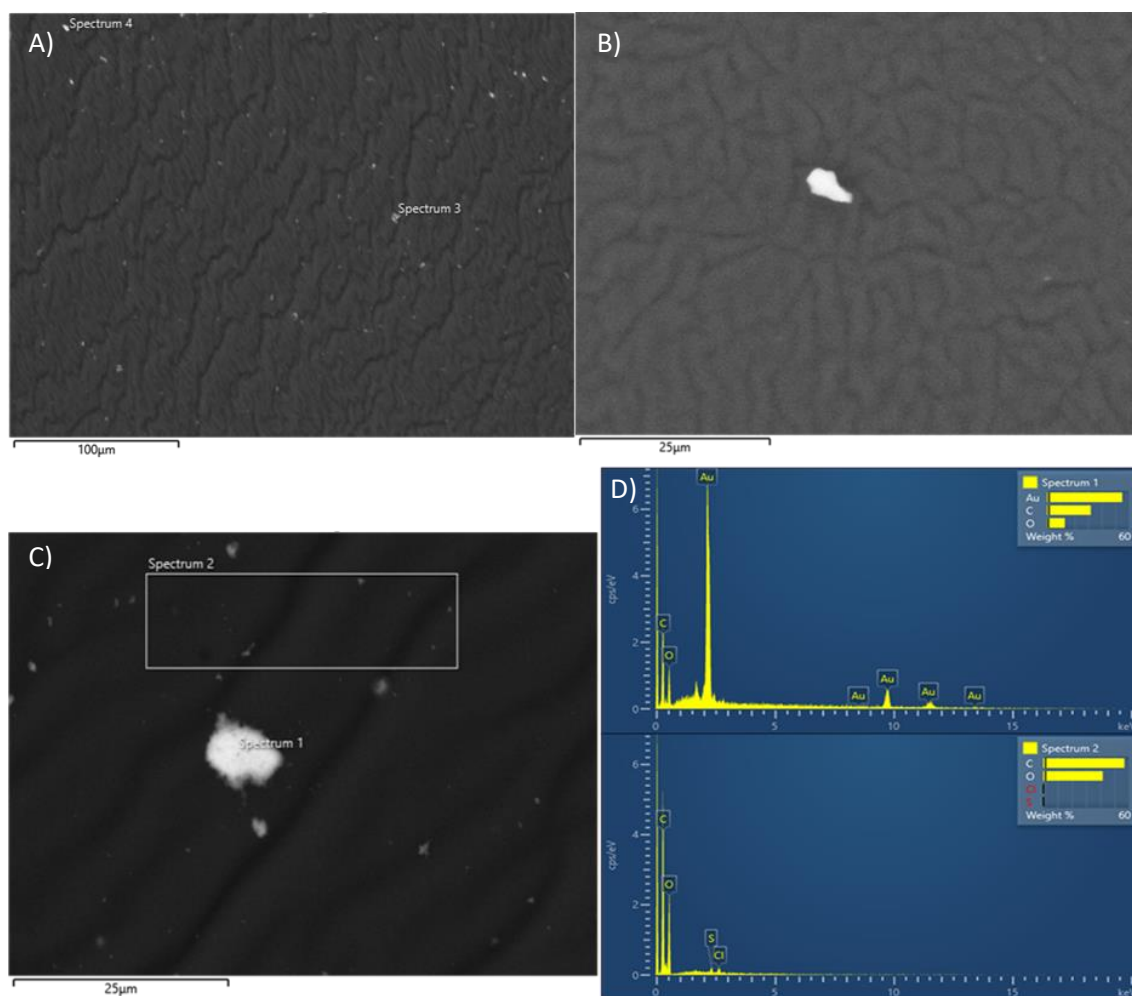


Figure 2.22: A, tris-HCl 10 % polyacrylamide with DMAP AuNPs. B, ATP tris-HCl 10 % polyacrylamide gel with DMAP AuNPs. C, DMAP AuNPs cluster in tris-HCl 10 % polyacrylamide gel. D, elemental spectrums for image C.

Similarly to Figure 2.21, Figure 2.22 A and B exhibit the same visible striations indicative of desiccation of the pores located closely to the gel surface. Interestingly when using tris-HCl buffer the DMAP AuNPs appear to sit within these striations as demonstrated by Figure 2.22 A, B and C. Again as in Figure 2.21 C, we visualise a DMAP AuNPs cluster in Figure 2.22 C, as confirmed by the accompanying elemental spectra representing the presence of gold (see Figure 2.22 D).

If aggregation of the DMAP AuNPs was a significant problem within the polymerisation of polyacrylamide gel we would expect to visualise more nanoparticle clusters at the surface of the gels. Additionally under visual inspection, the red-purple colour appeared uniform. However we do not and from this we infer that the DMAP AuNPs are relatively monodisperse throughout the polyacrylamide matrices, in junction with the OCT results. However further analysis is required

with more sensitive techniques such as transmission electron microscopy and atomic force microscopy, initial efforts to obtain these results were unsuccessful.

2.7 Conclusions:

We have successfully characterised both gold nanoparticles and polyacrylamide gels. We have established that DLS while being a very useful tool in the characterisation of nanoparticles has weaknesses when applied to molecules which form clusters or have non-spherical morphologies. However this technique does provide a useful point of reference for further characterisation by other methods and does take into account hydration spheres.¹⁰⁷ UV-Vis, was employed to characterise the size of gold nanoparticles using the plasmon resonance peak with varying success, the method being developed from citrate AuNPs showed accurate sizing.⁹⁹ However the effect of batch synthesis and different ligands causes this method to be unreliable for DMAP and CTAB protected AuNPs. Further characterisation of DMAP AuNPs by TEM confirmed that the synthesised DMAP AuNPs had an average diameter range of 6 – 8 nm, as reported in the literature.¹⁰⁵

DMAP AuNPs containing polyacrylamide gels were exhibiting unusual behaviour during polymerisation in both TBE and tris-HCl gels, such as; colour changing and slowing the polymerisation process. We investigated the properties of polyacrylamide gels with and without DMAP AuNPs at different concentrations. The rheological data showed a general reduction in the loss modulus or elasticity of the gel across all polyacrylamide concentrations. However the storage moduli showed little variation between gold and non-gold gels, what variation was recorded occurred in gels with percentages below 15 %, this may be attributed to the increased polymer crosslinking in higher percentage polyacrylamide gels. Although these differences are statistically relevant they do not greatly change the properties, in fact the addition of gold nanoparticles appear to stabilise the linear viscoelastic range and improve the recovery time of the different percentage gels.

Optical coherence tomography and scanning electron microscopy were used to visualise the presence of DMAP AuNPs in polyacrylamide gels. What we established from these experiments were that clustering of gold nanoparticles do occur in polyacrylamide gels. However the fact that more of these clusters are not present suggest that the DMAP AuNPs appear to be relatively monodisperse throughout the polyacrylamide gel matrices. We then took these materials forward to testing with biological analytes.

Chapter 3: Analysis of Biomolecules using Gold Nanoparticles as Adjuncts in Polyacrylamide Gel Electrophoresis.

3.1 Introduction:

Biomolecules form four primary classifications: peptides, carbohydrates, lipids and nucleic acids.^{3,5,6,22} These biomolecules all have important functions which support life, an important sub-group of these molecules are ones which contain the element sulfur. Sulfur containing biomolecules carry out a great many functions; from phosphorylation, to controlling protein structure and molecular signalling.^{8,22,42} They also have applications in the synthetic world, particularly with regards to therapeutics and biotechnology.^{8,83,84} Synthetically modified biomolecules have been developed such as phosphorothioated DNA. Modifications with sulfur reduce the susceptibility of DNA to be degraded by DNA enzymes and aid in the development of chemical applications for DNA such as data storage and medicine.^{6,34,52} Sulfur containing RNAs are naturally occurring and show promise as therapeutics,³³ this has led to a demand for the separation of sulfur containing RNAs (tRNAs) from un-thiolated biomolecules. A method was developed by Biondi and Burke,⁵³ which uses mercury to achieve this by exploiting the hard soft acid base (HSAB) chemistry of sulfur and mercury. HSAB theory states that sulfur and mercury are both 'soft' elements and because of this will readily form strong interactions.⁵⁶ They were able to successfully separate tRNAs⁵³ however the safety and cost of using mercury makes this method undesirable. Mercury is a toxic element when absorbed into the human body and because of this disposal is very expensive.⁵⁵ Gold nanoparticles (AuNPs) have recently become popular in a wealth of research due to their high functionality and potential therapeutic properties.^{59,60,110} Like mercury, gold is also considered a 'soft' element and therefore forms strong interactions with sulfur containing molecules.^{111–113} We theorise that by replacing mercury with gold nanoparticles in polyacrylamide gel electrophoresis, we can separate sulfur containing biomolecules similarly to Biondi and Burke.⁵³

3.2 Experimental:

3.2.1 Materials:

Hydrogen tetrachloroaurate; aliquat[®] 336 and sodium borohydride, urea, EDTA and isopropanol were purchased from Acros. 4-Dimethylamino pyridine was purchased from Fluorochem. Toluene, boric acid and acrylamide/bisacrylamide 37.5:1 solution was purchased from Fisher Scientific. Ammonium phosphate, N, N, N', N'-tetramethylethylenediamine, (TEMED) and cetyltrimethyl-ammonium bromide were purchased from Sigma Aldrich. Tris; glycine, glycerol, bromophenol blue, expedeon instant blue and Ellman's reagent were also purchased from Sigma Aldrich. Sodium citrate was purchased from Fisons. Stains-all was purchased from Alfa Aesar. Protein samples were purchased from Sigma Aldrich and reduced using Ellman's reagent. DNA strands were purchased from Link Technologies and diluted as recommended. All chemicals were used as provided and not purified further unless stated otherwise.

3.3 Methods:

3.3.1 DNA Samples:

Single Stranded DNA (ss-DNA) samples were analysed by TBE or TAMg denaturing polyacrylamide gel electrophoresis with gold nanoparticles as adjuncts. A parent strand of DNA was used to develop other strands with phosphorothioates at different points along the length, this was to ensure that all the strands had the same length and similar molecular weights. The parent strand of DNA was called SS4-54 (DNA reference), this strand was originally chosen because of its ability to bind multiple organophosphate groups in the literature,⁸¹ the other strands were modifications from this strand:

DNA (Reference): AAGCTTTTTTGACTGACTGCAGCGATTCTTGATCGCCACGGTCTGGAAAAAGAG.

The following four ss-DNA strands contain phosphorothioates in different positions along the strand and differing numbers, (*).

ExtS: A*AGCTTTTTTGACTGACTGCAGCGATTCTTGATCGCCACGGTCTGGAAAAAGAG.

IntS: AAGCTTTTTTGACTGACTGCAG*CGATTCTTGATCGCCACGGTCTGGAAAAAGAG.

2S: A*AGCTTTTTTGACTGACTGCAG*CGATTCTTGATCGCCACGGTCTGGAAAAAGAG.

3S: A*AGCTTTTTTGACTGACTGCAG*CGATTCTTGATCGCCACGGTCTGG*AAAAAGAG.

The final strand contained the -5ThiolMC6D linker (see figure 3.1 A).

Thiol:

-5ThiolMC6D-AAGCTTTTTTGACTGACTGCAGCGATTCTTGATCGCCACGGTCTGGAAAAAGAG.

The ss-DNA strands have been labelled with asterisk indicate the position or number of phosphorothioates within the strand.

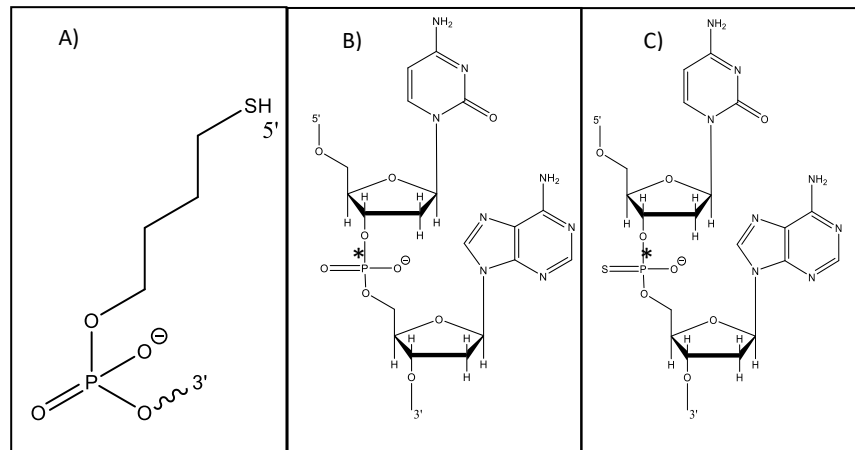


Figure 3.1: A) -5ThiolMC6D, thiol modifier. B) Phosphodiester linkage between adenosine and cytosine. C) Phosphorothioate linkage between adenosine and cytosine.

The phosphorothiolate modification occurs when the double bonded oxygen on the phosphodiester linkage is replaced with sulfur (*) see figure 3.1 B, C.

3.3.2 DNA Sample Preparation:

DNA samples were purchased as powders from IDT; 100 mM stock solutions were prepared as directed. The thiol strand required reduction by the oxygenation of the solution. Electrophoresis samples were prepared as follows; 1 μ L of 100 mM stock DNA was diluted in 20 μ L of 8 M urea and 20 μ L deionised water. 20 μ L of each sample was loaded onto the polyacrylamide gel. The DNA was prepared in denaturing conditions to avoid the formation of dimers through sulfur bridging.

3.3.3 Tris Borate EDTA (TBE) Native Denaturing PA Gel:

TBE denaturing polyacrylamide gels were prepared from a denaturing 20 % polyacrylamide stock solution and TBE buffer, with a final concentration of 12 % polyacrylamide, without AuNPs and 15 %, with AuNPs. The gels were polymerised between glass plates with 0.75 mm spacers. The gel was poured between the plates to the top (control) a 0.75 mm comb was inserted and the gel left to fully polymerise. For an AuNPs containing gel the cassette was 80 % filled and left to completely polymerise. The AuNPs modified gel was prepared and poured between the plates to fill the remaining 20 %, a 0.75 mm comb was inserted and the gel allowed to fully polymerise. The comb was removed after polymerisation and the wells were flushed with deionised water then buffer. 20 μ L of each sample was loaded onto the gel with a 1 kba ladder.

3.3.4 Tris Magnesium Acetate (TAMg) Native PA Gel:

The TAMg gels were prepared from a 12 % polyacrylamide stock solution, with a final concentration of 12 % polyacrylamide for both with and without AuNPs. The gels were prepared as above.

All gels were run at maximum voltage (300 V), 15 mAmps per gel, for 90 minutes and in TAMg buffer unless otherwise stated. Gels were stained in Stains-All prepared in isopropanol-tris buffer, for a minimum of 30 minutes; the gels were then rinsed of excess stain using water before being imaged on an Epson scanner. Images were visually enhanced as required using windows photo editor software.

3.3.4 Protein Reduction:

5 mg of lysozyme was dissolved in 3 mL 6 M guanidine in 20 mM tris. To this 0.5 M NaOH was added to pH 8. Absorbance at 280 nm showed 1.223 down from 12.33, signalling a 1 in 10 dilution of the protein in solution. Using the mass extinction coefficient of the lysozyme (2.33) the mg mL^{-1} was calculated to be 4.67 mg mL^{-1} which is equivalent to 326 μM protein. To this 100 μL of 1 M DTT was added, which was a final concentration of 33 mM of DTT. The solution was rolled overnight and a PD10 column purification was completed using 0.1 M acetic acid. The resultant solution was the tested using Ellman's reagent to test for unbound thiols. 100 μL of 1

M tris solution was combined with 50 μL of Elman's reagent and 840 μL H_2O , this was tested for absorbance at 280 nm, and the absorbance was measured as zero. 10 μL of the lysozyme solution was added and the sample retested, the absorbance was measured at 0.594 abs. This signal combined with the colour change from colourless to yellow signifies the presence of reduced thiols. All proteins were reduced by this method and then analysed by tris-HCl native PA gel electrophoresis.

3.3.5 Tris-HCl Native PA Gel:

Tris-HCl gels were prepared from 30 % acrylamide stock solution. The stacking, resolving and non-AuNPs gels were prepared with 0.375 M tris-HCl buffer, the AuNPs gel was prepared with 1.5 M tris-HCl buffer. The stacking gel final concentration was 4 %; the resolving gel final concentration was 10 % unless stated otherwise. The AuNPs +/- gels were a final concentration of 10 %. Control and test gels were prepared, the resolving gels were poured into cassettes and left to polymerise before the AuNPs +/- gels were poured into the cassettes. Once polymerised the stacking layers were poured and combs inserted into the gels and left to polymerise.

3.3.6 SDS Gradient Polyacrylamide Gel (4-15 %):

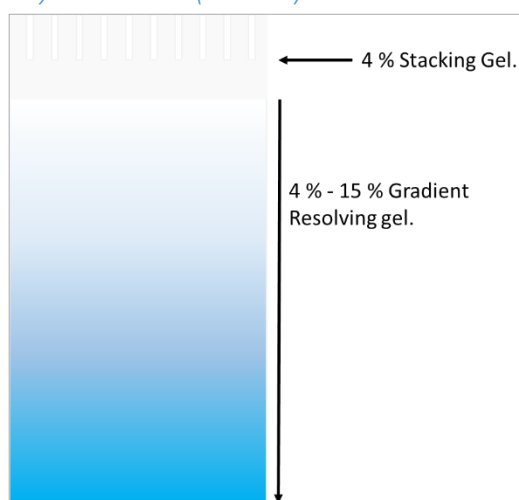


Figure 3.2: Showing the principle behind the SDS gradient gel, colour is used to highlight the principle.

SDS gels were prepared from a 30 % polyacrylamide stock solution; with autoclaved water, upper tris for the higher percentage gels (10-15 %) and lower tris buffer for the low percentage gels (4 %) gels. The resolving gels had a final concentration of 4 % and 15 %, the stacking gels final concentration was 4 %. A control gel was prepared by drawing up the 4 % and then the 15

% resolving gels in equal quantities, mixing was achieved by introducing a bubble to the pipette before depositing the mixture into a cassette. This was left to polymerise before the stacking gel was poured and a comb inserted.

3.3.7 Tris-HCl Native Gradient Gels:

Gel solutions were prepared from a 30 % acrylamide stock solution, diluted with 0.375 M tris-HCl for the resolving, stacking and AuNPs – gels. The AuNPs + gel was made using 1.5 M tris-HCl. Resolving gel solutions were prepared at 4 %; 10 % and 15 %. The stacking gel was prepared at a concentration of 4 %, the AuNPs +/- gels were prepared at a concentration of 10 %. The 4-15 % gradient gel was prepared by combining equal quantities of the 4 and 10 % resolving gels by introducing a bubble to the pipette, the solution was deposited into two cassettes and left to polymerise. Each cassette was filled with either the AuNPs +/- gel, once polymerised the stacking gel was poured into the cassettes and a comb inserted. Figure 3.3 shows a visual representation of the gradient gel principle and configuration.

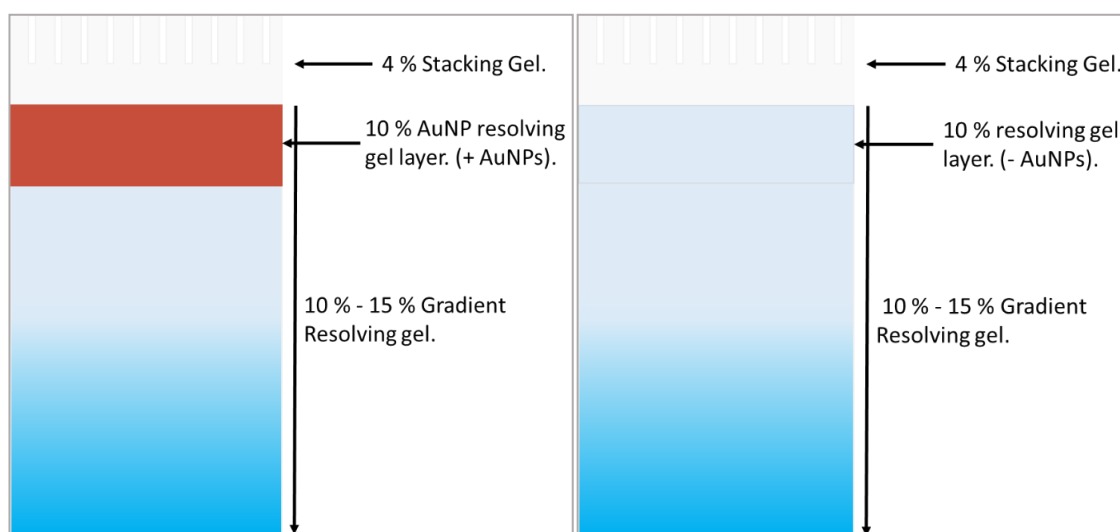


Figure 3.3: Representation of tris-HCl Native gradient PA gels, left: Gel containing gold nanoparticles, right: Control gel without gold nanoparticles.

3.3.8 ATP Tris-HCl Native PA Gel Buffers:

The ATP native PA gel buffer solutions were prepared from a 100 mM stock solution of ATP, which was prepared by dissolving 5 g of ATP in 100 mL of autoclaved water. From this stock buffers of; 8, 15 and 32 mM ATP were made 0.375 M and 1.5M tris-HCl buffer.

3.3.9 ATP Tris-HCl Native PA Gel:

10 and 15 % resolving gels; 10 % AuNPs – and a 4 % stacking gels, were prepared from a 30 % polyacrylamide stock solution diluted with 8 mM ATP 0.375 M tris-HCl buffer. The AuNPs + gel was prepared from a 30 % stock solution of polyacrylamide diluted with 8 mM ATP, 1.5 M tris-HCl buffer. The gels were prepared by the same method outlined in section 3.3.7.

Unless stated otherwise all tris-HCl gels were run with the following protein samples; Lysozyme (Lys), RNase A (RNase), Bovine Serum Albumin (BSA) and Glutathione-S-Transferase (GST), they were purchased from Sigma. All samples were also investigated with the addition of N-ethylmaleimide (NEM). The samples were prepared by combining protein solutions (15 μ L) with 4 x native loading dye (10 μ L) (Bromophenol Blue). In the case of the NEM containing samples, protein solutions (15 μ L) were combined with 10 % NEM in 4 x native loading dye (10 μ L) (10 μ L NEM in 100 μ L dye). 12.5 μ L of each sample was loaded onto the gels. Gels were ran at 160 V for 1 hour and stained with expedon instant blue and placed on a rocking table overnight. The gels were visualised using an Epson Perfection 3200 scanner with the Epson Scan 3.04 software.

3.4 Results and Discussion:

3.4.1 AuNPs Gel Electrophoresis:

Previous work in the group investigated the use of concentrated citrate AuNPs with both the TBE and tris-HCl gels, although the results were unsuccessful they laid the foundation for this work¹¹⁴. It is from these previous experiments that I have developed my protocols for the following experiments. We investigated three types of nanoparticles and their interactions with phosphorothioated DNA, with varying positions and numbers of phosphorothioates.

3.4.2 Citrate-AuNPs Polyacrylamide Gel Electrophoresis:

The first experiments we conducted were using 12 % TBE polyacrylamide gels, with a 12 % modified gel layer with approximately 15 mg mL⁻¹ concentrated citrate AuNPs. These experiments showed no success with regards to the ss-DNA being retained within the gold layer due to 'soft – soft' interactions.

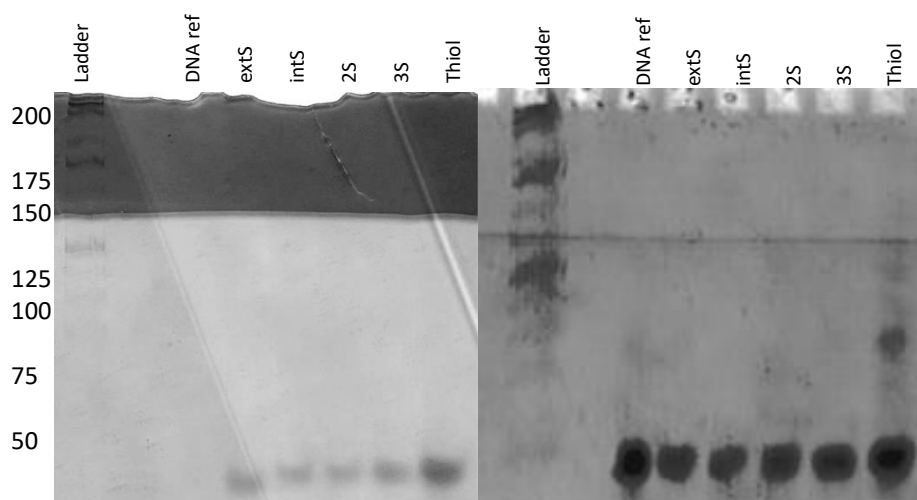


Figure 3.4: Left, 12 % TBE PAGE with modified citrate AuNPs (approximately 15 mg mL⁻¹) layer. Right, control 12 % TBE PAGE, without modified citrate AuNPs layer.

Figure 3.4 shows a direct comparison between a citrate AuNPs gel and a control gel, as can be seen there is no obvious obstruction to the migration of the ss-DNA by the citrate AuNPs. We believed that the concentration of gold was the limiting factor with regards to ss-DNA retention, we increased the citrate AuNPs concentration to approximately 60 mg mL⁻¹.

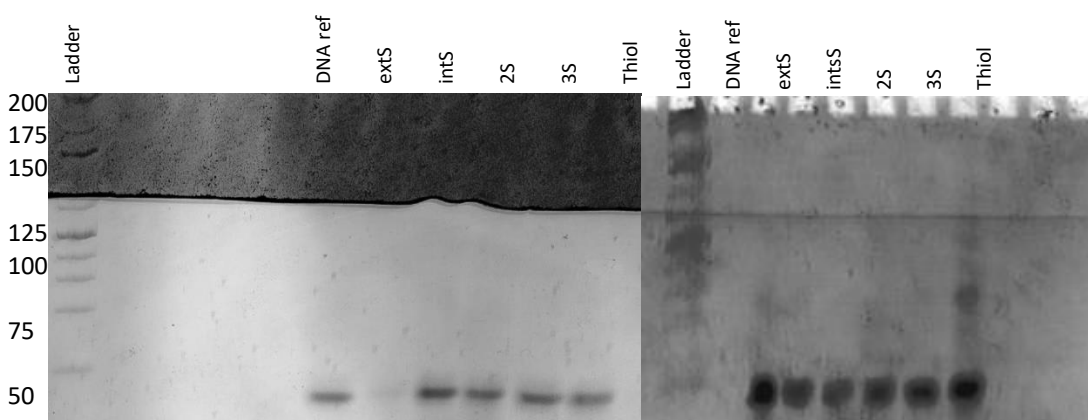


Figure 3.5: Left, 12 % TBE PAGE with citrate AuNPs (approximately 60 mg mL⁻¹) modified layer. Right, control 12 % TBE PAGE without citrate AuNPs.

Despite increasing the concentration of gold in the modified gel layer the ss-DNA migrated through the gel to a similar degree to that of the control gel (see figure 3.5). There was also no change in mobility between the different strands of DNA despite there being varying accessibility to phosphor-thiolates between the strands. DNA has an overall negative charge, this is why it moves through a gel in electrophoresis. The citrate ligand protecting the nanoparticles also has an overall negative charge. We theorised that the DNA was being repelled by the citrate ligand shell, not allowing the sulfurs on the ss-DNA to come close enough to the gold core, therefore

preventing the possibility of sulfur-gold 'soft' interactions. We believed if we neutralised the charge on the citrate ligand by introducing magnesium into the polyacrylamide gel solution and running buffer, we would be able to visualise gold-sulfur interactions in the modified gold gel layer. We ran a TAMg 12 % polyacrylamide gel with a 12 % citrate AuNPs modified gel layer, in TAMg buffer.

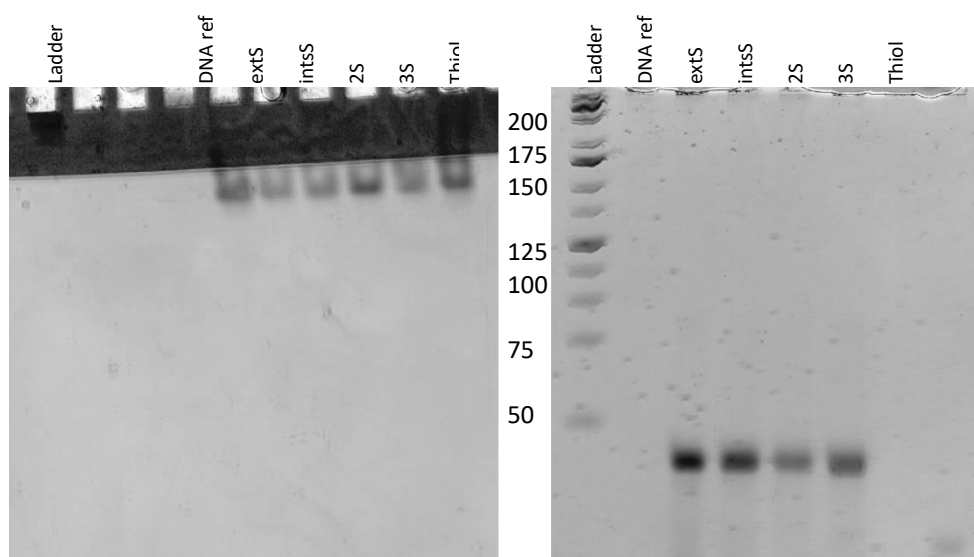


Figure 3.6: Left, TAMg 12 % PAGE with citrate AuNPs (approximately 60 mg / mL) 12 % modified gel layer. Right, control TAMg 12 % PAGE without modified citrate AuNPs layer.

Figure 3.6 shows, a reduction in the mobility of the DNA strands as a whole compared to the control gel, including the reference strand which does not contain any sulfur atoms. However there is no discernable difference between the migrations of the DNA strands related to their sulfur content. Unexpectedly, we were unable to repeat the stable dispersion of citrate AuNPs in the TAMg gel, figure 3.7 shows an example of this aggregation.



Figure 3.7: TAMg 12 % PAGE with citrate AuNPs (approximately 60 mg mL⁻¹) aggregation.

The aggregation of citrate protected AuNPs in TAMg buffer was consistent and we were unable to prevent it from occurring. We therefore stopped investigating citrate protected AuNPs as part of this work.

3.4.3 CTAB-AuNPS Polyacrylamide Gel Electrophoresis:

The second type of gold nanoparticles we investigated were CTAB protected nanoparticles, CTAB is a surfactant with a long carbon chain tail. Figure 3.8 is a schematical representation of CTAB.

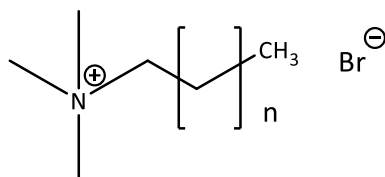


Figure 3.8: Structure of cetyltrimethyl-ammonium bromide (CTAB).

CTAB AuNPs from the outset proved problematic; the AuNPs when added to TBE buffer and denaturing polyacrylamide gel solution would aggregate. This resulted in large clusters of aggregated particles when the gel was polymerised, as demonstrated by figure 3.9. Despite the aggregation we decided to run the gel with the ss-DNA samples.

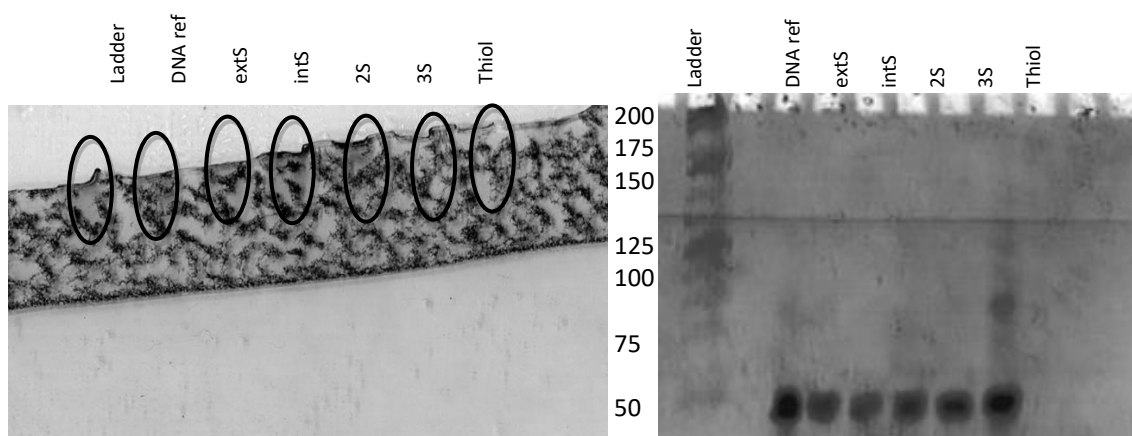


Figure 3.9: Left, TBE 12 % polyacrylamide gel with CTAB AuNPs (approximately 60 mg mL⁻¹) 12 % modified polyacrylamide gel layer. Right, control, TBE 12 % polyacrylamide gel without CTAB AuNPs.

The CTAB AuNPs made it difficult to visualise the DNA bands within the gold layer. The ss-DNA samples appear to have been retained within the gold layer regardless of sulfur content. It cannot be dismissed that the retention of the DNA may be due to the aggregation of the nanoparticles acting as a physical barrier to the DNA instead of gold-sulfur interactions. In an attempt to remove the aggregation of the CTAB protected AuNPs we ran the experiment using TAMg buffer. Polymerisation of the gold containing polyacrylamide gel solution now became a problem, in both gel types, this may be attributed to the aggregation of the AuNPs or the surfactant properties of CTAB interfering with polymerisation. We changed the amount of

initiator added to the gel but with no resolution, we chose to no longer investigate CTAB protected AuNPs in this project.

3.4.4 DMAP-AuNPs Polyacrylamide Gel Electrophoresis:

The third type of AuNPs we investigated were DMAP protected AuNPs. DMAP gives gold nanoparticles with a positive surface charge unlike the citrate and CTAB protected nanoparticles.⁵⁸ Figure 3.10 shows representation of DMAP being displaced by phosphorothioate.

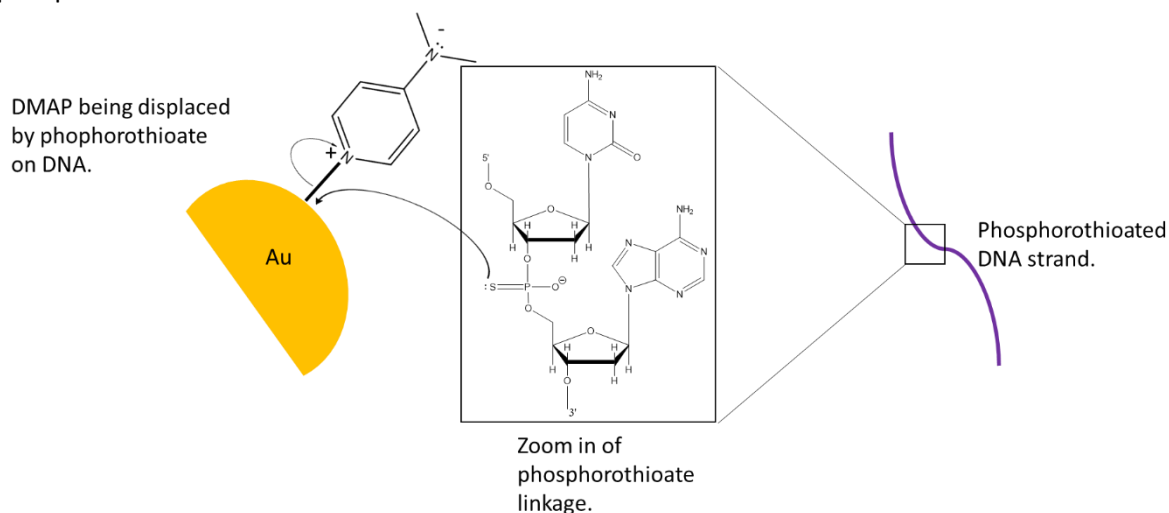


Figure 3.10: Schematical representation of DMAP being displaced by phosphorothioate on DNA at the surface of an AuNP.

Initial testing with these AuNPs gave rise to promising results. The ss-DNA should in theory be retained within the gold containing layer by different degrees, due to the number and positions of the phosphorothioates within the strands. Figure 3.11 shows the first successful representation of this retention of the DNA within the modified gold layer.

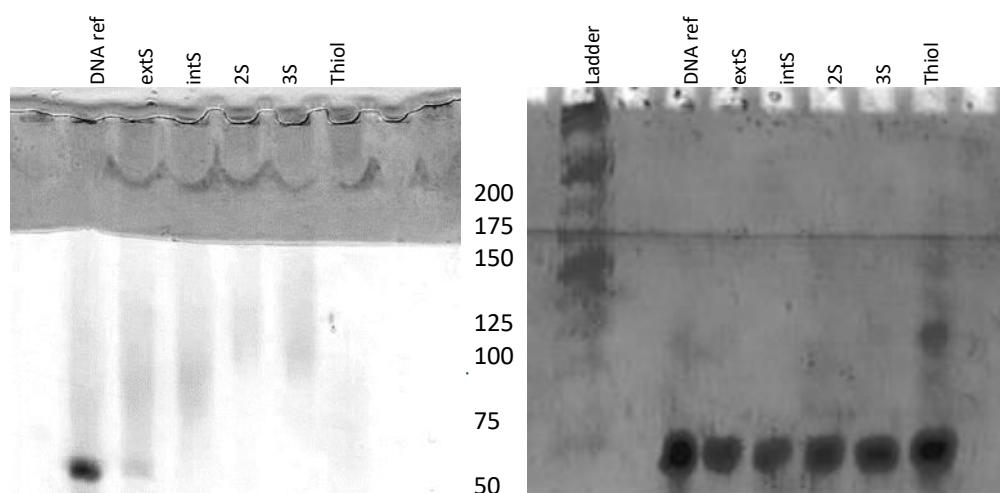


Figure 3.11: Left, TBE 12 % polyacrylamide gel with DMAP AuNPs (approximately 60 mg / mL) 12 % modified gel layer. Right, control, TBE 12 % polyacrylamide gel without DAMP AuNPs.

This demonstrated the expected reduction in mobility of the ss-DNA due to the different numbers of the phosphorothioates within in each strand. However replication of this result was challenging and shows retention of all of the DNA within the gold layer despite sulfur concentration, see figure 3.11.

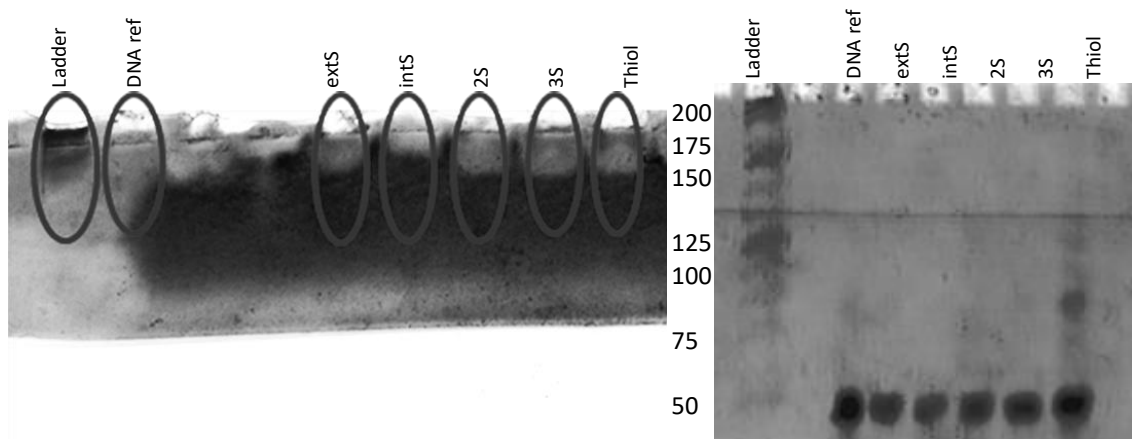


Figure 3.12: Left, TBE 12 % polyacrylamide gel with DMAP AuNPs (approximately 60 mg / mL) modified 12 % gel layer. Right, control, TBE 12 % polyacrylamide gel without DMAP AuNPs. The two images presented are not of the same scale.

In an attempt to achieve a repeatable graduated migration of the ss-DNA, we attempted to modify the conditions, by pre-running the gels, and increasing the time the gel was run for, however these resulted in similar results as in figure 3.11 or all of the DNA running through the gold layer into the un-modified gel layer. The reproducibility of this method has not been consistent with every attempt there has been enough promise to warrant further testing with proteins.

3.4.5 SDS Polyacrylamide Gel Electrophoresis:

The proteins we investigated were; lysozyme (lys), bovine serum albumin (BSA), RNase A (RNase) and glutathione-S-transferase (GST). Lysozyme, contains 147 amino acids, a theoretical PI of 9.36, contains 12 sulfurs and has 18 positively charged and 9 negatively charged residues. Bovine serum albumin, contains 607 amino acids, has a theoretical PI of 5.82, contains 40 sulfurs and has 99 negative and 86 positively charged residues. RNase A, contains 150 amino acids, a theoretical PI of 8.93, contains 13 sulfurs and has 10 negative and 16 positively charged residues. Glutathione-S-transferase, contains 209 amino acids, has a theoretical PI of 5.44, contains 6

sulfurs and has 23 negative and 20 positively charged residues. All of these parameters were calculated at pH 8 (running buffer pH), using the epoxy portal and protein data bank.

Investigating the retention of proteins by DMAP AuNPs was carried out in collaboration with Dr Dave Beal from the School of Biosciences at The University of Kent. Previously SDS-PAGE of proteins had been investigated using citrate-capped AuNPs, within the group, with no evidence of selective retention of proteins¹¹⁴. Similarly, we now found that there was no retention of the proteins by the DMAP AuNPs. This may be because the surfactant nature of the SDS is generating a secondary ligand sphere around the AuNPs, as DMAP is positively charged. This secondary shell maybe preventing the proteins from sufficiently interacting with the AuNPs. Figure 3.12 shows the DMAP AuNPs modified SDS PAGE results.

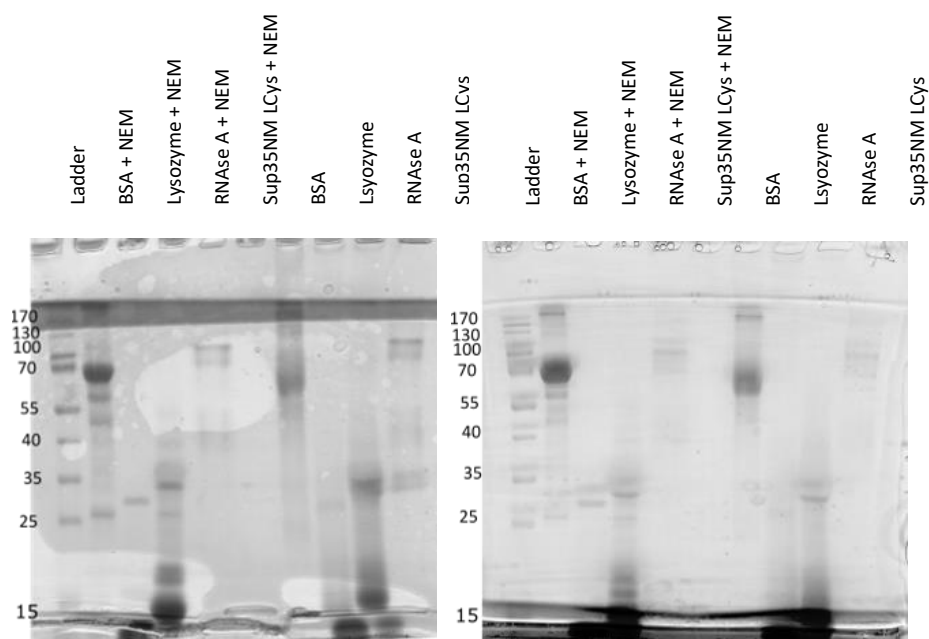


Figure 3.12: Left, 15 % SDS polyacrylamide gel with 15 % DMAP AuNPs modified gel layer and 4 % stacking gel. Right, control, 15 % SDS polyacrylamide gel with 4 % stacking gel, without DMAP AuNPs. Ladder is measured in kDa.

Because of the results obtained by myself and in the group previously, we decided to abandon using SDS Page to investigate protein AuNP interactions in this project.

3.4.6 Tris-HCl Polyacrylamide Gel Electrophoresis:

Our next avenue of testing was to use tris-HCl native PAGE to test the nanoparticles. Recreating a test previously used in the group, we used protein samples which contained sulfur competitors in an attempt to observe whether the proteins would still be retained by the DMAP AuNPs. We used β -mercaptoethanol (2-ME) and N-ethylmaleimide (NEM) as these competitors. The group had observed that the protein samples which were combined with β -mercaptoethanol caused the citrate AuNPs to be stripped from the gold modified layer of the gel and pulled into the main resolving layer. Figure 3.13 shows the experiment was repeated with DMAP AuNPs.

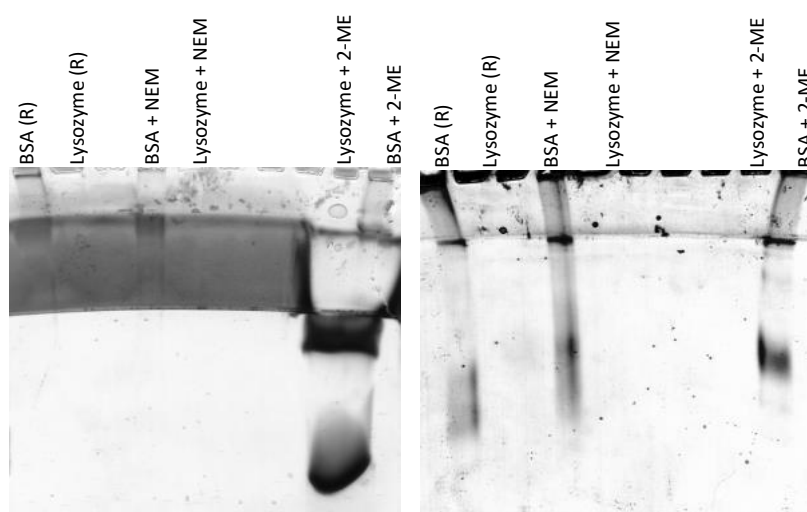


Figure 3.13: Left, tris-HCl 10 % polyacrylamide resolving gel, with 10 % DMAP AuNPs modified resolving layer and 4 % stacking gel. Right, control, tris-HCl 10 % polyacrylamide resolving gel without DMAP AuNPs modified layer and a 4 % stacking gel.

As can be seen from figure 3.13, BSA migrated into the control gel but was retained within the modified gold layer. Lysozyme is not visible on this gel, it was believed that the protein had run off the bottom of the gel. Figure 3.13 also shows the stripping of the DMAP AuNPs from their discrete layer into the main resolving gel. This phenomena was observed in previous work within the group and indicates that 2-ME as a sulfur competitor is too potent for our purposes, therefore we stopped using 2-ME in our experiments but continued to use N-ethylmaleimide as a sulfur competitor. We continued to test the DMAP AuNPs with proteins, however we began to encounter problems with small proteins being visualised in the gels as well how far they migrate into the gel. In an attempt to overcome this we tried running gradient gels, firstly with a wide acrylamide percentage range (4-15 %), (Figure 3.14).

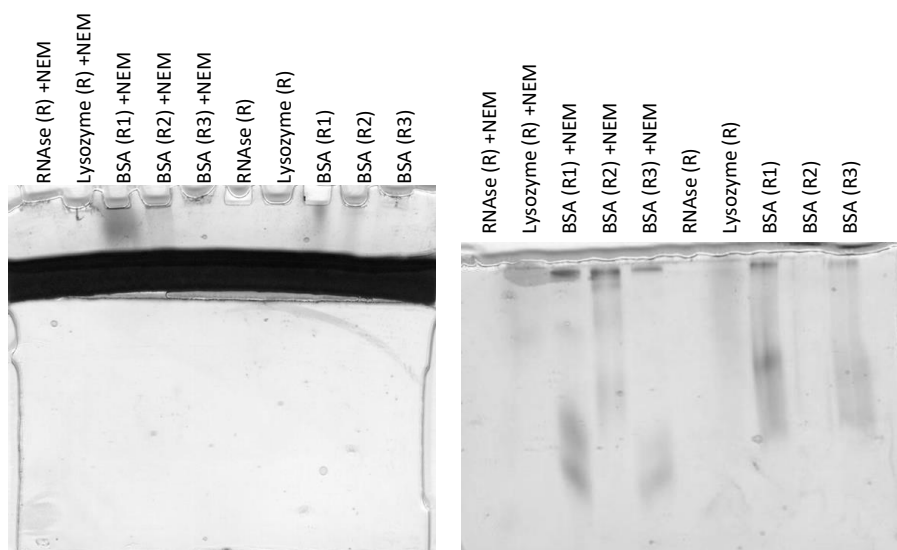


Figure 3.14: Left, tris-HCl 4 - 15 % gradient gel with 10 % DMAP AuNPs modified gel layer and 4 % stacking gel layer. Right, control, tris-HCl 4 - 15 % gradient gel, with 10 % gel layer and a 4 % stacking gel layer, R signifies reduced.

We used a gradient gel because we had continued difficulty visualising the small proteins, lysozyme and RNase A, we theorised that this would allow the smaller proteins to move into the resolving gel but not run to the bottom of the gel. Figure 3.14 allows us to see that the proteins were retained in the gold gel and there was reasonable difference in protein migration between the gold and control gels. Due to poor visibility of the proteins in the gold layer was due to the intensity of the colour, we reduced the amount of AuNPs solution we added to the gold gel layer fourfold (see figure 3.15). We believed it would be useful to reduce the acrylamide percentage range in the gradient gel to 10 – 15 % as this would match with the percentage of the gold and non-gold layers. Figure 3.15 shows the results of the 10 – 15 % gradient gels.

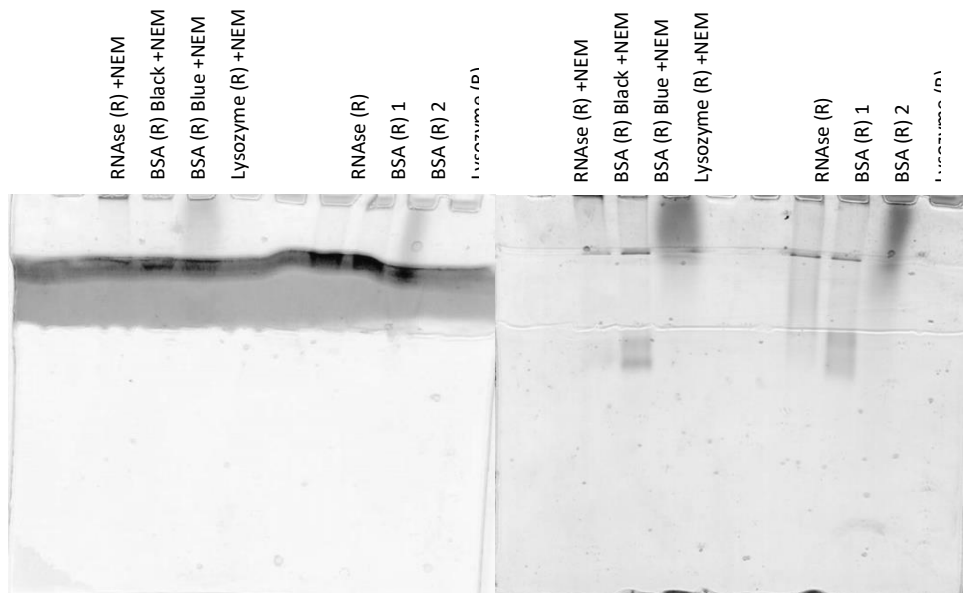


Figure 3.15: Left, tris-HCl 10 – 15 % gradient gel with 10 % DMAP AuNPs modified gel layer and a 4 % stacking gel. Right, control, tris-HCl 10 – 15 % gradient gel with 10 % non-AuNPs containing gel layer and a 4 % stacking gel.

Reducing the concentration of DMAP AuNPs in the modified layer did not impair the ability for the nanoparticle layer to retain the proteins, but there was still continued difficulty in visualising the proteins lysozyme and RNase. Analysis of the proteins using Epoxy portal and protein data from the Protein Data Bank (PDB) highlighted that, lysozyme and RNase have an overall positive charge which at pH 8, as listed at the beginning of section 3.4.5. Given that we are investigating these proteins using native PAGE, the proteins are not coated in a negative charge by the sample buffers as they would be in SDS PAGE for example. To investigate the migration of the smaller proteins we carried out a reverse polarity PAGE.

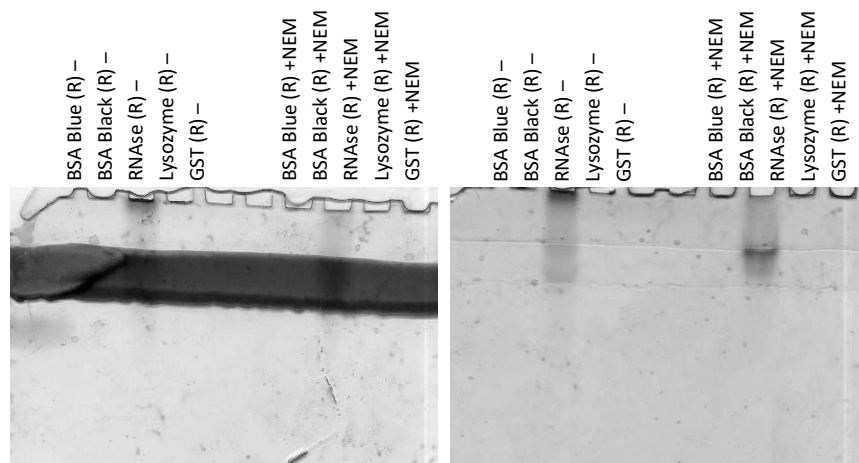


Figure 3.16: Left, tris-HCl 10 – 15 % reverse polarity gradient gel with 10 % DMAP AuNPs modified gel layer and a 4 % stacking gel. Right, control, tris-HCl 10 – 15 % reverse polarity gradient gel with 10 % without DMAP AuNPs and a 4 % stacking gel.

Figure 3.16 allows us to visualise RNase but none of the other proteins including lysozyme. A recent publication¹¹⁵ uses ATP as a hydrotope in the prevention of agglomeration of proteins, we have taken this principle and conducted a tris-HCl gel containing ATP. ATP is found in high concentrations within human cells (2-8 mM), meaning that it cannot be a denaturant¹¹⁵. However as it has been found to aid in protein solubility it must interact with their surface in some way possibly as a surfactant. Therefore ATP was used to coat the proteins in a negative charge, similarly to SDS but without the denaturing effects observed with the nanoparticles in previous SDS gels.

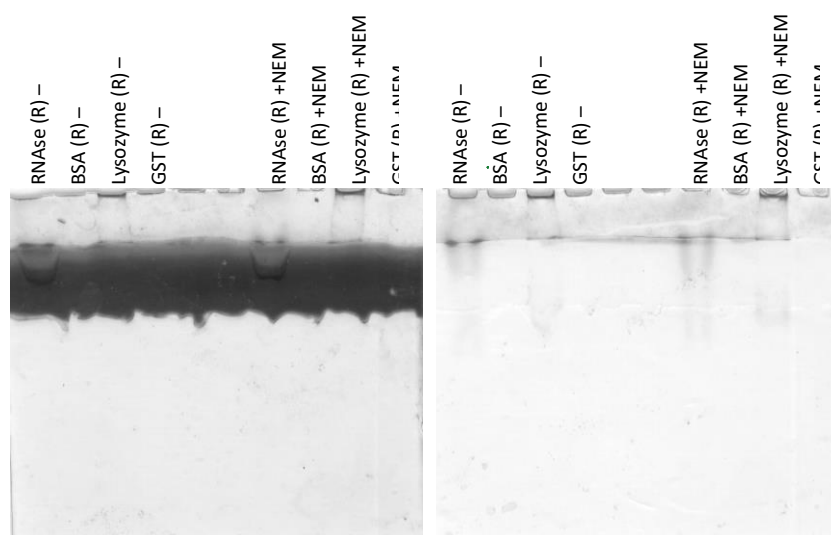


Figure 3.17: Left, ATP tris-HCl gradient 10 - 15 % gel with 10 % AuNPs gel layer and 4 % stacking gel. Right, ATP tris-HCl gradient 10 - 15 % gel 10 % without AuNPs gel layer and 4 % stacking gel (control).

Figure 3.17 shows the results of the ATP gel. RNase A has been retained by the gold layer but none of the other proteins are visualised. One distinct characteristic which the ATP gel had over the other gels was a lack of discolouration of the AuNPs modified layer; we believe this is because the ATP coated the AuNPs in a negative charge preventing them from interacting in the polymerisation process as previously thought and discussed in chapter 2. We were only able to visualise RNase most likely due to the ATP. However, this is a promising result, we were only able to conduct one attempt at this experiment due to time constraints. Given more time to develop the method we believe that this could be a promising area of research.

3.5 Conclusion:

We have discussed in detail the ability of three types of gold nanoparticles to retain sulfur containing biomolecules, with varying degrees of success. Citrate AuNPs have showed little success in retaining phosphorothioated DNA. We believed this firstly to be because of the concentration of gold within the modified gel layer, however on increasing the concentration we saw no changes in retention of the DNA. We theorised that the negative citrate ligand shell was causing repulsion of the DNA, so we investigated the AuNPs in TAMg polyacrylamide gel conditions. The magnesium ions were thought to neutralise the negativity of the citrate ligand shell; what we found was that these ions were disturbing the stability of the ligand shell, causing mass aggregation of the citrate AuNPs. No longer investigating citrate-capped AuNPs we looked at CTAB-capped AuNPs. These nanoparticles exhibited aggregation in both buffer types. We were able to polymerise a gel in TBE buffer which displayed retention of the DNA, but this retention was more likely due to the large aggregations acting as a physical barrier to the migration of DNA. Further testing was not possible as the polymerisation of gels containing CTAB AuNPs was not achievable.

DMAP-capped AuNPs showed the most promising results with initial testing with DNA. The results showed consistent retention of the phosphorothioated DNA but also the reference strand which contained no sulfur. Maintaining consistency with every gel was problematic. We investigated the proteins: lysozyme, bovine serum albumin, RNase A and glutathione-S-transferase using this method. The larger and negatively charged proteins, BSA and GST showed good retention within the gold layer; visualisation of the smaller positively charged proteins was consistently unachievable, despite trying different methods such as the gradient gel. We theorised that this was because the native tris-HCl gel we were using was not coating the positive proteins in a negative charge. Which prevented the smaller proteins migrating through the gel during electrophoresis we attempted to test this by performing a reverse polarity gel. This was only marginally successful in allowing us to visualise RNase and not lysozyme. We developed an ATP containing gradient gel based on the principle that ATP, being found in high

concentrations within cells and aiding in protein solubility would act as a surfactant in a similar way to SDS. This method allowed us only to visualise RNase and not lysozyme, BSA or GST but it did aid in the polymerisation of the gold layer which had been consistently difficult.

Our research has had limited success when investigating citrate and CTAB protected nanoparticles but we have had promising results when using DMAP protected nanoparticles with both phosphorothioated DNA and proteins. Further research would be useful in being able to successfully visualise lysozyme and RNase consistently, as well exploring techniques such as the ATP containing and gradient gels in more detail. I believe that this work has successfully explored the ability of DMAP AuNPs to separate sulfur containing biomolecules by polyacrylamide gel electrophoresis and formed a solid foundation for future work in this area.

Chapter 4: Catalytic DNA Aptamers.

4.1 Introduction:

Enzymes make biology possible; without enzymes the processes involved would take years, not microseconds.⁷¹ They have an enormous range of chemical and biological functions, with developments emerging in synthetic photosynthesis, biological tagging and therapeutics.^{20,24,84} Enzymes are biological catalysts, working by reducing the activation energy of a reaction pathway. This is because enzymes tertiary structures form active sites (pockets), which are complementary to transition state structure of the reaction for which they catalyse.¹¹⁶ Competitive inhibition of enzyme activity occurs when molecules with a similar structure to the transition state of the reaction bind to the active site of the enzyme.⁹⁰ Aptamers can also bind analytes through similar methods.⁸⁹ Aptamers are single stranded lengths of nucleic acids. Naturally occurring aptamers are RNA based and synthetic aptamers are generally DNA based.^{34,117} Aptamers can be discovered by *in vivo* selection; enabling a wide range of specificity, these aptamers can be developed to bind any analyte. The analyte we have chosen is pepstatin, which is an aspartic acid protease inhibitor with an affinity for Pepsin. Pepsin is an enzyme found in the stomach, which catalyses the hydrolysis of peptide bonds¹. Statine, one of the constituents of Pepstatin, has a tetrahedral structure which is a transition state analogue of peptic catalysis.^{90,91} We have chosen to use pepstatin and pepsin because they are well documented and simple, as well as the availability of biological assays which allow us to assess the catalytic activity of pepsin and our aptamer. We theorise that if we select an analyte which acts as an inhibitor for an enzyme, we would produce an aptamer with catalytic activity similar to that of the enzyme for which the inhibitor targets.

4.2 Materials:

Biotin-CE: dA-CE, dC-CE, dG-CE, and dT-CE phosphoramidites were purchased from Link Technologies and diluted as recommended. Deblock, cap A, cap B, oxidiser and ETT activator

reagents were purchased from Link Technologies. Dry acetonitrile, urea and EDTA were purchased from Acros. Acrylamide/bisacrylamide 37.5:1 solution was purchased from Fisher Scientific. Ammonium phosphate, N, N, N', N'-tetramethylethylenediamine (TEMED) and citric acid were purchased from Sigma Aldrich. Sodium citrate was purchased from Fisons. All materials were used as provided, without further purification unless otherwise stated.

4.3 Methods:

4.3.1 Aptamer Library Design.⁹²

Figure 4.1 represents our DNA aptamer library design. We used a library design from the literature,⁹² with three known regions and two unknown to allow us to produce a high sequence diversity, but also to allow us to control the folding of the aptamer. Each constant region has a complimentary binding sequence, region 1, 2 and 3 compliment primer 1, antisense biotin and primer 2 respectively. Keeping constant regions double stranded helps to ensure that the unknown variable regions are responsible for any binding affinity exhibited with pepstatin, while aiding in amplification by polymerase chain reaction (PCR). We have used biotinylated DNA to act as the binding agent between the library and the streptavidin columns which would be instrumental in separating binding sequences from non-binders.

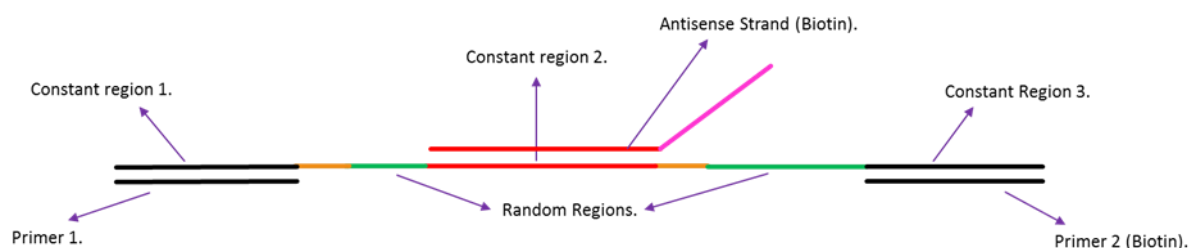


Figure 4.1: Schematic of our aptamer library design.

The variable regions were produced by mixing phosphoramidites of all four bases in the following ratio: A - 1.4 mL: C - 1.4 mL: G - 1.2 mL: T - 1 mL.¹¹⁸ These ratios were chosen based on the lower reactivity of bases C and G over A and T. The letter M in the below sequence represents a base which has been taken from the mixture of phosphoramidites to produce the variable regions.

Library strand:

CCTGCCACGCTCCGC**AAGCTT**MMMMMMMMMMMM**CTGCAGCGATTCTTGATCG**MMMMMMMMMMMM
MMMMMMMMMMMMMM**TAAGCTTGGCACCCGCATCGT**

Primer 1:

GCGGAGCGTGGCAGG

Biotin Antisense strand:

Biotin-TACCGCAAAAAAAAA**CAAGAATCGCTGCAG**

Biotin primer 2:

ACGATGCGGGTGCCAAGCTTA-*Biotin*

The above oligomers are written in standard 5'- 3' notation. All library components were synthesised on an Expedite 8909 system provided by Biolytic. Phosphoramidites were dissolved in dry acetonitrile to the concentrations as suggested by the supplier, solvents were used as provided. Oligomers were synthesised on a 1 μ M scale.

4.3.2 Cleavage, Deprotection and Purification of Synthesised DNA Components:

Oligomers were cleaved and deprotected from the synthesis columns at the same time. The solid support resin was removed from the column and placed into a screw-cap centrifuge tube and to this 1.5 mL of ammonia was added. The oligomers were incubated at 55 °C overnight in a stirring water bath. The oligomers are then placed in a centrifugal vacuum concentrator to remove the ammonia solution. The strands were re-suspended in 200 μ L of autoclaved water.

The DNA library required purification by PAGE. A 1.5 mm 10 % denaturing PAGE gel was produced by diluting 25 mL of 20 % denaturing stock solution with 25 mL of 1 x TBE buffer, to this 50 μ L of TEMED and 130 μ L of 40 % APS stock solution were added to induce polymerisation. The gel was poured between two glass plates and a 1.5 mm comb was inserted. The comb was removed after casting and the well washed with TBE buffer, the gel was pre-ran at 300 V for 1 hour before the sample loaded. The DNA library with 8 M urea was loaded onto the gel and ran at 150 V for half an hour before being run for a further 2 hours at 300 V. The gel was removed from the glass plates and placed onto cling film, which was then placed onto a silica TLC plate;

the gel was illuminated with UV light to visualise the DNA band which cast a shadow on the fluorophore in the TLC plate. The DNA band was cut out of the bulk gel and placed into a 15 mL falcon tube. The gel was homogenised and 8 mL of autoclaved water was added. The solution was mixed and rapidly frozen in liquid nitrogen before being incubated overnight at 60 °C in a water bath. The solution was split into two equal portions and centrifuged for five minutes, the supernatant was collected and the pellet washed with 2 mL autoclaved water. This was repeated a further two times. The supernatants were dried by centrifugal vacuum concentration at 60 °C for five hours and the pellets were re-suspended in a total of 1 mL autoclaved water.

The complimentary strands: primer 1, primer 2 with and without biotin and the antisense strand were desalted by ethanol precipitation, the samples were incubated with 3 M sodium acetate and 100 % ethanol over night before being centrifuged at 21.1 x g for 20 minutes. The supernatant was removed and the pellet washed with 1 mL 70 % ethanol and centrifuged again, this was repeated a total of three times for each sample. The samples were then left to air dry before being re-suspended 200 µL autoclaved water.

4.3.3 Quantification:

The DNA aptamer components were analysed using UV-Visible spectroscopy using a nanodrop, 1 µL of sample was diluted in 100 µL of autoclaved water. Using the value obtained at an absorbance of 260 nm and the OD 260 value¹¹⁹ we calculated the DNA concentration in nmol / mL.

4.3.4 Selection Buffers:

An acidic buffer was chosen as our selection buffer because pepsin has a pH range of 4-6.5^{1,120} and pepstatin has a pH range of 4.5-7.¹²¹ Since DNA is stable only in slightly acidic conditions, we chose a buffer with pH 6, as it sits within the stable activity ranges of the selection materials. We made two buffer components when combined in a known volume would produce a selection buffer of pH 6. We produce 0.1 M component buffers of citric acid and sodium citrate, dissolved

in 18.2 mΩ purified water up to 1 L. A denaturing buffer was chosen as our washing buffer. 5 M urea buffer was made by dissolving urea in 1 x TBE up to 1 L.

4.4 Results and Discussion:

Based upon the literature⁹² we developed an in vitro selection method which would allow us to separate inactive aptamer sequences from aptamer sequences which bind pepstatin. The selection method would take place using streptavidin spin columns, with multiple incubation, elution and purification steps. Around twelve rounds of selection are anticipated.⁹² Figure 4.2 shows a schematic of our in vitro selection process.

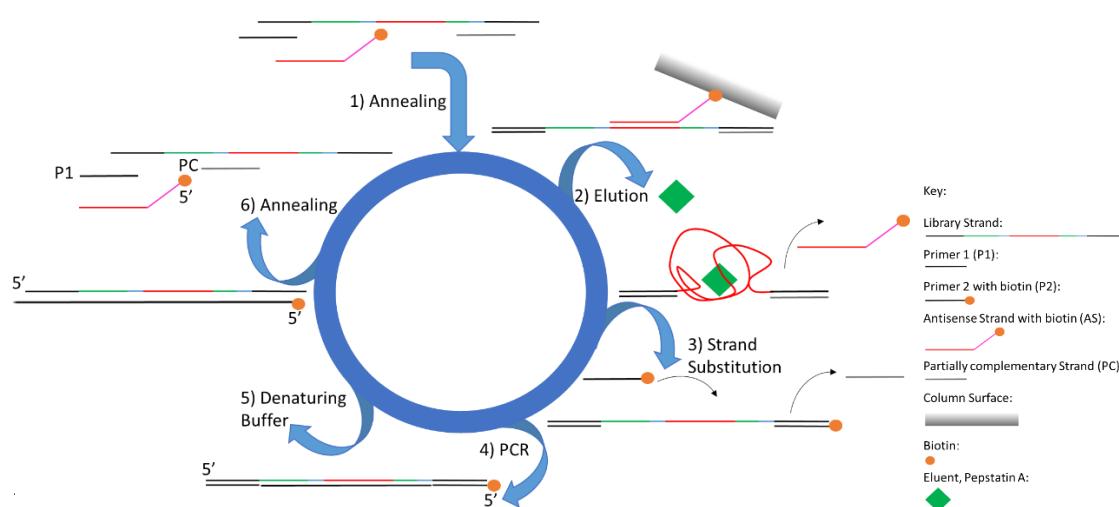


Figure 4.2: Representation of the proposed in vitro selection process.

DNA solutions would be prepared at concentrations used in the literature.⁹² The DNA library would be prepared at a concentration of 2 nmol, the biotinylated antisense strand would be at a concentration of 10 nmol.⁹² Both primers, 1, 2 and the semi-complimentary strand would be prepared at concentrations of 2.5 nmol⁹² in selection buffer. The selection protocol has been designed as follows.

- Prepare column: The storage solution would be removed from the columns by centrifugation at 150 x g for 1 minute.
- Equilibrate column: The columns would be then equilibrated, 400 μL of binding buffer would be added to the column then it would be centrifuged for 1 minute, this process would be repeated a further two times.

- Bind biotinylated DNA: The biotin antisense strand of DNA would then be added to the column. 200 μL of sample would be added and the column would be sealed and slowly inverted for a period of twenty minutes. After this period the column would be centrifuged to remove any unbound strands, for 1 minute at 150 x g. See figure 4.2, step 1.
- Wash column: The column would then be washed with 400 μL of binding buffer, then centrifuged for 1 minute at 150 x g. This step would be repeated a further two times.
- Bind target DNA: 200 μL each of, DNA library and primer 1 and the partially complementary strand, would be added to the column. The column would be incubated for 60 minutes while undergoing slow inversion. After this period the column would be centrifuged for 1 minute at 150 x g to remove any unbound sequences. The flow-through would be collected. See figure 4.2, step 1.
- Wash column: 400 μL of binding buffer would be added and the column centrifuged at 150 x g for 1 minute. This would be repeated a further four times, the flow-through from each would be collected.
- Wash with target analyte: A 400 μL solution of Pepstatin A would be added to the column, and the column inverted to ensure mixing. The column would then be centrifuged at 150 x g for one minute. See figure 4.2, step 2.
- Elute Target DNA: 200 μL of elution buffer would be added to the column and mixed by inversion. The column would then be centrifuged for one minute at 1000 x g to remove the target DNA aptamers. The eluent would be collected. This process would be repeated a further two times.
- Strand Substitution: The Eluted Strands would have the partially complimentary strand replaced by the biotinylated DNA, as strands which are more complimentary would displace less complimentary strands. This would aid in separation of the double stranded DNA after PCR. See figure 4.2, step 3.

Columns would be centrifuged in 2 mL micro-centrifuge tubes, in order to collect the eluents. Tubes would be changed between each step. The PCR protocol is adapted from one used within the group, PCR would be conducted after each round of selection in order to amplify the isolated sequences. See figure 4.2, step 4.

- A PCR bead would be placed into a 300 μ L micro centrifuge tube to this 10 μ L of primer 1 (2.5 nmol DNA / mL) and 10 μ L primer 2 (2.5 nmol DNA / mL) would be added to the tube.
- 5 μ L of the isolated DNA library would be added to the tube. The tube would then be sealed and flicked to ensure the bead has dissolved.
- The tube would then be centrifuged at 1,000 rpm for 1 minute to ensure all of the liquid is at the bottom of the tube.
- The micro centrifuge tube would then be placed into the thermocycler and run under the following programme:
 1. 94 °C for 2 minutes.
 2. 94 °C for 30 seconds, 55 °C for 30 seconds, 72 °C for 30 seconds, for 30 cycles.
 3. 72 °C for 5 minutes, then held at 4 °C.
- The resultant DNA would then be treated with denaturing urea buffer to separate the double stranded DNA into single strands. See figure 4.2, step 5.
- The separated DNA would then undergo the selection process again, this would be repeated for approximately 12 rounds of selection or until the exponential increase by amplification begins to flattern.⁹² See figure 4.2, step 6.
- The successful sequences would then be sequenced by an in vivo method.^{122,123} The sequences would be cloned into vectors, which when exposed to a bacterial host would be amplified into plasmid colonies. The sequences would be purified from the colony and sequenced to obtain the full sequence for future solid phase synthesis.^{122,123}

Once sequenced the aptamers would be tested using a pepsin activity assay to test the ability of the aptamer to catalyse haemoglobin. Pepsin would also be tested and the results compared to assess the level of catalytic activity of the aptamers.

We began the synthesis of the components required for selection, although purity of the synthesised components was very low. The purity of the synthesised library was analysed by polyacrylamide gel electrophoresis, figure 4.3 shows the resultant gel.

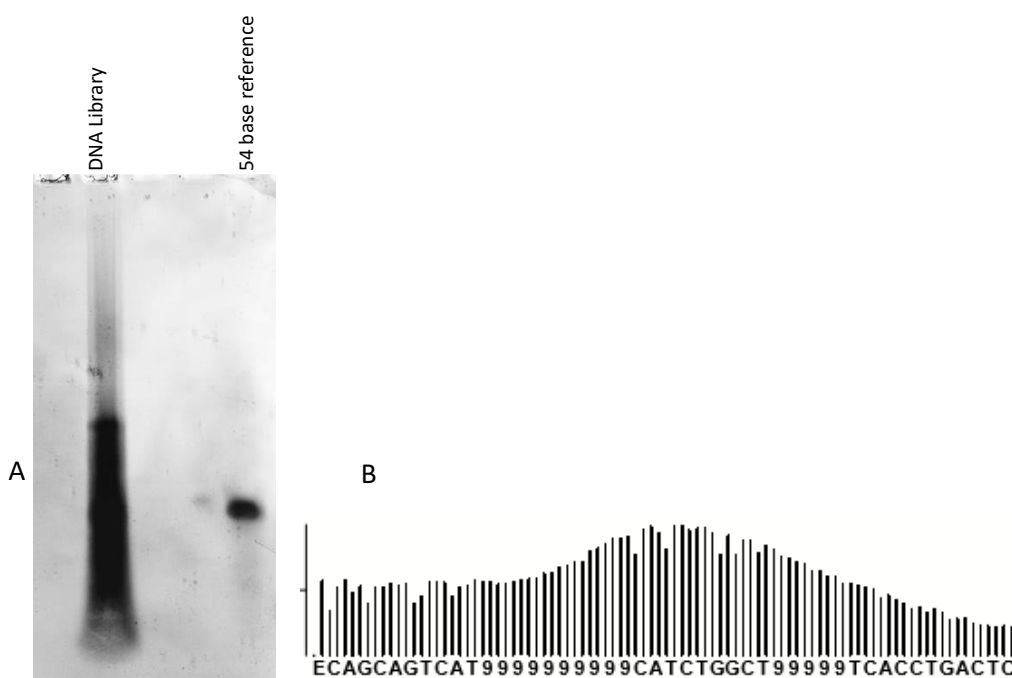


Figure 4.3: A, 20% denaturing Polyacrylamide gel of DNA library and 54 base reference strand. B, trityl graph of DNA library synthesis, 9 represents a coupling made from the mixed phosphoramidites M.

The DNA library is a 91 base oligomer and should not travel as far as the 54 base reference strand (Figure 4.3 A) the DNA library causes a large smear due to its impurity. The top of the darkest part of the smear is where the full length library should migrate too, however there are shorter sequences which migrate past this point. Therefore we purified the Library by PAGE and obtained the concentration of DNA there was an insufficient amount of DNA to be able to begin the selection process. The concentrations of the antisense and primer 2 biotinylated samples also had an insufficient concentration of DNA. Primer 1 was synthesised to a sufficient concentration to begin selection. These strands required re-synthesising to increase the

concentration of DNA, however due to time constraints we were unable to progress this research beyond this point.

4.5 Conclusions:

We have developed a route which would in theory, lead to the creation of aptamers with catalytic activity. However we have had problems with the synthesis of DNA components, which was a process which required a large amount of optimisation. This process led to the development of impure DNA sequences which required further purification. Purification was successful and the correct length components were isolated but low concentration yields for the library and biotinylated DNA required re-synthesis. Due to the time constraints on this project we were unable to progress this research further. Given the opportunity we would attempt the selection process on the newly synthesised aptamer components and carry out the research as described in detail above.

Chapter 5: Conclusions, Further Work and References.

5.1 Conclusions and Further Work:

This work has discussed the analysis and application of biomolecules. Chapter 2 describes the methods by which we synthesised and characterised gold nanoparticles and polyacrylamide gels. Three types of gold nanoparticles: citrate, CTAB and DMAP protected AuNPs, were successfully characterised using DLS, UV-Vis and TEM. There was little similarity between the two methods, DLS and UV-Vis. This was caused by a number of factors, DLS reports size data based on hydration spheres and is unsuitable for the analysis of non-spherical samples and clusters. The data obtained from UV-Vis gave inconsistent data for the DMAP and CTAB AuNPs which may be attributed to the method used, being developed using citrate AuNPs⁹⁹. In conjunction DLS and UV-Vis form a basis for further testing, TEM imaging of DMAP AuNPs gave an average diameter of between 4 and 8 nm which is concordance with literature⁹⁸.

Gold containing polyacrylamide gels showed slowed polymerisation when compared to non-gold containing gels. Characterisation by rheology, OCT and SEM allowed us to successfully characterise the distribution and effects the addition of gold has on polyacrylamide gels. Rheological results suggest there is reduction in the elasticity of gold containing polyacrylamide gels when compared to non-gold gels. However the addition of gold does stabilise the LVER of polyacrylamide gels and does not affect the efficiency of polyacrylamide as a separation medium. OCT and SEM allowed us to successfully visualise clustered DMAP AuNPs within polyacrylamide gels the lack of more clusters would suggest that the majority of DMAP AuNPs are monodisperse throughout the polyacrylamide matrices. These materials were then taken forward to analyse biomolecules.

Chapter 3 discusses the efficacy of gold nanoparticle modified polyacrylamide gels in the separation of sulfur containing biomolecules. Citrate AuNPs showed little success when investigated with phosphorothioated DNA this was believed to be due to the negative ligand shell. However when interrogated with magnesium containing polyacrylamide gel

electrophoresis there was no change in the results, with aggregation becoming a problem. Testing using citrate AuNPs halted and we turned to CTAB AuNPs. We have seen problems from the outset, with agglomeration and polymerisation of polyacrylamide gel was unreproducible, leading to the discontinuation of testing with CTAB AuNPs.

In contrast DMAP AuNPs showed interaction with DNA, with the retention of all of the samples including the un-thiolated strand although some selectivity was seen. Although reproducibility of the same result was not consistent we moved onto testing these gold nanoparticles with proteins: lysozyme, RNase, GST and BSA. GST and BSA showed continued retention by the DMAP AuNPs modified polyacrylamide gels. However, there were continued problems with the visualisation of lysozyme and RNase, which at pH 8 are positively charged. We believed that this charge caused the proteins in native PAGE to move up the gel, leading to the development of ATP buffered polyacrylamide gel electrophoresis. ATP being a naturally occurring molecule which prevents the agglomeration of proteins, likely through surface interactions similarly to a surfactant, we believed that this could be used to coat lysozyme and RNase in a negative charge. This experiment resulted in the visualisation of RNase but not lysozyme. We believe, with method development that this technique may be promising. We were able to successfully use DMAP AuNPs to analyse sulfur containing biomolecules in polyacrylamide gel electrophoresis, through the principle of thiol substitution chemistry. Further investigation is needed to obtain consistent results as well as obtaining the successful visualisation of lysozyme.

Chapter 4 discusses the method by which we would have synthesised an aptamer library to select for catalytic activity with pepstatin. We were able to successfully synthesis the DNA components required for selection. However, issues with synthesis led to the need for extensive purification, especially for the DNA aptamer library sequence. Low yields were also an issue, resulting in the resynthesis of the biotinylated and library strands. Due to time constraints we were unable to complete the project; given more time we would complete the selection and

amplification of the successful sequences. Before then sequencing and testing the effectiveness of the selected aptamers to catalyse the hydration of peptide bonds in haemoglobin.

5.2 References:

1. Bailey D, Carpenter E, Coker A, Coker S, Read J, Jones A, Erskine P, Aguilar C, Badasso M, Toldo L, Rippmann F, Sanz-Aparicio J, Albert A, Blundell T, Roberts N, Wood S, Cooper J *Acta Crystallographica Section D: Bio. Cryst.* vol. 68, issue 5 (2012) pp. 541-552
2. Protein Data Bank. RCSB - Pepstatin Summary Page. Available at: http://www4.rcsb.org/bird/PRD_000557. (Accessed: 7th September 2017)
3. Muro, E., Ekin Atilla-Gokcumen, G. & Eggert, U. S. Lipids in cell biology: how can we understand them better? *Mole. Bio. Cell.* **25**, (2014).
4. Alberts, B. *et al. Mole. Bio.Cell.* (Garland Science, 2002) ISSN:[1059-1524](https://doi.org/10.1016/S1522-2675(02)00000-0) .
5. Bush, C. A., Martin-Pastor, M. & Imberty, A. Structure and confirmation of complex carbohydrates of glycoproteins, glycolipids, and bacterial polysaccharides. *Annu. Rev. Biophys. Biomol. Struct* **28**, 269–93 (1999).
6. Ganesh, K. & Krishnan, Y. Nucleic Acids – Chemistry and Applications. *J. Org. Chem* **78**, 12283–12287 (2013).
7. Asif, M. *et al.* Amino acids : A review article Amino acids : A review article. *J. Med. plants Res.* **5**, 3997–4000 (2011).
8. Li, Q. & Lancaster, J. R. Chemical foundations of hydrogen sulfide biology. Nitric Oxide - Biology and Chemistry, vol. 35 (2013) pp. 21-34
9. Editorial, N. Biology and brimstone. *Nat. Chem. Biol* **2**, 169 (2006).
10. Kessler, D. Enzymatic activation of sulfur for incorporation into biomolecules in prokaryotes. *FEMS. Microbiol. Rev.* vol. 30, issue 6 (2006) pp. 825-840
11. Gibson, D. T. Significant studies in the organic chemistry of sulfur, *Chem. Rev.* vol. 14, issue 3 (1934) pp. 431-457.
12. Wang, W., Yang, B., Qu, Y., Liu, X. & Su, W. FeS/S/FeS₂ Redox System and Its Oxidoreductase-like Chemistry in the Iron-Sulfur World. *Astrobiol.* **11**, 471–476 (2011).
13. Koniev, O. & Leriche, G. Selective Irreversible Chemical Tagging of Cysteine with 3- Arylpropionitriles. *Bioconj. Chem.* **25**, 202–206 (2014).
14. Ren, H. *et al.* A Biocompatible Condensation Reaction for Labeling of Terminal Cysteines on Proteins Graphical. *Angew. Chem. Int. Ed. Engl.* **48**, 9658–9662 (2009).
15. Hermanson, G. T. *Bioconj. Techn.: Third Edition* (2013) pp. 1-1146 Published by Elsevier Inc.
16. Hermanson, G. *Bioconjugate techniques Bioconj. Techn.: Third Edition* (2013) pp. 1-1146 Published by Elsevier Inc, Chapter28.
17. Volkman, G. & Liu, X.-Q. Protein C-Terminal Labeling and Biotinylation Using Synthetic Peptide and Split-Intein. *PLoS. ONE.* vol. 4, issue 12 (2009)
18. Andringa, K. K. & Bailey, S. M. 6 - Detection of Protein Thiols in Mitochondrial Oxidative

Phosphorylation Complexes and Associated Proteins. 83-108 (2010).

19. Jalili, P. R., Sharma, D. & Ball, H. L. Enhancement of Ionization Efficiency and Selective Enrichment of Phosphorylated Peptides from Complex Protein Mixtures Using a Reversible Poly-Histidine Tag. *J. Am. Soc. Mass. Spectrom.* **18**, 1007–1017 (2007).
20. Baldwin, A. D. & Kiick, K. L. Tunable Degradation of Maleimide Thiol Adducts in Reducing Environments. *Bioconj. Chem.* **22**, 1946–1953 (2011).
21. Jackson, D. Y. Processes for Constructing Homogeneous Antibody Drug Conjugates. *Org. Process. Res. Dev.* **20**, 852–866 (2016).
22. Ariyasu, S. & Hayashi, H. Site-Specific Dual Functionalization of Cysteine Residue in Peptides and Proteins with 2- Azidoacrylates. *Bioconj. Chem.* **28**, 897–902 (2017).
23. Zakeri, B. & Fierer, J. Peptide tag forming a rapid covalent bond to a protein, through engineering a bacterial adhesin. *Proc. Natl. Acad. Sci.* vol. 109, issue 12 (2012) pp. E690-E697
24. Seitz, O. & Beck-Sickinger, A. Peptide-tags for site-specific protein labelling in vitro and in vivo. *Mol. Biosyst.* **12**, 1731–1745 (2016).
25. Meyer, M., Stenzel, U., Myles, S., Prü, K. & Hofreiter, M. Targeted high-throughput sequencing of tagged nucleic acid samples. *Nucleic. Acids. Res.* vol. 35, issue 15 (2007)
26. Zearfoss, N. R. & Ryder, S. P. End-labeling oligonucleotides with chemical tags after synthesis. *Methods Mol. Biol.* **941**, 181–93 (2012).
27. Hermanson, G. T. & Hermanson, G. T. in *Bioconj. Techn.:* Third Edition (2013) pp. 396–497 Published by Elsevier Inc.
28. Goodchild, J. Review Conjugates of Oligonucleotides and Modified Oligonucleotides: A Review of Their Synthesis and Properties. *Bioconjug. Chem.* vol. 1, issue 3 (1990) pp. 165-187
29. Gaffney, B. L., Veliath, E., Zhao, J. & Jones, R. A. One-Flask Syntheses of c-di-GMP and the [R p ,R p] and [R p ,S p] Thiophosphate Analogues. *Org Lett* **12**, 3269–3271 (2010).
30. Shigi, N. Biosynthesis and functions of sulfur modifications in tRNA. *Front. Genet.* **5**, 1–11 (2014).
31. Leidel, S. *et al.* Ubiquitin-related modifier Urm1 acts as a sulphur carrier in thiolation of eukaryotic transfer RNA. *Nat.* vol. 458, issue 7235 (2009) pp. 228-232
32. Barciszewski, J. & Clark, B. F. C. *RNA Biochemistry and Biotechnology.* (Springer Netherlands, 1999).
33. Bonetta, L. RNA-Based Therapeutics: Ready for Delivery? *Cell.* vol. 136, issue 4 (2009) pp. 581-584
34. Burnett, J. C. & Rossi, J. J. Chemistry & Biology Review RNA-Based Therapeutics: Current Progress and Future Prospects. *Chem. Biol.* **19**, 60–71 (2012).
35. Katare, D. RNA based therapeutics. *Int. J. Pharm. Pharm. Sci.* **4**, 1–11 (2012).
36. Giner Martínez-Sierra, J., Galilea San Blas, O., Marchante Gayón, J. & García Alonso, J. Sulfur analysis by inductively coupled plasma-mass spectrometry: A review. *Spectrochim. Acta Part B At. Spectrosc.* **108**, 35–52 (2015).
37. Neubauer, K. R. Determination of Phosphorus and Sulfur with Dynamic Reaction Cell ICP-MS. pp. 1-5, 2004.

38. X-ray Photoelectron Spectroscopy (XPS) Reference Pages: Sulphur. Available at: <http://www.xpsfitting.com/2009/06/sulphur.html>. (Accessed: 21st July 2017)
39. Godat, E. & Madalinski, G. Mass Spectrometry-Based Methods for the Determination of Sulfur and Related Metabolite Concentrations in Cell Extracts. *Meth. Enzymol.* vol. 473 (2010)
40. Yaneva, M. & Tempst, P. Isolation and Mass Spectrometry of Specific DNA Binding Proteins. **338**, 291–303
41. Paulsen, C. & Carroll, K. Cysteine-Mediated Redox Signaling: Chemistry, Biology, and Tools for Discovery. *Chem. Rev.* 4633–4679 (2013). doi:10.1021/cr300163e
42. Kolluru, G. K., Shen, X., Bir, S. C. & Kevil, C. G. Hydrogen sulfide chemical biology: Pathophysiological roles and detection. *Nitric. Oxide.* **35**, 5–20 (2013).
43. Giner Martínez-Sierra, J. *et al.* Evaluation of different analytical strategies for the quantification of sulfur-containing biomolecules by HPLC-ICP-MS: Application to the characterisation of 34 S-labelled yeast. *JAAS.* vol. 25, issue 7 (2010) pp. 989-997
44. Fantauzzi, M., Elsener, B., Atzei, D., Rigoldi, A. & Rossi, A. Exploiting XPS for the identification of sulfides and polysulfides. *RSC. Adv.*, vol. 5, issue 93 (2015) 75953-75963
45. Castner, D. G., Hinds, K. & Grainger, D. W. X-ray Photoelectron Spectroscopy Sulfur 2p Study of Organic Thiol and Disulfide Binding Interactions with Gold Surfaces. *Langmuir.* vol. 12, issue 21 (1996) pp. 5083-5086
46. Epiotis, N. D. *et al.* Rates of Thiol-Disulfide Interchange Reactions between Mono- and Dithiols and Ellman's Reagent'. *J. Org. Chem.* **42**, 332–338 (1977).
47. TRII, D., Shasha, B. S. & Russell, C. R. Thiolation of Starch and Other Polysaccharides. *J. Appl. Polym. Sci.* **17**, 1607–1615 (1973).
48. Peng, H. *et al.* Thiol Reactive Probes and Chemosensors. *Sensors.* **12**, 15907–15946 (2012).
49. Rudyk, O. & Eaton, P. Biochemical methods for monitoring protein thiol redox states in biological systems. *Redox Bio.* vol. 2, issue 1 (2014) pp. 803-813 Published by Elsevier B.V.
50. Greenfield, N. J. Using circular dichroism spectra to estimate protein secondary structure. *Nat. Protoc.* **1**, 2876–2890 (2006).
51. Kelly, S. M., Jess, T. J. & Price, N. C. How to study proteins by circular dichroism. *Biochem. Biophys.* **1751**, 119–139 (2005).
52. Igloi, G. L. Interaction of tRNAs and of Phosphorothioate-Substituted Nucleic Acids with an Organomercurial. Probing the Chemical Environment of Thiolated Residues by Affinity Electrophoresis+. *Biochem. Arch. Biochem. Bio-Ray Biochem. J. Infect. Dis. Znt. J. Chem. Kinet Arch. Biochem. Biophys. J. Biol. Chem. Biochem.* **27**, 3842–3849 (1988).
53. Biondi, E. & Burke, D. H. Separating and Analyzing Sulfur-Containing RNAs with Organomercury Gels. *Methods in Molecular Biology*, vol. 883 (2012) pp. 111-120 Published by Humana Press Inc.
54. WHO. Exposure to Mercury: A major public health concern. *World Heal. Organ.* (2007).
55. Bernhoft, R. A. Mercury toxicity and treatment: A review of the literature. *J. Environ. Pub. Heal*, vol. 2012 (2012) Published by Hindawi Publishing Corporation
56. Lopachin, R. M., Gavin, T., Decaprio, A. & Barber, D. S. Application of the Hard and Soft,

- Acids and Bases (HSAB) Theory to Toxicant Target Interactions. *Chem. Res. Toxicol* **25**, 239–251 (2012).
57. Sharma, N., Bhatt, G. & Kothiyal, P. 3. Gold Nanoparticles synthesis, properties, and forthcoming applications – A review. *Indian J.Pharm.Biol.Res* **3**, 13–27 (2015).
 58. Rucareanu, S., Gandubert, V. J. & Lennox, R. B. 4-(N,N-Dimethylamino)pyridine-Protected Au Nanoparticles: Versatile Precursors for Water-and Organic-Soluble Gold Nanoparticles. *Chem. Mater.* **18**, 4674–4680 (2006).
 59. Tomar, A. & Garg, G. Short Review on Application of Gold Nanoparticles. *Glob. J. Pharmacol.* **7**, 34–38 (2013).
 60. Huang, X. & El-Sayed, M. A. Gold nanoparticles: Optical properties and implementations in cancer diagnosis and photothermal therapy. *J. Adv. Res.* **1**, 13–28 (2010).
 61. Yannick Tauran, Arnaud Brioude, Anthony W Coleman, Moez Rhimi, B. K. Molecular recognition by gold, silver and copper nanoparticles. *World J. Biol. Chem.* **4**, 35–63 (2013).
 62. Hornos Carneiro, M. F. & Barbosa, F. Gold nanoparticles: A critical review of therapeutic applications and toxicological aspects. *J. Toxicol. Environ. Heal. Part B* **19**, 129–148 (2016).
 63. Das, M., Shim, K. H., An, S. S. A. & Yi, D. K. Review on gold nanoparticles and their applications. *Toxicol. Environ. Health Sci.* **3**, 193–205 (2011).
 64. Van Santen, R. Catalysis in Perspective: Historic Review. *Catalysis: From Principles to Applications* (2012) pp. 3-19 Published by Wiley-VCH
 65. Dokukin, V. Catalysis by DNA enzymes: Roles of lanthanide(III) ions and DNA aptamer modules. (University of Illinois at Urbana-Champaign, 2014).
 66. Pang, X., Zhao, L., Han, W., Xin, X. & Lin, Z. A general and robust strategy for the synthesis of nearly monodisperse colloidal nanocrystals. *Nat. Nano. Tech.*, vol. 8, issue 6 (2013) pp. 426-431
 67. Widegren, J. A. & Finke, R. G. A review of the problem of distinguishing true homogeneous catalysis from soluble or other metal-particle heterogeneous catalysis under reducing conditions. *J. Mol. Catal. A Chem.* **198**, 317–341 (2003).
 68. Weisz, P. B. Heterogeneous catalysis. *Annu. Rev. Phys. Chem.* **21**, 175–196 (1970).
 69. Ma, J. *et al.* A short review of catalysis for CO₂ conversion. *Catalysis Today*, vol. 148, issue 3-4 (2009) pp. 221-231
 70. Geletii, Y. V. *et al.* An All-Inorganic, Stable, and Highly Active Tetra Ruthenium Homogeneous Catalyst for Water Oxidation. *Angew. Chemie.* **120**, 3960–3963 (2008).
 71. Cooper, G. M. The Central Role of Enzymes as Biological Catalysts. *The Cell: A Molecular Approach*, issue National Library of Medicine (2000)
 72. Lever, G. Large-Scale Quantum-Mechanical Enzymology. 9–19 (2015).
 73. Liu, C. T. *et al.* Probing the Electrostatics of Active Site Microenvironments along the Catalytic Cycle for Escherichia coli Dihydrofolate Reductase. *JACS* **136**, 10349–10360 (2014).
 74. Schwartz, T. J. *et al.* Engineering Catalyst Microenvironments for Metal-Catalyzed Hydrogenation of Biologically Derived Platform Chemicals. *Angew. Chemie Int. Ed.* **53**, 12718–12722 (2014).

75. Alamillo, R., Crisci, A. J., Gallo, J. M. R., Scott, S. L. & Dumesic, J. A. A tailored microenvironment for catalytic biomass conversion in inorganic-organic nanoreactors. *Angew. Chemie - Int. Ed.* **52**, 10349–10351 (2013).
76. Silverman, S. K. Catalytic DNA: Scope, Applications, and Biochemistry of Deoxyribozymes. *Trends Biochem. Sci.* **41**, 595–609 (2016).
77. Blackburn, G. M., Kang, A. S., Kingsbury, G. A. & Burton, D. R. Catalytic antibodies. *Biochem. J* **262**, 381–390 (1989).
78. Min, J. *et al.* A Recombinant Secondary Antibody Mimic as a Target-specific Signal Amplifier and an Antibody Immobilizer in Immunoassays. *Sci. Rep.* vol. 6, issue April (2016) p. 24159 Published by Nature Publishing Group
79. Chames, P., Regenmortel, M. Van, Weiss, E. & Baty, D. VECTOR DESIGN AND DRUG DELIVERY REVIEW Therapeutic antibodies: successes, limitations and hopes for the future Therapeutic antibodies: coming of age. *Br. J. Pharmacol.* **157**, 220–233 (2009).
80. Ma, S., Tang, N. & Tian, J. DNA Synthesis, Assembly and Applications in Synthetic Biology Gene Synthesis. *Current Opinion in Chem. Bio.* vol. 16, issue 3-4 (2012) pp. 260-267
81. Wang, L. *et al.* Selection of DNA aptamers that bind to four organophosphorus pesticides. *Biotechnol. Lett.* **34**, 869–874 (2012).
82. Li, Y. & Sen, D. A catalytic DNA for porphyrin metallation. *Nat. Struct. Biol.* **3**, 743 (1996).
83. Chalker, J. M., Bernardes, G. J. L. & Davis, B. G. A 'tag-and-modify' approach to site-selective protein modification. *Acc. Chem. Res.* **44**, 730–741 (2011).
84. Barber, J. & Tran, P. D. From natural to artificial photosynthesis. *J. R. Soc. Interface.* vol. 10, issue 81 (2013) pp. 20120984-20120984
85. Lindner, T., Kolmar, H., Haberkorn, U. & Mier, W. DNA libraries for the construction of phage libraries: Statistical and structural requirements and synthetic methods. *Mole.* **16**, 1625–1641 (2011).
86. Yarnell, A. & Washington, C. Hammond postulate. *Sci. Technol.* **81**, 42 (2003).
87. Solà, M. & Toro-Labbé, A. The Hammond Postulate and the Principle of Maximum Hardness in Some Intramolecular Rearrangement Reactions. *J. Phys. Chem. A*, vol. 103, issue 44 (1999) pp. 8847-8852
88. Hammond, G. A Correlation of Reaction Rates. *J. Am. Chem. Soc.*, vol. 77, issue 2 (1955) pp. 334-338 Published by American Chemical Society
89. Jayasena, S. D. Aptamers: An Emerging Class of Molecules That Rival Antibodies in Diagnostics. *Clinical Chemistry*, vol. 45, issue 9 (1999) pp. 1628-1650 Published by American Association for Clinical Chemistry Inc.
90. Marciniszyn, J., Hartsuck, J. A. & Tang, J. Mode of Inhibition of Acid Proteases by Pepstatin. **251**, 70–8
91. Schmidt, P. G., Bernatowicz, M. S. & Rich, D. H. Pepstatin Binding to Pepsin. Enzyme Conformation Changes Monitored by Nuclear Magnetic Resonance. *Biochem.* **21**, 6710–6716 (1982).
92. Nutiu, R. & Li, Y. In vitro selection of structure-switching signaling aptamers. *Angew. Chemie - Int. Ed.* **44**, 1061–1065 (2005).
93. Lead, J. R. & Wilkinson, K. J. Aquatic colloids and nanoparticles: Current knowledge and

- future trends. *Environ. Chem.* **3**, 159–171 (2006).
94. Hornos Carneiro, M. F. & Barbosa, F. Gold nanoparticles: A critical review of therapeutic applications and toxicological aspects. *J. Toxicol. Environ. Heal. Part B* **19**, 129–148 (2016).
 95. Daniel, M. C. M. & Astruc, D. Gold Nanoparticles: Assembly, Supramolecular Chemistry, Quantum-Size Related Properties and Applications toward Biology, Catalysis and Nanotechnology. *Chem. Rev.* **104**, 293–346 (2004).
 96. Toma, H. E., Zamarion, V. M., Toma, S. H. & Araki, K. The coordination chemistry at gold nanoparticles. *J. Braz. Chem. Soc.* **21**, 1158–1176 (2010).
 97. Hutchings, G. J., Brust, M. & Schmidbaur, H. Gold—an introductory perspective. *Chem. Soc. Rev.* vol. 37, issue 9 (2008) p. 1759
 98. Brust, M., Walker, M., Bethell, D., Schiffrin, D. J. & Whyman, R. Synthesis of Thiol-derivatised Gold Nanoparticles in a Two-phase Liquid-Liquid System. *J. Chem. Soc. Chem. Commun.* (1994).
 99. Haiss, W., Thanh, N. T. K., Aveyard, J. & Fernig, D. G. Determination of size and concentration of gold nanoparticles from UV-Vis spectra. *Anal. Chem.* **79**, 4215–4221 (2007).
 100. Schindelin, J. *et al.* Fiji -an Open Source platform for biological image analysis. *Nat. Methods.* vol. 9, issue 7 (2012) pp. 676-682
 101. Haiss, W., Thanh, N. T. K., Aveyard, J. & Fernig, D. G. Determination of Size and Concentration of Gold Nanoparticles from UV – Vis Spectra. **79**, 4215–4221 (2015).
 102. Zimbone, M., Calcagno, L., Messina, G., Baeri, P. & Compagnini, G. Dynamic light scattering and UV–vis spectroscopy of gold nanoparticles solution. *Mater. Lett.* **65**, 2906–2909 (2011).
 103. Frens, G. Controlled Nucleation for the Regulation of the Particle Size in Monodisperse Gold Suspensions. *Nat. Phys. Sci.* **241**, 20–22 (1973).
 104. Lucius, A. L., Veronese, P. K. & Stafford, R. P. Dynamic light scattering to study allosteric regulation. *Methods Mol. Biol.* **796**, 175–86 (2012).
 105. Gandubert, V. & Lennox, R. Assessment of 4-(dimethylamino) pyridine as a capping agent for gold nanoparticles. *Langmuir* **21**, 6532–6539 (2005).
 106. Brust, M., Walker, M., Bethell, D., Schiffrin, D. J. & Whyman, R. Synthesis of Thiol-derivatised Gold Nanoparticles in a Two-phase Liquid-Liquid System. *J. Chem. Soc., Chem. Commun.* (1994).
 107. Tianyu Zheng, Steven Bott, and Q. H. Techniques for Accurate Sizing of Gold Nanoparticles Using Dynamic Light Scattering with Particular Application to Chemical and Biological Sensing Based on Aggregate Formation. *ACS Appl. Mater. Interfaces* 21585–21594 (2016).
 108. Zheng, T., Bott, S. & Huo, Q. Techniques for Accurate Sizing of Gold Nanoparticles Using Dynamic Light Scattering with Particular Application to Chemical and Biological Sensing Based on Aggregate Formation. *ACS Applied Materials & Interfaces*, vol. 8, issue 33 (2016) pp. 21585-21594
 109. Waigh, T. A. *et al.* Physical properties of polyacrylamide gels probed by AFM and rheology. *EPL*. vol. 109, issue 3 (2015) p. 38003

110. Dykman, L. A. & Khlebtsov, N. G. Immunological properties of gold nanoparticles. *Chem. Sci.*, vol. 8, issue 3 (2017) pp. 1719-1735
111. Bürgi, T. Properties of the gold–sulphur interface: from self-assembled monolayers to clusters. *Nanoscale* **7**, 15553–15567 (2015).
112. Zhao, W. & Hsing, I.-M. Facile and rapid manipulation of DNA surface density on gold nanoparticles using mononucleotide-mediated conjugation. *Chemical Communications*, vol. 46, issue 8 (2010) p. 1314
113. Häkkinen, H. The gold–sulfur interface at the nanoscale. *Nature Chemistry*, vol. 4, issue 6 (2012) pp. 443-455
114. Cavuoto, S. Development of modified polyacrylamide gels for use as selective electrophoresis media for examination of biological analytes. (2016). (Unpublished).
115. Patel, A. *et al.* ATP as a biological hydrotrope. *Sci.* vol. 356, issue 6339 (2017) pp. 753-756
116. Paola Travascio. DNA and RNA catalyts with peroxidase activity: An investigation into structure and mechanism. (Simon Frazer University, 2000).
117. Krylova, S. M., Koshkin, V., Bagg, E., Schofield, C. J. & Krylov, S. N. Mechanistic Studies on the Application of DNA Aptamers as Inhibitors of 2-Oxoglutarate-Dependent Oxygenases. doi:10.1021/jm300243h
118. Pollard, J. Pool Design, Complexity, and Purification. *Unpublished* (1998). Available at: <https://molbio.mgh.harvard.edu/szostakweb/protocols/rnapool/rnapool.html>. (Accessed: 19th September 2017)
119. IDT. OligoAnalyzer 3.1. *Unpublished* Available at: <https://www.idtdna.com/calc/analyzer>. (Accessed: 19th September 2017)
120. Piper, D. W. & Fenton, B. H. pH stability and activity curves of pepsin with special reference to their clinical importance. *Gut*, vol. 6, issue 5 (1965) pp. 506-8
121. Xie, D. *et al.* Dissection of the pH Dependence of Inhibitor Binding Energetics for an Aspartic Protease: Direct Measurement of the Protonation States of the Catalytic Aspartic Acid Residues. *Biochem*, vol. 36, issue 97 (1997) pp. 16166-16172
122. Bruno, J. G. *et al.* Development, screening, and analysis of DNA aptamer libraries potentially useful for diagnosis and passive immunity of arboviruses. *BMC. res. notes*. vol. 5 (2012) p. 633
123. Sudha, P. *et al.* Selection and Characterization of Aptamers Using a Modified Whole Cell Bacterium SELEX for the Detection of Salmonella enterica Serovar Typhimurium. *ACS Combinat. Sci.* vol. 18, issue 6 (2016) pp. 292-301 Published by American Chemical Society